MONTE CARLO SIMULATIONS OF SYSTEMS OF LIGHT ALCOHOLS + WATER + N-DODECANE AND WATER SOLUBILITY AND STRUCTURES IN POLYTETRAFLUOROETHYLENE

Matthew Lasich

In fulfillment of the degree of Master of Science in Engineering, Faculty of Engineering, University of KwaZulu-Natal

July 2011

Supervisor: Prof. D. Ramjugernath

Co-supervisor: Dr. E.L. Johansson

As the candidate's Supervisor I agree/do not agree to the submission of this thesis

_____

Prof. D. Ramjugernath

DECLARATION

I ..... declare that

(i) The research reported in this dissertation/thesis, except where otherwise indicated, is my original work.

(ii) This dissertation/thesis has not been submitted for any degree or examination at any other university.

(iii) This dissertation/thesis does not contain other persons' data, pictures, graphs or other information, unless specifically acknowledged as being sourced from other persons.

(iv) This dissertation/thesis does not contain other persons' writing, unless specifically acknowledged as being sourced from other researchers. Where other written sources have been quoted, then:

a) their words have been re-written but the general information attributed to them has been referenced;

b) where their exact words have been used, their writing has been placed inside quotation marks, and referenced.

(v) Where I have reproduced a publication of which I am an author, co-author or editor, I have indicated in detail which part of the publication was actually written by myself alone and have fully referenced such publications.

(vi) This dissertation/thesis does not contain text, graphics or tables copied and pasted from the Internet, unless specifically acknowledged, and the source being detailed in the dissertation/thesis and in the References sections.

Signed: _____

Acknowledgements

I would like to acknowledge the following individuals and institutions:

- My supervisors, Prof. Deresh Ramjugernath and Dr. Erik Lennart Johansson, for all of their knowledge and guidance
- The National Research Foundation (NRF) for their financial assistance
- The School of Engineering at University College of Borås in Sweden for allowing the use of their computing facilities
- Dr. Erik Lennart Johansson and Mr. Suren Moodley, for all of their advice and assistance on the topic of simulations
- My fellow postgraduates and colleagues, and the academic and support staff of the Thermodynamics Research Group, for creating a pleasant working and learning environment
- My friends and family, for all of their support during this project

Abstract:

Polytetrafluoroethylene (Teflon®) is encountered in many environments – frying pans, clothing, osmotic distillation membranes, to name a few – yet the solubility and clustering behaviour of water with this material was not found in the open literature. This information may be useful in applications where an absence of water is desired, such as in clothing and textiles. Previous work on polyethylene + water has shown that small water clusters form in the amorphous portion of the polymer. This work investigated this phenomenon for the case of polytetrafluoroethylene + water.

Initially, a test system of light alcohols + water + n-dodecane was investigated using Gibbs Ensemble Monte Carlo simulations and compared to previous laboratory experiments. This test system was investigated in order to gain expertise in the methodologies and theory behind Monte Carlo simulation, as well as to gain experience with using the necessary software. For this test system, it was found that the TraPPE parameters representing the interactions between the alcohols and the n-dodecane were not adequate and lead to increasing deviations with increasing carbon number in the alcohol.

To replicate the conditions of the amorphous polymer matrix, liquid-liquid equilibrium between water and the polymer was investigated. Gibbs Ensemble Monte Carlo simulations have been performed for systems of perfluoroalkanes and water to determine the influence of temperature and carbon number on the solubility and clustering behaviour of water within the perfluoroalkanes. The temperature range in this study was from 450 K to 600 K, and the perfluoroalkane carbon number range was from 8 to 300 carbon atoms. With increasing carbon number, it was found that there was an asymptotic value of 98.0 mole percent water in the polymer phase. With increasing temperatures it was found that there were exponential increases in solubility of water into the polymer matrix. Previous work on clustering and supramolecular structure of perfluoroalkanes described the rigidity of the perfluoroalkane chains in comparison to alkane chains, thus explaining the large increases in free volume with increasing temperature in the polymer matrix observed in this work. A discontinuity with regard to both solubility and clustering behavior was observed for a polymer carbon number of 10 to 12 carbon atoms. Prior work on the energy contributions towards the helical structure of perfluoroalkanes showed a shift in the energy contribution regime for carbon numbers larger than ~10 carbon atoms, which may explain this discontinuity. It was found that linear water clusters accounted for up to ~90 percent of the water clusters, concurring with previous work on water clustering in polyethylene.

Contents:

List of tables:

Note: The tables in the manuscripts in the appendices are not included in this list.

List of figures:

Note: The figures in the manuscripts in appendices are note included in this list.

Nomenclature:

Latin symbols:

A	Bond angle.
C	The number of chemical species in a system.
c	Torsional potential energy model parameter.
D	Dihedral angle formed between two adjacent pairs of atoms or molecules.
F	The degrees of freedom of a system (thermodynamic).
k	Model parameter.
k_{ij}	Interaction parameter to account for non-idealities between elements “i” and “j”.
l	Bond length.
P	The number of phases in a system.
q	Electrical charge.
r	Intermolecular/interatomic distance.
U	Potential energy.

Greek symbols:

ε	Lennard-Jones parameter describing the potential well depth.
ε_0	The permittivity of free space.
π	The ratio of a circle's circumference to its diameter.
Σ	Denotes a summation of the elements of a series or set.
σ	Lennard-Jones parameter describing the distance at which the potential function equals zero.

Subscripts:

$_{0}$	A rest value at equilibrium.
$_{0, 1, 2, 3, \ldots}$	Subscripted numerical identification of torsional potential energy model parameters.
$_{bend}$	Associated with bond bending.
$_{Coulombic}$	Associated with the Coulombic (electrostatic) potential.
$_{i,j,ii,jj,ij}$	Describes the interactions between the i^{th} and the j^{th} elements.
$_{LJ}$	Associated with the Lennard-Jones potential.
$_{stretch}$	Associated with bond stretching.
$_{torsion}$	Associated with torsion (i.e. dihedral twisting).

CHAPTER 1: INTRODUCTION

In order to predict the interactions of chemical species during the process design stage of any engineering project, it is vital that experimental measurements be undertaken. From such measurements, the desired properties can be measured, and possibly have existing models fitted to them, in order to aid prediction at varied conditions. One shortfall with physical experiments is feasibility, as certain conditions may not be attainable in many laboratories. To this end, molecular simulation can prove useful, since it is not constrained by such physical limitations. Additionally, simulating systems at the molecular level can provide insight that would otherwise be impossible to gain via macroscopic physical experiments.

The work to be described in this project concerned the interactions of polytetrafluoroethylene (PTFE), otherwise known by its DuPont trademarked name Teflon®, with the common industrial solvent water. Molecular studies on these interactions have been lacking in the open literature, and since PTFE is found in many applications, such a study could prove useful. For example, PTFE is already in use in membrane processes; such as fuel cells, as discussed by Lin et al (2005), and osmotic distillation, as discussed by Courel et al (2000). PTFE is also used in many common, everyday applications, such as a hydrophobic coating for frying pans and textiles, and also as a tape used to seal pipe joints. The chemical inertness of PTFE, due to its fluorine sheath, may also make it an attractive material for other applications in the future.

The course that was to be followed in this work was to determine the solubility of water in the perfluoroalkane phase over a range of temperatures and carbon numbers. This would allow for any trends in terms of these variables to be determined, which would be useful for any future design or research work. In addition, the clustering of water molecules in the perfluoroalkane phase would be analyzed, as this would show the behavior of the water at a molecular level. Both of these approaches would be compared to previous work on polyethylene by Johansson and Ahlström (2007) and Johansson et al (2007).

In order to become familiar with molecular simulation procedures and methodologies, a test system was initially measured. This was necessary since molecular simulation did not form any part of

the undergraduate curriculum which was studied prior to this project. The test system chosen was that of light alcohols + water + n-dodecane, namely; methanol + water + n-dodecane at T = 313.14 K and P = 101.325 kPa, and T = 350 K and 400 K and P = 600 kPa, and ethanol/isopropanol + water + n-dodecane at T = 333.15 K and P = 101.325 kPa, and T = 350 K and 400 K and P = 600 kPa. These systems were a continuation and extrapolation of previous work done on light alcohols + water + n-dodecane by Lasich et al (2011). The simulation of such systems would also illustrate the predictive capacity (or lack thereof) of molecular simulation in predicting phase equilibria. It would also allow for comparison with experimental data. This comparison would then allow one to determine whether or not the models used in such simulations should be used in an industrial application. If the simulation models do not provide a close match to the experimental data, then it would illustrate the limitations of said models in industry. It should be noted that some of the temperatures used in the simulations (i.e. 350 K and 400 K) could not be attained using the LLE apparatus in the Thermodynamics Research Unit.

With regard to simulating the systems of water + polymer, an important aspect to note was that water condenses on the sample surface at temperatures greater than ~0.7 T_C, according to Johansson et al (2007). This may be seen to be due to the gravimetric nature of these experiments. The procedures which are followed for such tests are contained within standards such as, for example, ASTM D5229/D5229M-92. This translates to a temperature of approximately 453 K.. Since this is within the temperature range required to form the polymer molecules into an amorphous mass, experimental measurements of water solubility into the polymer would be inaccurate, and thus molecular simulation would be a preferred option.

For the simulations of the solubility of water with perfluorocarbons, the procedure of Johansson et al (2007) was used. This entailed the simulations of a specific carbon number over a wide temperature range, followed by the simulations of of systems of water + perfluoroalkanes. The perfluoroalkanes in these systems contained varied chain lengths. This constant temperature would have to be sufficiently high to result in a LLE situation for all carbon numbers, including the polymers, in order to simulate the amorphous portions of the solid polymer. The amorphous portion of the polymer are more akin to the liquid phase, in that there is no regular structure within it, and thus it is considered to be amorphous. The simulations for variable carbon number at a fixed temperature would illustrate the effect of the molecule size on the solubility of water in the perfluorocarbon. The simulations for varied temperature values at a fixed carbon number would then illustrate what effect temperature would have on the solubility of water in the perfluorocarbon. As illustrated in the work of Johansson and Ahlström (2007) and Johansson et al (2007), the general trend which may be observed in this work would be that of an increase in water solubility in the organic phase with an increase in carbon number. As the solubility of the water is

temperature- and not pressure-dependent, according to Tsonopoulos (1999), one could expect that the solubility determined in this work would greatly increase with temperature, which was also observed in the aforementioned work of Johansson and Ahlström (2007) and Johansson et al (2007).

The importance of analysing the clustering of water molecules within a polymer matrix may be illustrated by work such as that of Johansson (2007). In this study, it was found that clustering of water molecules around charged ions withing the polyethylene (PE) matrix cause degradation of the polymer over time. Therefore, determination of the clustering behaviour of water with respect to temperature and polymer carbon number will then illustrate the possibility or lack thereof of degradation of the polymer with respect to these two variables.

It should be noted that the approach of studying the systems of light alcohols + water + n-dodecane as well as water + perfluoroalkanes/PTFE will inevitably result in two disparate parts to the body of the study presented in this dissertation. However, closer examination may illustrate that these two parts are not entirely dissimilar. Both studies involve the analysis of liquid-liquid equilibria by way of Monte Carlo simulation using the Gibbs ensemble. In addition, both studies involve the use of the same model (i.e. transferrable potentials for phase equilibrium) for alcohols, alkanes and perfluoroalkanes, which illustrates the transferrable nature of this model. Also, two very similar, related models were used for water in these two studies (i.e. simple point charge and simple point charge-extended), illustrating the application of models which, although not identical, are nonetheless intimately related.

CHAPTER 2: THEORETICAL BACKGROUND

2.1 Theoretical considerations:

The theory to be discussed in this chapter is only that which is immediately relevant to the project at hand, such as non-standard algorithms and procedures which were necessary for the project. There were many standard texts to be found on the elementary theory required for this work. For an excellent overview and description of molecular simulation itself, Frenkel & Smit (2001) is a useful text. Smith et al (2005) provides a good discussion of thermodynamic fundamentals and molecular thermodynamics. Haile & Mansoori (1983) also provides a good discussion of molecular thermodynamics, and also delves into some fundamentals of Monte Carlo simulations. Two volumes from the work of Landau and Lifshitz (1980) are also useful as a reference for information regarding statistical mechanics and statistical physics, which are fundamental to molecular simulation. In addition, previous studies from the Thermodynamic Research Unit on molecular simulation can be found in the work of Du Preez (2005), Clifford (2006), McKnight (2006) and Moodley (2008).

2.1.1 Intra- and intermolecular interactions & mixing rules:

To determine the total potential energy of any system of molecules, one needs to account for not only the intermolecular interactions, but also the intramolecular interactions, which can become rather significant as the molecules themselves become larger. The total potential energy is then the sum of the intermolecular and intramolecular components and the electrostatic energy. It should be noted that all of the equations presented below are included within the Transferrable Potentials for Phase Equilibrium-United Atom (TraPPE-UA) model of Martin & Siepmann (1998).

The stretching of inter-atomic bonds results in an associated deformation energy. This is usually modeled by means of a Taylor series centered at the equilibrium bond length;

$$U_{stretch} = U_0 + dU / dl\,(l - l_0) + (1 / 2!)\, d^2U / dl^2\,(l - l_0)^2 + \ldots \qquad \text{Eq. (1)}$$

The base energy, U_0, is usually set to zero, since this is merely a reference point, and internal energy is a relative value. Commonly, terms higher than the quadratic term are ignored, as their contribution to the total stretching potential energy is insignificant. Also, since the change in stretching potential is zero at the natural bond length, the whole series simplifies to a harmonic potential, parameterized by a stretching constant, $k_{stretch}$;

$$U_{stretch} = (k_{stretch}) (l - l_0)^2 \qquad \text{Eq. (2)}$$

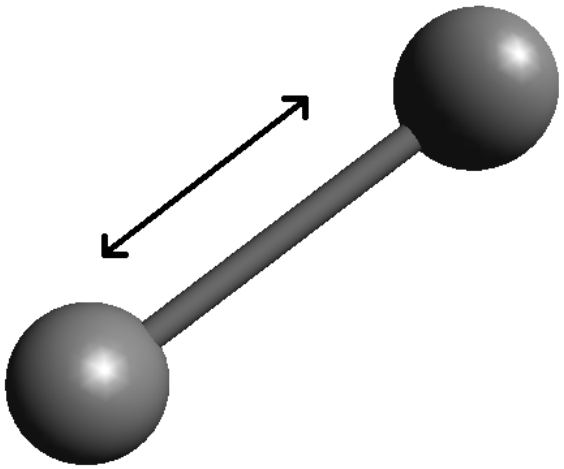

Figure 2-1: Illustration of intramolecular bond stretching.

When a molecule consists of 3 or more atoms or atomic groups, then a bond angle, *A*, naturally forms. While often represented in elementary chemistry texts as a constant value, it is in fact subject to slight variation due to electrostatic interaction as well as the geometry and packing of nearby atoms and molecules. This potential energy is parameterized in a similar manner to the stretching potential energy, using the bending constant, k_{bend}, based upon the rest bond angle, A_0;

$$U_{bend} = (k_{bend}) (A - A_0)^2 \qquad \text{Eq. (3)}$$

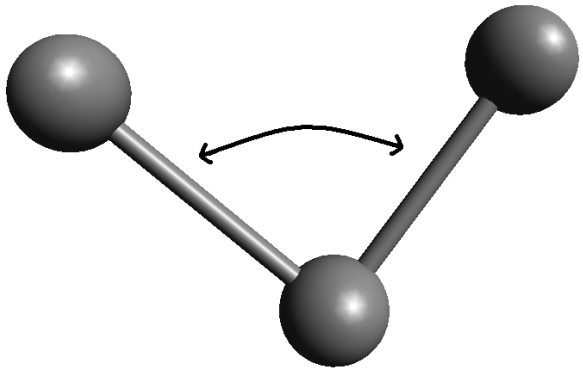

Figure 2-2: Illustration of intramolecular bond bending.

Once a molecule consists of four or more atoms, twisting, or torsional potential energy, comes into play. This torsion is parameterized according to the dihedral angle, D, formed by adjadcent pairs of atoms or atomic groups, usually by means of a cosine series with several parameters, c_i, such as;

$$U_{torsion} = (c_0) + (c_1)\,(1 + \cos[D]) + (c_2)\,(1 - \cos[2D) + (c_3)\,(1 + \cos[3D]) \qquad \text{Eq. (4)}$$

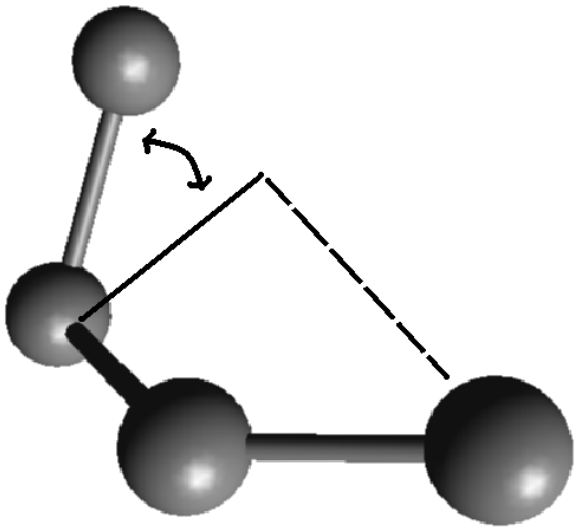

Figure 2-3: Illustration of intramolecular torsion.

However, it is possible for variations in this regard, as there are often several ways to parameterize the torsional potential energy. This is to be seen later on in this work in chapter 2.1.8, where a different functional form of the torsional potential energy was used for perfluorinated alkanes, in the

interests of improved accuracy.

In addition to these aforementioned intramolecular interactions, one should also consider the intermolecular interactions, namely the attractive van der Waals force and the Pauli repulsion. The former of these forces results in a long-range attraction between atoms and molecules, whilst the latter results in repulsion at shorter ranges. The van der Waals attraction is caused by the intermolecular correlation of electrons between atoms. The work of Lennard-Jones (1931) led to the development of a formula to calculate the van der Waals interaction;

$$U_{LJ} = 4\varepsilon_{ij} [(\sigma_{ij} / r_{ij})^{12} - (\sigma_{ij} / r_{ij})^{6}] \qquad \text{Eq. (5)}$$

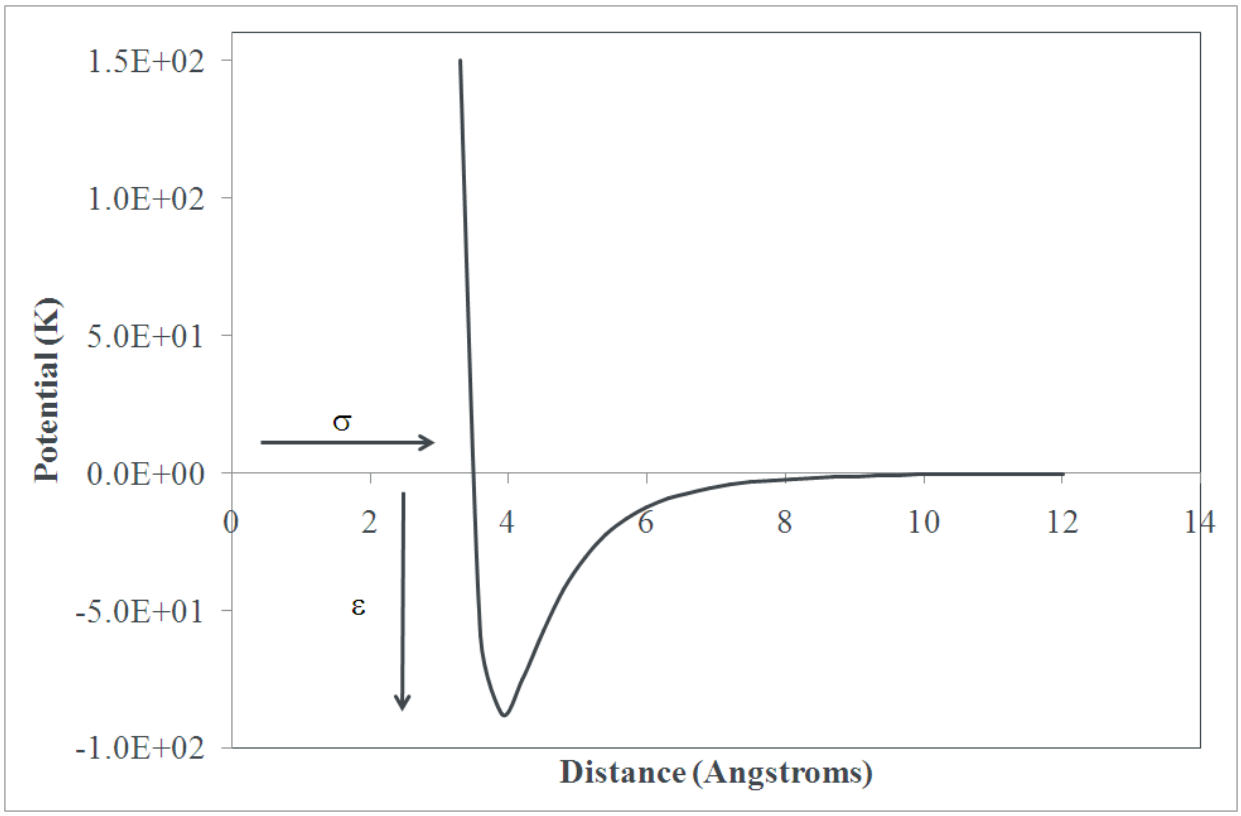

Figure 2-4: Sample graph of the Lennard-Jones potential for the water + methyl pair.

This van der Waals potential is thus the interaction between different Lennard-Jones groups. This formula has been improved upon since 1931, and there are now several more accurate methods for calculating the van der Waals energy, with the iterative exponential-6 model of Buckingham (1938) being a notable example to be found in the fundamental literature.

Calculating the electrostatic interactions is a complex procedure, in which one would use an extension of the same equation used to determine the Coulombic potential energy between two point charges;

$$U_{Coulombic} = q_i q_j / 4\pi\varepsilon_0 r_{ij} \qquad \text{Eq. (6)}$$

However, it is important to note that the relationship presented above in eq. (6) only ever applies to two distinct point charges. In determining the electrostatic interactions between elements of a much larger system, such as in a molecular simulation, the complex Ewald summation is often used. This summation technique accounts for the long-range effects of the Coulombic forces. The long ranges of these forces preclude the use of tail corrections after truncation. This technique has been discussed previously by Ewald (1921) de Leeuw et al. (1980a, 1980b and 1983) and Frenkel and Smit (2002).

One must also consider that the interacting sites between molecules are heterogeneous, and to account for this, mixing rules are used. The well-known Lorentz-Berthelot mixing rules, from the work of Lorentz (1881) and Berthelot (1898), use simple averages to find the cross-term parameters for each i-j pair;

$$\varepsilon_{ij} = (\varepsilon_{ii}\, \varepsilon_{jj})^{0.5} \qquad \text{Eq. (7)}$$

$$\sigma_{ij} = 0.5\, (\sigma_{ii} + \sigma_{jj}) \qquad \text{Eq. (8)}$$

Thus, by use of equations (2) through (8), it becomes apparent that there are clear parameters which need to be specified, such as $k_{stretch}$, c_i, and so forth. It is by choosing a particular model, such as TraPPE-UA (to be discussed further along in chapter 2.1.5), that one would assign values to these parameters, and these parameters form the core of any simulation.

2.1.2 Monte Carlo simulations:

In order to simulate systems of atoms or molecules, there are two primary approaches one can use; Molecular Dynamics (MD) and random sampling, or the Monte Carlo (MC) approach. Molecular dynamics involves the determination of the forces on each molecule due to interactions with other molecules (due to, for example, electrostatics). The magnitudes of these forces are then used to determine

the motion of each molecule over time, according to Newton's laws of motion.

The random sampling approach is different to the MD approach in that the behavior over time of the system is not considered. Instead, the average value of the system's properties for number of different acceptable configurations is determined. Another name for this random sampling approach is the "Monte Carlo" approach, as it relies upon randomly generated numbers and probabilities, much like gambling in a casino. Various changes to the system are performed, at random, and for each change there is a probability to accept each change. The chance to accept these changes depends upon the difference in energy of the new configuration as compared to the old configuration. If the change in energy is above a pre-determined tolerance, the move is rejected. In this way, a statistical average across many states can be determined. Since chemical and phase equilibria are dependent upon energy and not upon time, this approach of using statistical averages may be more efficient than using time averages. In addition, the data produced by an MD simulation (i.e. molecular positions and velocities) are not directly comparable with laboratory experiments, in which such data is generally not known. This statistical averaging also overcomes the problem of the amount of time which may be required for a system to reach equilibrium, which may be computationally expensive.

2.1.3 Ensembles:

In molecular simulations there are several ensembles which are possible; a few examples of which are the canonical, isobaric-isothermal and grand-canonical ensembles. The canonical ensemble (also known as the standard ensemble) was used in the very first Monte Carlo simulations by Metropolis et al (1953), and involves fixing the total number of molecules (N), the system volume (V) and the system temperature (T) – hence its abbreviated designation as the “NVT” ensemble. In this ensemble, only molecule displacements are allowed, both in terms of translation and orientation of the molecules.

In the isobaric-isothermal (“NPT”) ensemble, as the name suggests, the system pressure (P) and temperature (T) are maintained at a constant specified value, along with the total number of molecules in the system (N). In this type of simulation, translation/rotation is still allowed, but in addition, so are volume fluctuations. NPT simulations have a greater flexibility that NVT simulations, and also mimic the behavior of physical laboratory experiments, in which pressure and temperature are frequently the controlled variables (the total number of molecules in an experiment should not change much either, unless the apparatus is leaking).

The third type of ensemble mentioned above, the grand-canonical (μVT) ensemble, maintains the

total chemical potential (μ) of the system within a fixed volume (V) and at a fixed temperature (T). In such a simulation, molecules' displacements are permitted moves, along with molecular insertions into the enclosed system volume in which the chemical potential is being monitored. This type of simulation is not suitable for phase equilibrium analysis and is instead used when analyzing adsorption, according to Frenkel & Smit (2001).

2.1.4 The Gibbs ensemble:

The Monte Carlo simulation method used in this work was that of the Gibbs ensemble method of Panagiotopoulos (1987). A major hurdle in molecular simulations is the effect of interfacial surfaces. Molecular simulations are often considered small systems, due to the presence of 10^2 to 10^3 molecules in the system. Due to this small size, a high percentage of molecules will lie on the exterior boundary or surface of a system in space. This is easily illustrated when considering the surface area to volume ratio of a droplet of water as compared to the same ratio for a swimming pool. In this way, the bulk properties of a system are impossible to determine with any certainty, due to such a small percentage of molecules in the system not being involved in surface interactions. The Gibbs Ensemble eliminates this problem by removing the physical exterior boundaries of the system. The Gibbs ensemble reduces a system to a set of “boxes”, each containing only the bulk material of each interacting phase. These two (or more) boxes are “connected” via the possibility to transfer particles from one phase to another. Thus the interfacial surface area has been functionally replaced by an action to either or all of the relevant phases.

In order to replicate the natural motion and rearrangement occurring inside each phase, there are then three fundamental types of “moves” which are allowed to occur in the system, namely:

1. Volume change to one or any combination of the two phases,

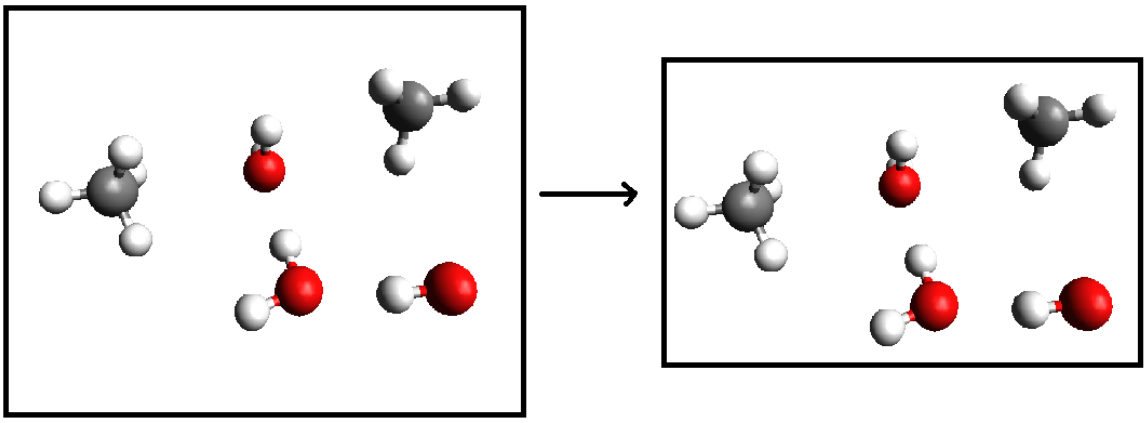

Figure 2-5: Illustration of MC volume change.

2. Particle translation/rotation within each phase,

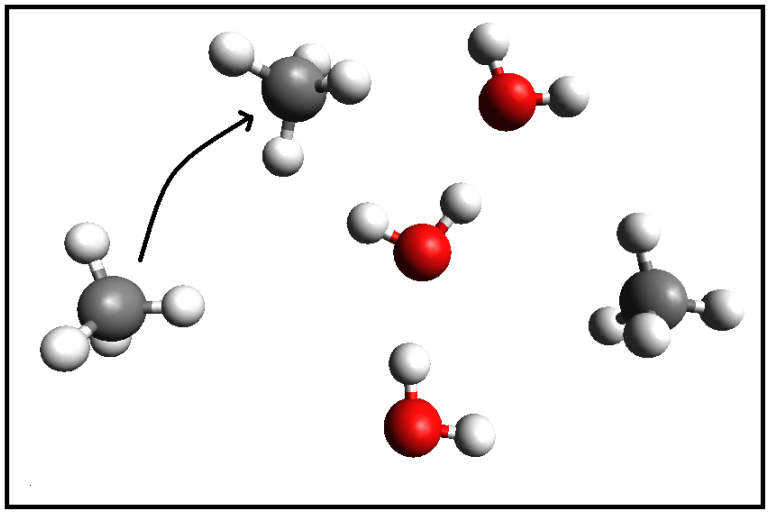

Figure 2-6: Illustration of MC translation/rotation.

3. Particle exchange between each phase (as described previously).

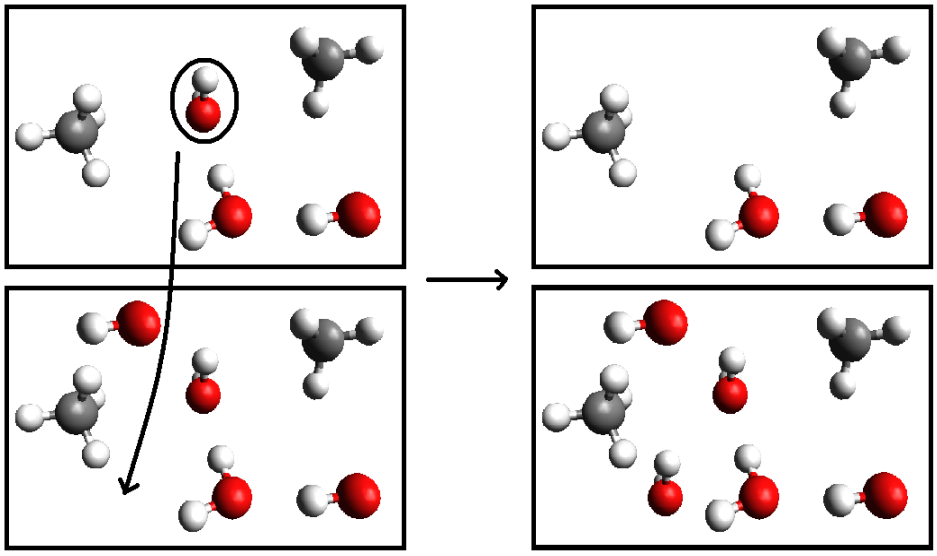

Figure 2-7: Illustration of MC particle exchange.

As was discussed by Gubbins (1993), the first of these moves is to attain mechanical equilibrium, the second is to attain internal equilibrium, and the third is to attain chemical equilibrium.

The primary drawback of the Gibbs ensemble, as was discussed by both Gubbins (1993), and Johansson (2007), has to do with the acceptance rate of the third type of move if the system is not at a sufficiently low density or if the constituent molecules are very large. If the molecules are large and relatively closely packed, then there are unlikely to be sufficiently large enough voids in that phase for molecules to be inserted without producing a large change in the internal energy of the phase. Such a large change in internal energy would not be accepted, and thus the move would not be accepted. It is this drawback that ultimately limits the use of the Gibbs ensemble at low temperatures and with very large molecules, as such simulations would take impractically long periods of time to generate sufficiently good statistics. It should also be noted that the density or packing of a system of molecules is significantly affected by the system temperature, as discussed by both Landau & Lifshitz (1980) and Tsonopoulos (1999).

2.1.5 Configurational bias Monte Carlo (CBMC):

A problem which would be encountered in simulations involving large, complex molecules would be that of a high probability of rejection in the insertion or displacement of such large molecules. This would be due to the fact that the acceptance of the displacement of an entire molecule would depend on the unanimous acceptance of the displacement of all of its constituent pseudo-atoms. This would then result in a computationally expensive simulation scenario. To surmount this obstacle, the configurational-bias method was introduced into simulations by Siepmann (1990). This method itself was not entirely new and was based upon prior work on a lattice-based method by Rosenbluth & Rosenbluth (1955). In essence, this method entails the construction of each molecule, atom-by-atom. The acceptance or rejection of each atomic insertion is then determined. If an atom is rejected, another random but feasible location is determined for the insertion. The comparison for this insertion is based upon the Rosenbluth weights of each of the previous configuration and the new "trial" configuration of a particular molecule. The Rosenbluth weights are determined using the intermolecular energy of each of the configurations. Each atom is then inserted into the region of space that is most energy-favorable in such a way that the entire molecule is "grown" atom-by-atom.

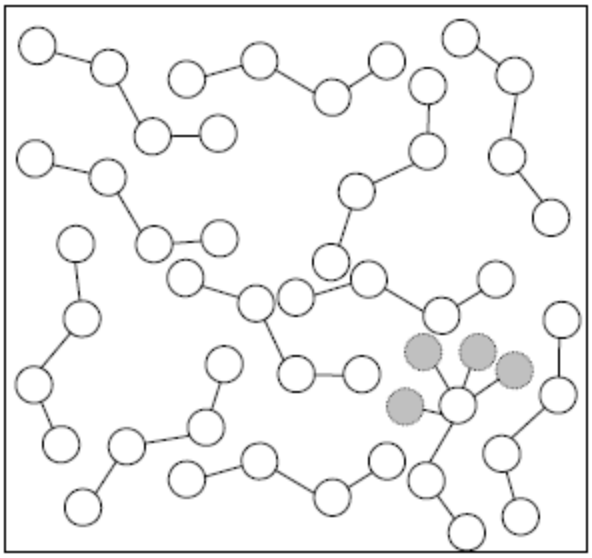

Figure 2-8: Illustration of the configurational-bias approach. To complete the growth of the molecule, the most energy-favorable position is chosen. Image taken from Moodley (2008).

2.1.6 The united-atom approach:

The TraPPE-UA model for linear alkanes, developed by Martin and Siepmann (1998), was used in this work to represent all of the test system species excluding water. A different model was used to describe water, which is described in chapter 2.1.7. The TraPPE-UA model approximates complex molecules as strings of Lennard-Jones functional groups. For example, n-hexane would be broken down into two CH_3 groups and four CH_2 groups. This methodology greatly decreases computational complexity and calculation time, since not every single atom is handled individually, and instead groupings of atoms are handled as pseudo-atoms. The TraPPE-UA model is easily used to account for all of the intramolecular interactions for a variety of molecule types. It is important to note that the TraPPE-UA model was not used to account for the torsional potential energy of the perfluorocarbons handled in this work. The torsional potential model used for the perfluorocarbons was of a different mathematical form to the standard TraPPE-UA. It was shown by Cui et al (1998) to yield a difference of less than 5 percent to experimental density measurements.

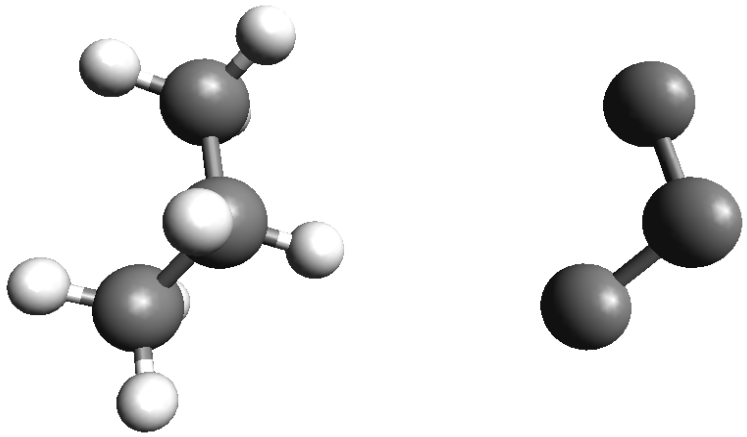

Figure 2-9: Illustration of the united atom approach. N-propane is shown on the left with explicit hydrogen atoms, on the right as three methyl pseudo-atoms.

What should also be noted about models used for representing molecules in simulations is that there are many models in existence, and not just the TraPPE-UA model. An advantage of the TraPPE-UA model was that it rigorously accounted for all of the possible motions and interactions of the atoms or pseudo-atoms in a molecule, whereas many other models are not as rigorous. Rigorous in this context refers to the types of behavior that are accounted for; that is, stretching, bending, and so forth. Also, the TraPPE model is intended to be transferrable; that is, it is not specific to a particular species and can be used rather generally. A further reason for using the TraPPE-UA model was that since the previous work

on polyethylene, which was to be used as a comparison for this work, was performed using this approach, the same methodologies should be followed as much as possible in order to draw a direct comparison. An example of a different model, for n-alkanes, was that of Weber (1978) and Ryckaert & Bellemans (1975), in a combined form, as presented by Haile and Mansoori (1983).

2.1.7 Water models:

There are over 100 models in existence which have been used to describe the water molecule, although only two very popular models will be discussed here. The models which were used to represent water in these molecular simulations were the Simple Point Charge (SPC) and the Simple Point Charge-Extended (SPC-E) models. The SPC force field was initially developed by Berendsen et al (1981), and then reparametrized by Berendsen et al (1987) to develop the SPC-E model. The SPC-E model is generally preferred for saturated liquid density measurements, whilst the SPC model is preferred for saturated vapor pressure measurements, according to Boulougouris et al (1998). Johansson (2007) showed that the SPC model also provides a closer match between simulated and experimental vapor densities at low temperatures.

The SPC water model describes the water molecule as consisting of a single Lennard-Jones site and 3 electrostatic sites. The single Lennard-Jones site contains all of the atoms constituting the water molecule (i.e. the oxygen atom and the 2 hydrogen atoms). The 3 electrostatic sites are located to mimicking the actual locations of the oxygen atom and the hydrogen atoms within this single pseudo-atom,

The SPC-E water model is fairly similar to the SPC water model. The key difference being that the SPC-E water model possesses a large dipole moment than the SPC water model. This is effected by differences in the values of the charges on the electrostatic sites as compared to the SPC water model. This may be seen in tables A-1-1 and A-1-2 in the appendix to this work. The SPC-E water model was found to better represent the liquid phase as compared to the SPC water model. However, the SPC-E water model provided a poorer description of the vapour phase as compared to the SPC water model.

For the test system in this work, the only criterion to consider when selecting a water model was the degree of previous simulations' accuracy with regard to the water-alkane interactions. In this case, the work of Johansson (2007) showed that the SPC model gave significantly closer fits to experimental solubility measurements than the SPC-E model for the system of water + n-decane.

For the study involving perfluorinated alkanes and water, a different criterion was important, namely the critical temperature of the water which was predicted by the chosen water model. This was the deciding factor, since the simulations may have to occur at up to 600 K, according to DuPont (2006), in

order to liquefy the PTFE molecules. It was then apparent that only the SPC-E model would satisfy this criterion, since the work of Boulougouris et al (1998) showed that the critical temperature of the SPC model ranged between 587 and 596 K, whilst also showing that the critical temperature of the SPC-E model was between 630 and 640 K. It may also be noted that the SPC-E model agrees more closely with the experimental critical temperature of 647.3 K for water.

2.1.8 Torsional potential energy of perfluoroalkanes:

A slight departure from standard simulations was encountered when dealing with perfluoroalkanes. This departure was to be found in the parametrizing of the torsional potential energy of perfluoroalkanes. Usually, the 4 parameter TraPPE-UA torsion potential model is sufficient, and was in fact used in the test system in this work. The relevant TraPPE-UA model equation is of the form presented by eq. (4). For perfluoroalkanes, this model is less accurate at determining the torsional potential energy, as discussed by Cui et al (1998). Instead, the torsion potential model of Cui et al (1998) was used. This model has the form:

$$U_{torsion} = \Sigma\{(c_i)\cos^i[D]\}, \text{ for } i = [0, 7] \qquad \text{Eq. (9)}$$

This potential is similar in form to the alkane torsional potential from the work of Karayiannis et al (2002), although with 7 parameters instead of the 8 parameters of the aforementioned "Karayiannis model". A further discussion of the use of the Cui model used in this work was presented by Zhang & Siepmann (2005), along with adjusted parameters which resulted in improved correlation with experimental measurements.

2.1.9 Boundary conditions and cut-off radius:

The original Gibbs ensemble program used in this work employed the method of periodic boundary conditions and minimum image convention. This topic was discussed in great detail by Frenkel & Smit (2001). Essentially, this method requires that an interacting molecule must not interact with any molecules which are situated outside of a box which is of the same size as the simulation box, but is centered at the interacting site itself. To generate the other “virtual” molecule co-ordinates, the simulation box is repeated once in every direction surrounding the box. What is important to note about this method

is that no molecule must interact with its periodic image, or with two periodic images of the same molecule, since this would result in the introduction of an artificial periodicity to the system, according to Allen and Tildesley (1987). This periodicity would result in an ordered system, as opposed to a random system. The ordering of such a system would invalidate the intended statistical analysis on such a system, as the sample would not be random.

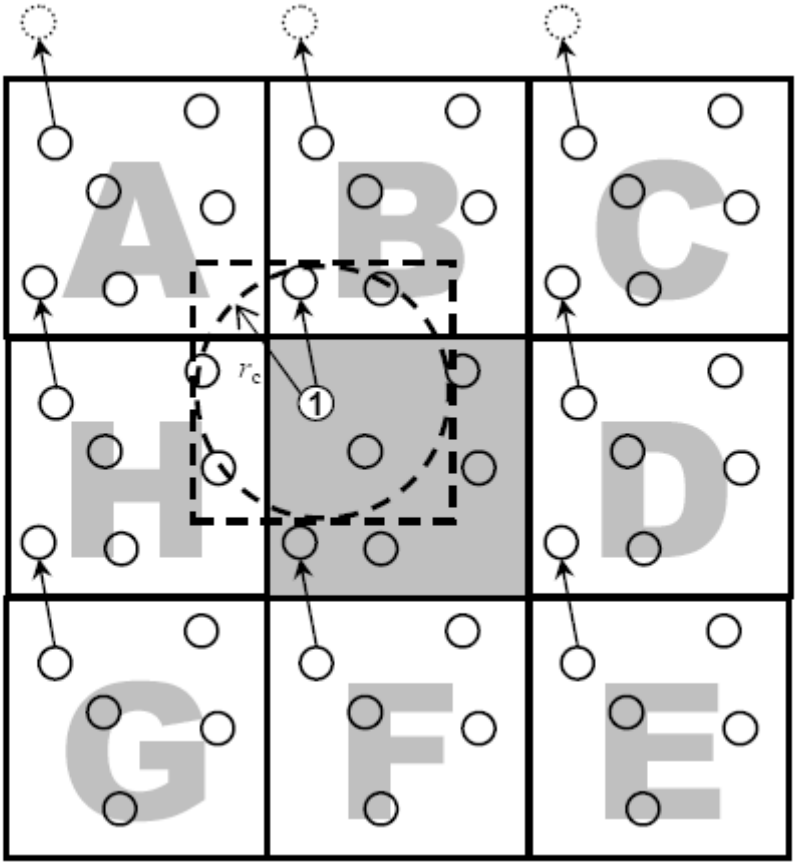

Figure 2-10: Illustration of periodic boundary conditions for a 2-D system. From Allen & Tildesley (1987).

In the modified form of the Gibbs ensemble program used in this work, a cut-off radius was used to speed up computations. To calculate the total interaction from all of the molecules on one particular molecule, there would be two separate summations which should occur. The summations considered would be for the total van der Waals contribution and the total electrostatic contribution. To determine the total van der Waals contribution, the contribution from within the box being analyzed is taken into account, up to a certain cut-off radius. This cut-off radius would need to be less than half of the length of the cubic box's side, in order to avoid periodicity errors. In order to account for interactions from molecules outside the cut-off radius, intermolecular interactions would be truncated using an analytical tail correction which assumes that the number density outside the cut-off radius is the same as the inside,

according to Frenkel & Smit (2001). This tail correction can be used only for the van der Waals interactions, due to the short ranges of these interactions. In order to determine the total contribution from the electrostatic interactions, a tail correction cannot be used, since Coulombic forces act over a much longer range than van der Waals forces. Thus, a different summation technique would be used, of which there are many varieties. The most commonly used, and the method which was used in the programs relevant to this work, is the Ewald summation, which was discussed in great detail by Frenkel & Smit (2001). The reason the Ewald summation was used was due to its high accuracy, according to Frenkel and Smit (2001). What was important to note about this algorithm, however, is that it actually uses up most of the processor time during computations, and would thus be the rate-limiting step in molecular simulation, as it can use up to 90 % of the CPU time, according to Johansson (2007). Therefore, this increased accuracy comes with the attached cost of increased computation time.

2.1.10 Polymer configuration:

In order to generate the initial co-ordinates of the PTFE molecules to be used in the polymer simulations a program was written in the open source interpreted scripting language Python. This language was chosen as it was compatible across different platforms. Since it was an open source language, a Python interpreter was easily available on many systems or online, and comes standard with the popular Ubuntu operating system.

The accuracy of the initial positions for the pseudo-atoms was found to be of great importance when a simple test was conducted. In this situation, the polymer program crashed, and thus it was concluded that the bond lengths needed to be accurate to approximately 10^{-11} Ångströms for the polymer simulations to commence. This was due to the precision of the stored variables used in the polymer program itself.

The program operated by utilizing the initial co-ordinates of a 4-atom PTFE chain. These co-ordinates were determined by the free molecular modeling program Avogadro (see references), and were then adjusted to the desired precision. This adjustment was undertaken by incrementally increasing or decreasing the Cartesian co-ordinate values of each pseudo-atom in turn until the bond lengths were of the required precision. This unit was then repeated within a "box" of specified dimensions. The 1st atom in each unit was placed using randomly generated numbers, scaled by the length of the cubic box's side. Relative to the 1st of these 4 atoms, the position of the other 3 atoms was determined. The direction of each modular addition was determined by means of random number generation using the Python module

"random". Alternatively, there was also an option to generate completely linear molecules, in which case the direction would only be chosen for the initial addition of atoms. Once the direction had been determined, the next 3 atoms would be added. Each set of 3 atoms would then be added onto the 4^{th} atom of the preceding unit. This procedure was then repeated for every molecule. Once each molecule had been generated, it would then be checked for overlaps with the preceding molecules, as well as a check for whether or not the molecule lay within the specified enclosed cubic space. Overlap checking was performed using all of the co-ordinates generated thus far, with a user-specified minimum distance, which in the case of this work, was set to be the bond length of each CF_2 group, as this would ensure a decent spread of PTFE molecules throughout the cubic box. The reason for performing checks on a molecule-by-molecule basis was that the density of the polymer melt was expected to be low (~100 kg/m^3 or less), according to the work of Johansson (2007). Therefore, one would expect the probability of rejection of a new molecule to be fairly low, and thus the total computation time should be faster than if checks were performed on an atom-by-atom basis.

2.1.11 PTFE structural considerations:

In order to determine the solubility of water within a polymer such as PTFE, it is important to know what form the polymer exists as. PTFE exist primarily in two forms: amorphous and crystalline. The amorphous PFTE is sold as granules, and is the form in which PTFE is produced industrially before it is applied to a particular surface, according to DuPont (2007). PTFE takes on its crystalline form once it has been applied to a surface or molded into a particular shape. However, what is of great importance to note is that any polymeric structure does not simply consist of either one phase or the other, and is always a combination of the two phases. This is where the degree of crystallinity of the polymer becomes important, as discussed by Gedde (1995).

It is of key importance to know which form of the polymer will be taking part in the simulation, as this can drastically alter the nature of the simulation to be undertaken. According to the aforementioned work of Gedde (1995), during the formation of a solid polymer mass, crystals of the polymer form around nucleation sites. This results in a structure consisting of crystalline nodules surrounded by amorphous material. This structure is due to the manner in which a crystalline polymer is formed, as described by Gedde (1995) and Johansson (2007). During crystallization, crystals form at different locations upon cooling. The radius of gyration of the polymer chains does not change during this crystallization process, and the chains are folded locally along with other chains. These localized folded regions form the polymer crystals. The unfolded regions forming the packing in between these crystals then forms the

amorphous portion of the polymer. The MD work of Pal et al (2005) illustrated that water molecules cannot diffuse through the crystals themselves. Therefore, the phase of interest was the amorphous phase in between the polymer crystals. Thus, it was necessary to perform solubility analysis on the PTFE at a temperature above its melting point of ~600 K, according to DuPont (2006), in order to form the PTFE into an amorphous mass. This was the same method followed by Johansson et al (2007). The complication here would be the issue of the water vaporizing, and thus pressures would be needed which would keep the water in liquid form. The pressure necessary to maintain water as a liquid at 600 K would be far greater than atmospheric pressure, although atmospheric pressure would be most desirable from a practical standpoint. What is important here then is the work of Tsonopoulos (1999) which showed that the solubility of water in linear non-polar alkanes was not significantly pressure-dependent. Since the perfluoroalkanes to be examined in this work are also non-polar, a similar pressure dependency would be expected.

2.1.12 Monte Carlo simulations of polymers:

In considering the simulations involving the polymers, there were a number of different Monte Carlo moves to be considered which differed slightly from the Gibbs ensemble moves mentioned in chapter 2.1.4. The different types of Monte Carlo moves which were used were reptation, end mer rotation, monomer flip, dimer flip, and end-bridging. As was done with the Gibbs ensemble program, fluctuations to the box volume were also allowed. Brief descriptions of each type of polymer-specific move can be found below;

(i). Reptation – An atom is removed from one end of a polymer chain, and then added to the opposite end of said chain. This procedure emulates the snake-like movement of long molecules in the liquid state.

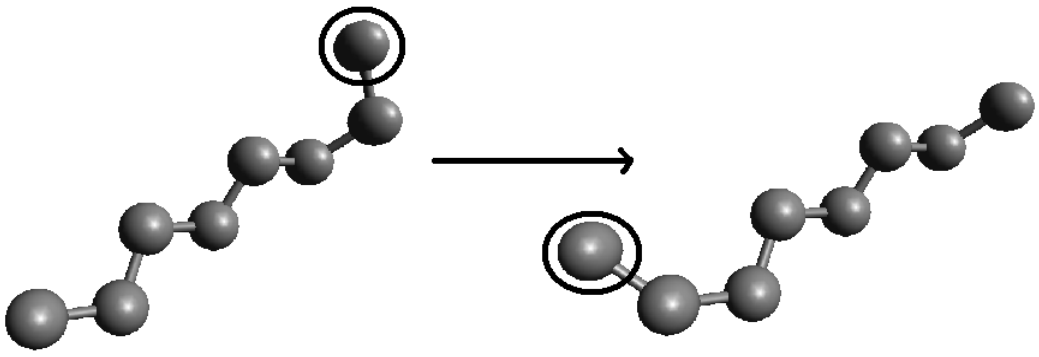

Figure 2-11: Illustration of the reptation polymer MC move.

(ii) End mer rotation – The last atom in a polymer chain is rotated about the axis formed by the second- and third-to-last atoms in the chain. This procedure emulates the gyration of the end pseudo-atoms of long polymer molecules.

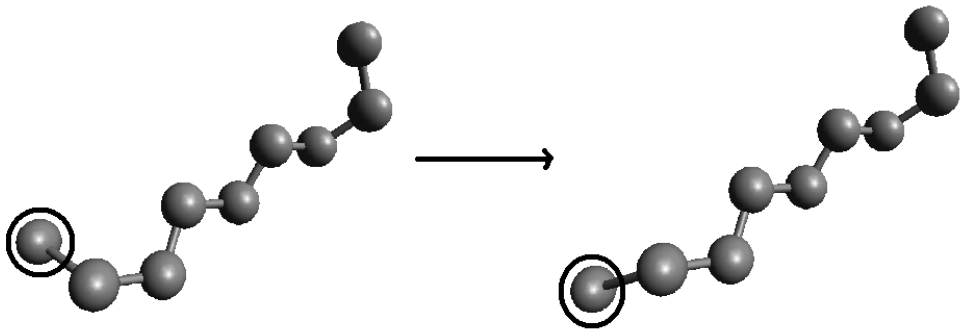

Figure 2-12: Illustration of the end-mer rotation polymer MC move.

(iii) Monomer flip – An atom in the chain is spun about the axis formed by the atoms adjacent to it. This procedure emulates the gyration of a single pseudo-atom about the central axis of the long polymer molecule.

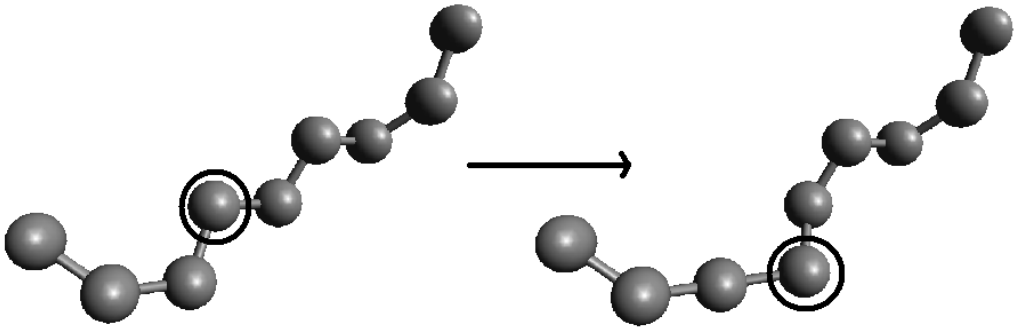

Figure 2-13: Illustration of the monomer flip polymer MC move.

(iv) Dimer flip – The same procedure as for monomer flip, but performed on a pair of neighboring atoms instead of a single atom. This procedure emulates the gyration of an adjacent pair of pseudo-atoms about the central axis of the long polymer molecule.

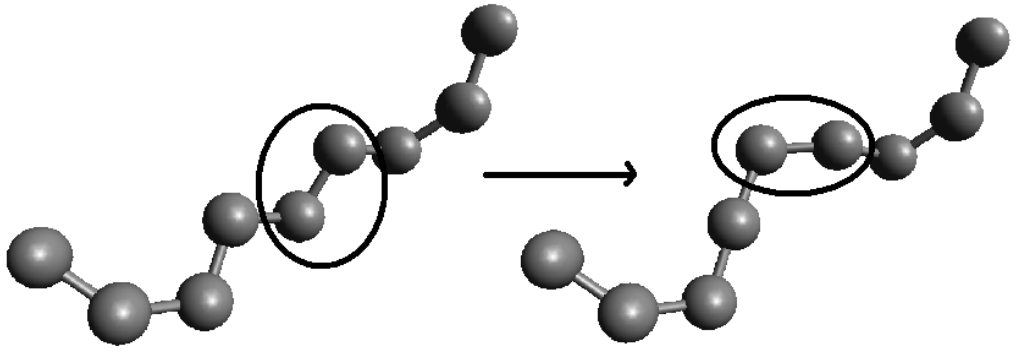

Figure 2-14: Illustration of the dimer flip polymer MC move.

(v) End-bridging – This is a highly important move to consider when performing polymer simulations, as it used in a situation where configurational bias methods would not be feasible. This difficulty would arise due to the greater length of the molecules, as compared to those handled by the Gibbs ensemble. If one had to use configurational bias Monte Carlo instead of end-bridging for polymer simulations, the simulations would be several orders of magnitude more costly in terms of computational time required. This issue was discussed by Mavrantzas et al (1999). The essence of the end-bridging algorithm is the separation of one end of a trimer from one chain, and the reconnection of the free end of the detached trimer onto an interior atom of a nearby chain from which an attempt to remove atoms is being made. The lengths of all of the chains concerned would change. Thus, in order to maintain the same number of chains throughout the simulation, an upper and lower bound for the length of the polymer chains were set. The mean carbon number of all of the chains would thus be halfway between the bounds. For this work a variance of 50% of the mean length was used to determine the bounds. The condition for this move to be performed must be that the distance between the two molecules at this point in space must be shorter than the distance that the proposed trimer can bridge. As long as this criterion is satisfied, there will always be a geometric solution, and thus the new configuration can be determined. End-bridging was discussed in further detail by Pant & Theodorou (1995). The end-bridging procedure essentially emulates the translational movement of long polymeric molecules.

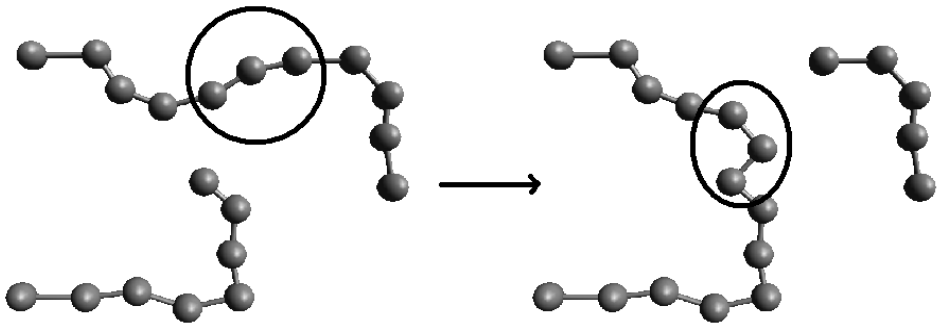

Figure 2-15: Illustration of the end-bridging polymer MC move.

2.1.13 Cluster definitions:

The definition of a water cluster may significantly influence the results obtained from any cluster analysis. Therefore, it is important to describe the definitions to be used in this study. Some definitions used in the literature may take into account either intermolecular distances or intermolecular energy, or both. The earliest definition, a purely distance-based criterion of an intermolecular distance of 3.8 Å (for example), was by Stillinger (1963). The cluster definition used in this work was that proposed by Kalinichev & Bass (1997). This definition made use of dual intermolecular distance and intermolecular energy criteria of < 2.4 Å and < - 10 kJ/mol respectively. This cluster definition has been used in a previous study on the polyethylene + water system by Johansson (2007).

2.1.14 Radial distribution function:

In the course of molecular simulations, it may be important to examine the radial distribution function (RDF). This function is the variation of the atomic (or molecular) density with distance from a particular atom (or pseudo-atom). The values of this function may be acquired through the co-ordinates of the pseudo-atoms or molecules stored during a Monte Carlo simulation. Examination of this data may then reveal more information about the molecular system in question. A useful text on this matter is Widom (2002).

2.2 Literature data:

Previous experimental measurements of light alcohols + water + n-dodecane were conducted within the Thermodynamics Research Unit to which the simulations in this work could be compared to. Data on the systems of perfluoroalkanes + water were found to be scarce in the open literature, and any sources of relevance, even not immediately so, are discussed following.

2.2.1 Previous experiments:

With regard to the test system, there existed prior work by Bhownath (2008) and Kontogeorgis et al (1999). The work in both of these prior projects resulted in LLE data for light alcohols + water + alkanes which was to be used for comparison. Additionally, the work of Bhownath (2008) was directly tied into the bulk of the reference experimental data used in this project in the form of the work by Lasich et al (2011).

Experimental measurements on the solubility of water in n-heptane and various perflouro- and fluorocompounds were undertaken by Freire et al (2006), (2010). These results yielded an observed solubility of water in perfluorinated alkanes of between ~1.88 x 10^{-2} and ~12.0 x 10^{-2} mole percent, over a temperature range of 288.15 K to 318.15 K and a carbon number of from 6 to 10 carbon atoms. While this data is not at the same temperatures examined in this work, it may still be useful is one considers this work as an extrapolation, via simulation, of solubility measurements towards higher temperatures. The results of the relevant study have been provided following.

T/K	C_7H_{16} $10^4(x \pm \sigma^a)$	C_6F_{14} $10^4(x \pm \sigma^a)$	C_7F_{16} $10^4(x \pm \sigma^a)$	C_8F_{18} $10^4(x \pm \sigma^a)$	C_9F_{20} $10^4(x \pm \sigma^a)$
288.15	2.9 ± 0.1	1.88 ± 0.06	2.23 ± 0.05	2.27 ± 0.06	2.53 ± 0.08
293.15	3.84 ± 0.08	2.46 ± 0.04	2.8 ± 0.1	3.1 ± 0.1	3.3 ± 0.1
298.15	4.96 ± 0.04	3.10 ± 0.07	3.8 ± 0.1	4.0 ± 0.2	4.51 ± 0.04
303.15	6.2 ± 0.1	4.4 ± 0.3	4.7 ± 0.1	5.0 ± 0.3	5.4 ± 0.3
308.15	7.80 ± 0.06	5.4 ± 0.1	6.4 ± 0.1	6.8± 0.1	7.41 ± 0.06
313.15	9.3 ± 0.2	7.3 ± 0.4	7.9 ± 0.2	8.2 ± 0.3	9.6 ± 0.4
318.15	11.5 ± 0.1	8.4 ± 0.4	10.2 ± 0.5	11.0 ± 0.3	12.0 ± 0.4

Table 2-1: Table of water solubility in n-heptane and various perfluoroalkanes as a function of temperature. The solubility values are in mole fraction. The data is from Freire et al (2006).

There also existed previous experimental work on the solubility of water in polyethylene, namely

the work of McCall et al (1984). In this work it was shown that the solubility of water in the polymer was of the order of 10^1 to 10^2 parts per million.

Testing of water absorption of PTFE according to German standards, namely DIN 53495, has resulted in less than 0.01 % absorption of water into the polymer, according to ElringKlinger (see references). The same result was obtained using the American ASTM standard D570, according to Omega Engineering (2010). What should be noted for these experimental measurements is that they were performed for the bulk polymer, not for the purely amorphous phase. The "bulk polymer" is the entirety of the polymer material, including both crystals and the amorphous material in between the crystals. The "amorphous phase" is the amorphous portions of the polymer material in between the polymer crystals. Thus, these values must be adjusted to account for the lack of water within the impermeable crystalline phase within the polymer. The work on PTFE crystallinity of Lennert et al (1996) and Rae & Dattelbaum (2004) was used in conjunction with the data presented by DuPont on their PTFE products (see references) in order to perform the aforementioned adjustment. This adjusted value was then used to compare to the results of the simulations of the polymers.

With regard to the internal structure of PTFE, there existed previous work involving positron decay to determine the average hole size in polymer matrices. Dlubek et al (1998) used this positron decay technique to investigate the size of holes in both PE and PTFE. In this work, it was found that the average holes in the PTFE matrix were roughly double the volume of those found in PE.

2.2.2 Previous simulations:

Previous simulation work of the nature in this project was also found to be lacking in the open literature. There exists work by Johansson & Ahlström (2007) and Johansson et al (2007) on influence of temperature and carbon number on the solubility of water in linear alkanes and polyethylene. In this aforementioned work it was found that, on a mass basis, the solubility of water in linear hydrocarbon chains was asymptotic with carbon number, with a leveling-off occurring with carbon numbers greater than ~16 carbon atoms. It was also found that the solubility of water in linear hydrocarbons increased exponentially with temperature, with significant increases in solubility once the temperature reached values greater than approximately 450 K. Similar data was also to be found in the work of Johansson (2007).

There existed a wealth of data on the subject of normal alkanes and water, and there was even data on perfluorinated alkanes. Excellent data on the former subject can be found in the work of

Boulougouris et al (2000) and Tsonopoulos (1999), and also in the aforementioned work of Johansson et al (2007) and Johansson (2007). Cui et al (1998) and Zhang & Siepmann (2005) have dealt with the latter subject, although the only data of relevance in their work were the liquid densities of the perfluorinated alkanes and the new torsional parameters. Of this data, the torsional parameters of Zhang & Siepmann (2005) were used in this work for the perfluorinated alkanes and the PTFE. The Lennard-Jones parameters used in this work were those used by Cui et al (1998), which were unmodified by a review of the models concerned as undertaken by Zhang & Siepmann (2005).

There was also work by Pal et al (2005) on the MD simulation of the interactions of water with the surface of perfluorinated alkane crystal bodies, in which it was found that water did not penetrate the crystal body, and did not even adhere strongly to the surface of the crystal, due to aforementioned hydrophobic nature of such perfluorinated alkanes, as discussed by Courel et al (2000). The results of Pal et al (2005) yielded a concentration of water adjacent to the surface of the crystal of less than ~0.3 g/cm^3. It was also found that immediately beyond this surface layer, intermediate between the surface and the bulk liquid, there was a layer in which the concentration of water was between ~1.3 and ~1.9 g/cm^3. This can be compared to the bulk concentration of between ~0.7 to ~1.1 g/cm^3 (which was approximately the expected density of liquid water, ~1 g/cm^3). In holes which were generated on the surface of the solid in the work of Pal et al (2005), it was found that the surface layer of extremely low water concentrations became thicker along the insides of the hole when compared to the surface of the surrounding crystal. This information would of course be of great use once a practical design of any PTFE structure to be used in water treatment is begun.

An MD clustering study on alkanes and perfluoroalkanes was conducted by Friedemann et al (2001) on decane and eicosane and the perfluorinated forms of both of those species respectively. Friedemann et al (2001) found that there was greater rigidity in the perfluorinated alkanes, and that there was also greater supramolecular ordering as compared to alkanes under identical conditions.

A computational study on the source of helicity in perfluoroalkanes was conducted by Jang et al (2003). The various energy contributions towards the helical molecular structure of perfluoroalkanes was investigated by Jang et al (2003), and the influence of parameters such as torsional angle, temperature and carbon number were determined. It can be inferred from the data that there was a change in the energy contribution regime at a carbon number of ~10, with perfluoroalkanes longer than 10 carbon atoms possibly following a different molecular structuring regime than those smaller than and equal to 10 carbon atoms in length.

CHAPTER 3: HARDWARE AND SOFTWARE CONSIDERATIONS

3.1 Beowulf clusters:

A Beowulf Cluster consists of several computer processors running in parallel, such that as a group, they can accomplish many tasks simultaneously. This is accomplished by assigning jobs to each processor by using a central “master” processor. The individual processors are connected via an internal network in order to facilitate communication. Each processor plus its attached connection is referred to as a “node”. Interfacing with the cluster as a whole is undertaken via the master node. These computers are to be commodity hardware if the supercomputer is to be considered as a Beowulf-class cluster. There are a plethora of websites and the like which can provide details of the inner workings of such clusters, with a few extremely useful sources being Swendson (2004), Jain (2006) and Hurst (2000). Hurst (2000) discussed the installation of a cluster, complete with photographs of the setup procedure. The other two sources mentioned above provided detailed descriptions of clusters, along with relevant definitions and more detailed explanations, albeit in a less graphical form than Hurst (2000). Adams (2007) also provided details on a variation on the Beowulf cluster: Microwulf. This was an attempt at producing a more portable cluster, and while not particularly relevant to this project, was interesting nonetheless, and may provide ideas for future projects.

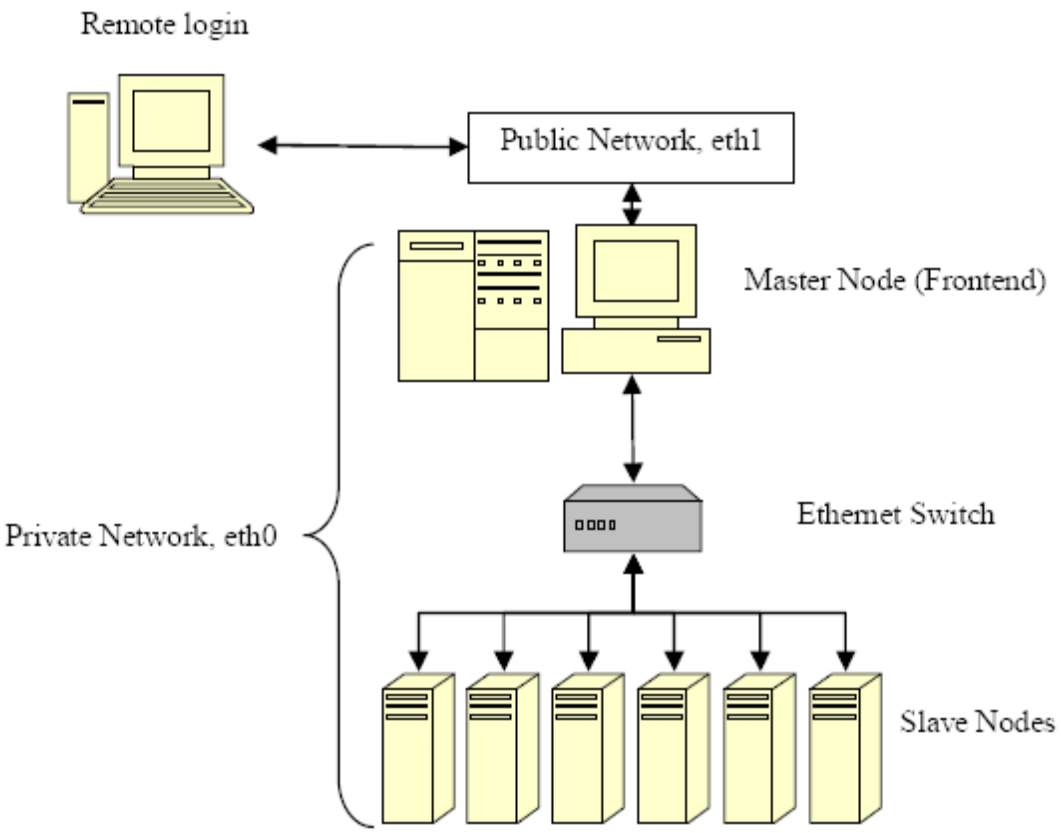

Figure 3-1: Schematic of a Beowulf cluster. From Moodley (2008).

As far as this project was concerned, the clusters to be used were “Howard1”, belonging to the Thermodynamics Research Group in the School of Chemical Engineering at the Howard College Campus of the University of KwaZulu-Natal, and "Ruby2", at the School of Engineering, University College of Borås, in Borås, Sweden. "Howard1" consisted of 6 quad-core computational processors, for a total of 24 computational nodes, and ran the CentOS 5 UNIX-like operating system. "Ruby2" consisted of 7 single- and 7 dual-core computational processors, for a total of 21 nodes, although only the dual-core processors were used in this work, due to the requirements of other users. To interface with both of the clusters, a secure-shell remote login was used, using the “ssh” bash command of many Linux operating systems. In particular, Ubuntu was used in this project, as it was freely available for download online and was also a fairly popular Linux operating system. The hyperterminal program “PuTTY” was also used on the Microsoft Windows XP and Windows 7 operating systems when Linux was not available. In this way, jobs could be remotely assigned to the cluster without direct physical access to the cluster itself.

	Master Node (x1)	Slave Nodes (x6)
CPU Speed	2.66 GHz	2.83 GHz
CPU Model	E7300 Intel Core2 Duo 64-bit	Intel Xeon Quad Core 64-bit
RAM	4 GB	4 GB
Hard Disk	695 GB	132 GB
Operating System	Linux version 2.6.18-92.1.13.e15 (CentOS 5)	

Table 3-1: Specifications of the Beowulf cluster "Howard1".

Once on the cluster itself, the Oracle computer program "Grid Engine" was used to manage the queuing of jobs to be run on the system. Grid Engine would assign jobs to available nodes and keep track of jobs which were submitted and unable to be run due to a lack of available computational nodes. These unassigned jobs would then wait in the "queue" until a node became free, at which point Grid Engine would assign the jobs to a free node. The priority of the jobs in the "queue" was determined simply by the order in which they were submitted.

3.2 The Gibbs ensemble program:

The Gibbs Ensemble program which was used in the test system was that of Errington & Panagiotopoulos (2000) in its original unmodified form, as of 22/01/2000. The program accepts the desired temperature, pressure and compositions of each phase to be studied as inputs. In addition, the relevant model parameters are also required as inputs. By default, the program is supposed to handle two phases and any number of components, which was ideal for the purposes of this work. Additionally, the user must specify which ensemble is to be used. The two choices are the isobaric-isothermal (NPT) and the canonical (NVT) ensemble. These different ensembles were discussed previously, in chapter 2.1.3. The NPT ensemble was most useful for this work, as both the pressure and temperature were fixed, as is common in a physical experiment. Thus, any simulation results obtained can be directly compared to experimental results, since they were obtained in essentially the same way.

What is of key importance to remember when performing simulations is whether or not the system has the correct degrees of freedom specified for the desired analysis. The equation used to check this is the well-known phase rule of Gibbs (1873) for non-reacting systems;

$$F = C + 2 - P \qquad \text{Eq. (11)}$$

In the case of this work, no inconsistencies were encountered in the use of the phase rule, as it was ensured that the system was correctly specified. It should be noted that if the system was incorrectly

specified, the simulations would be impossible, since the system would be either overspecified or underspecified. For a correctly specified system, at each temperature, pressure and overall composition, there could be only one possible set of individual phase compositions. Here, the overall composition refers to the number of molecules of each species in the entire system (i.e. both phases).

For the perfluorinated polymer analysis, a modified version of the original Gibbs ensemble program was used. This version was modified by Johansson (2007), and was changed to allow for different torsional potentials, a cut-off radius, as well as including external electric fields, among other features. However, only the first two additions were of importance to this work. It was then modified further to allow for the use of the torsional potential model of Cui et al (1998), which was achieved by changing the limits of the Karayiannis torsional potential calculation in the code from 8 terms to 7 terms.

The Gibbs ensemble program was written in Fortran90, and as such had to be compiled into machine code before use on the cluster. Compilation was performed in the standard manner, using the default Makefile, albeit with the required compiler directory. The Makefile contains the instructions for the compiler to use when instructed to compile the source code into machine code. The compiler used in this work was the Intel compiler on the Howard1 cluster. The GNU Compiler Collection was also used at times to compile the programs used in this work into machine code. A further modification of the Makefile was required for the polymer code when compilation was attempted, as the compile would not recognize files with the extension ".mod" as being written in Fotran90, but instead would recognize them as being written in Modula C. To rectify this, the line "%.o : %.mod" needed to be added near the beginning of the Makefile in order that the compiler handle the ".mod" files correctly and include them in the compiled machine code.

3.3 The polymer program:

The polymer program which was used in this work was that used by Johansson (2007). The polymer program as such is actually a merger of the original polymer program of Mavrantzas et al (1999) with the modified Gibbs ensemble program of Errington and Panagiotopoulos (2000). This modification was performed so that the Gibbs program can handle the non-polymer interactions while the polymer program handles the polymer interactions. The Gibbs program alone cannot be used for polymer simulations due the limitations discussed in chapter 2.1.4, and thus the polymer program was introduced to the arrangement to enable phase equilibrium studies involving polymers.

The inputs to this amalgamated program include portions for both the Gibbs ensemble part of the program and the polymer part. The Gibbs ensemble input file is fairly similar to the standard form found

in the original form, albeit with some slight modifications due to the work of Johansson (2007). The polymer program, however, requires several input files to be used, containing the various forcefield parameters, as well as the initial configuration of the polymers and the co-ordinates of the pseudo-atoms. The initial co-ordinates for the shorter polymer molecules were determined using the program described in chapter 2.1.10. For the initial co-ordinates of the longest polymer molecules, existing co-ordinates for polyethylene were used.

CHAPTER 4: SIMULATION DETAILS AND RESULTS

4.1 Test system:

The test system of light alcohols (methanol, ethanol and isopropanol) + water + n-dodecane was simulated using the Gibbs ensemble program of Errington & Panagiotopoulos, as discussed previously in chapter 3.2. The test systems were simulated using the NPT ensemble of the Gibbs ensemble program. The test systems consisted of the following:

- methanol + water + n-dodecane at;
  - T = 313.14 K and P = 101.325 kPa
  - T = 350 K and P = 600 kPa
  - T = 400 K and P = 600 kPa
- ethanol + water + n-dodecane at;
  - T = 333.15 K and P = 101.325 kPa
  - T = 350 K and P = 600 kPa
  - T = 400 K and P = 600 kPa
- isopropanol + water + n-dodecane at;
  - T = 333.15 K and P = 101.325 kPa
  - T = 350 K and P = 600 kPa

- T = 400 K and P = 600 kPa

To determine the initial volume of each box, a simple calculation using the approximate experimental value of the density of the expected dominant species in each phase as well as the molecular mass of the initial starting composition was undertaken. The initial compositions that were used were those for the same system at 313.14 K and 101.325 kPa found in the work of Lasich et al (2011). The number of molecules in each box was adjusted such that the sides of each cubic box would be at least 20 Ångströms in length. It was found, however, that for every initial configuration there were too few molecules to generate sufficiently good representative statistics (i.e. approximately 100 to 200 molecules or less), and thus the number of molecules in each setup was doubled, such that the total number of molecules was between 300 and 500. This doubling was found to be reasonable, since in the work of Johansson (2007), not less than 300 molecules were used in simulations of alkanes and water. However, it is important to note that these initial configurations need not be accurate at all, since the system will automatically adjust itself during the course of each simulation.

As for the TraPPE model parameters which were used in this work, they were acquired from a various sources; methanol from Martin & Siepmann (1998), n-dodecane and ethanol from Martin & Siepmann (1998) and Chen at al (2001), isopropanol from Martin & Siepmann (1998, 1999) and Chen et al (2001). The SPC water model parameters were taken from Berendsen et al (1987).

To begin with, each system was equilibriated in two stages. In the first, pre-equilibriation stage, no swap moves were allowed, and the system was run until it was seen that the internal energy and density of each phase had converged, and that no trends were observed in the properties of the system (i.e. phase compositions, etc). This generally took approximately one run of 45,000,000 Monte Carlo moves. Once each phase was at equilibrium, then the second, equilibriation stage was undertaken. This involved running the simulation until no changes in composition for each phase was observed and the compositions had stabilized to their respective average values. This generally took two runs of the aforementioned number of Monte Carlo moves. It was only once this two-phase equilibriation process was completed that production runs were attempted. Production runs were simulations which continued from where the equilibriation process had left off. These production runs were performed in order to generate enough data to reduce statistical uncertainty. The ratio of translation/rotation : volume change : interphase transfer : regrow moves used in the simulations was 0.340 : 0.0030 : 0.500 : 0.157. This ratio of volume change was chosen in order to limit the CPU time spent on volume changes, which are computationally costly, as mentioned by Moodley (2008), whilst letting the two most statistically important moves, i.e. translation/rotation and phase swapping, take up the majority of the CPU time.

As far as the production runs were concerned, it was found that the acceptance rate for a transfer of dodecane between phases was incredibly low, of the order of 0.05%. This was likely due to the aforementioned shortcomings of the Gibbs ensemble, as discussed in chapter 2.1.4. However, each production run was set at 45,000,000 Monte Carlo moves (as before). Several production runs were performed for each measurement to ensure that adequately representative statistics would be obtained of the system being analyzed. What should also be noted was that since the minimum composition change could be one molecule out of a total of 10^2 to 10^3, the corresponding precision of the simulated compositions were thus adjusted accordingly, and the results and their standard deviations (uncertainties) reflect this.

Presented following are the initial configuration of the system(s) and the tabulated results along with the relevant tie-line data and phase diagrams to graphically illustrate the results. (It should be noted that the same four initial points were used for each system and at each temperature);

	Point 1		Point 2	
Species	Phase I	Phase II	Phase I	Phase II
Water	0	0	0	82
n-Dodecane	46	2	60	2
Alcohol	10	300	4	280
	Point 3		Point 4	
	Phase I	Phase II	Phase I	Phase II
Water	0	220	0	280
n-Dodecane	50	0	50	0
Alcohol	1	180	0	60

Table 4-1: Initial number of molecules of each species in each phase for each simulated point.

x_{Water}	$x_{n\text{-}Dodecane}$	$x_{Methanol}$
	T = 313.14 K	
	Phase I	
0.000	0.991 ± 0.013	0.009 ± 0.013
0.000	0.997 ± 0.005	0.003 ± 0.005
0.000	0.998 ± 0.003	0.002 ± 0.003
0.000	0.998 ± 0.004	0.002 ± 0.004
	Phase II	
0.000	0.006	0.994
0.221	0.013	0.765
0.547	0.002	0.450
0.824	0.000	0.176
	T = 350 K	
	Phase I	
0.000	0.791 ± 0.022	0.209 ± 0.022
0.001 ± 0.001	0.969 ± 0.014	0.030 ± 0.014
0.001 ± 0.001	0.995 ± 0.003	0.004 ± 0.003
0.001 ± 0.001	0.996 ± 0.004	0.004 ± 0.004
	Phase II	
0.000	0.010	0.990
0.225 ± 0.001	0.000	0.775 ± 0.001
0.549	0.000	0.451
0.824	0.000	0.176
	T = 400 K	
	Phase I	
0.000	0.893 ± 0.064	0.107 ± 0.064
0.004 ± 0.004	0.931 ± 0.028	0.065 ± 0.027
0.011 ± 0.008	0.923 ± 0.028	0.066 ± 0.023
0.006 ± 0.004	0.975 ± 0.011	0.019 ± 0.010
	Phase II	
0.000	0.065 ± 0.003	0.935 ± 0.003
0.223 ± 0.001	0.015 ± 0.002	0.762 ± 0.002
0.552 ± 0.002	0.001 ± 0.001	0.447 ± 0.002
0.826 ± 0.001	0.000	0.174 ± 0.001

Table 4-2: Simulated LLE tie-line data for the water + n-dodecane + methanol system. Some values do not contain stated uncertainties as these uncertainties were less than 0.000 mole fraction.

x_{Water}	$x_{n\text{-}Dodecane}$	$x_{Ethanol}$
	T = 333.15 K	
	Phase I	
0.000	0.977 ± 0.020	0.023 ± 0.020
0.000 ± 0.001	0.993 ± 0.008	0.006 ± 0.008
0.000 ± 0.001	0.992 ± 0.008	0.007 ± 0.008
0.000 ± 0.001	0.993 ± 0.009	0.006 ± 0.009
	Phase II	
0.000	0.013	0.987
0.223	0.005	0.772
0.548 ± 0.001	0.001 ± 0.001	0.450 ± 0.001
0.824 ± 0.001	0.000	0.176 ± 0.001
	T = 350 K	
	Phase I	
0.000	0.645 ± 0.023	0.355 ± 0.023
0.009 ± 0.012	0.878 ± 0.021	0.113 ± 0.020
0.001 ± 0.001	0.979 ± 0.015	0.020 ± 0.015
0.001 ± 0.002	0.989 ± 0.012	0.010 ± 0.011
	Phase II	
0.000	0.024	0.976
0.224 ± 0.002	0.015 ± 0.001	0.761 ± 0.002
0.550 ± 0.001	0.000	0.450 ± 0.001
0.825 ± 0.001	0.000	0.175 ± 0.001
	T = 400 K	
	Phase I	
0.000	0.110 ± 0.029	0.890 ± 0.029
0.120 ± 0.017	0.311 ± 0.013	0.568 ± 0.019
0.011 ± 0.011	0.920 ± 0.045	0.069 ± 0.038
0.007 ± 0.007	0.954 ± 0.033	0.039 ± 0.029
	Phase II	
0.000	0.151 ± 0.019	0.849 ± 0.019
0.238 ± 0.012	0.036 ± 0.004	0.726 ± 0.011
0.547 ± 0.003	0.011 ± 0.003	0.442 ± 0.003
0.828 ± 0.005	0.001 ± 0.002	0.171 ± 0.004

Table 4-3: Simulated LLE tie-line data for the water + n-dodecane + ethanol system. Some values do not contain stated uncertainties as these uncertainties were less than 0.000 mole fraction.

x_{Water}	$x_{n\text{-}Dodecane}$	$x_{Isopropanol}$
	T = 333.15 K	
	Phase I	
0.000	0.553 ± 0.026	0.447 ± 0.026
0.122 ± 0.018	0.505 ± 0.013	0.373 ± 0.018
0.166 ± 0.029	0.520 ± 0.020	0.314 ± 0.024
0.128 ± 0.030	0.733 ± 0.028	0.139 ± 0.022
	Phase II	
0.000	0.000	1.000
0.219 ± 0.007	0.000	0.780 ± 0.007
0.575 ± 0.006	0.000	0.425 ± 0.006
0.843 ± 0.005	0.000	0.157 ± 0.005
	T = 350 K	
	Phase I	
0.000	0.946 ± 0.021	0.054 ± 0.021
0.006 ± 0.004	0.939 ± 0.022	0.054 ± 0.021
0.007 ± 0.006	0.970 ± 0.013	0.023 ± 0.012
0.008 ± 0.006	0.938 ± 0.023	0.053 ± 0.022
	Phase II	
0.000	0.003 ± 0.002	0.997 ± 0.002
0.225 ± 0.001	0.001 ± 0.002	0.774 ± 0.002
0.548 ± 0.001	0.003 ± 0.001	0.449 ± 0.001
0.830 ± 0.003	0.000	0.170 ± 0.003
	T = 400 K	
	Phase I	
0.000	0.702 ± 0.055	0.298 ± 0.055
0.034 ± 0.015	0.779 ± 0.054	0.187 ± 0.047
0.052 ± 0.013	0.754 ± 0.031	0.194 ± 0.027
0.051 ± 0.019	0.875 ± 0.033	0.074 ± 0.021
	Phase II	
0.000	0.007 ± 0.004	0.993 ± 0.004
0.219 ± 0.003	0.035 ± 0.006	0.746 ± 0.005
0.562 ± 0.003	0.001 ± 0.001	0.437 ± 0.003
0.813 ± 0.003	0.021 ± 0.003	0.165 ± 0.003

Table 4-4: Simulated LLE tie-line data for the water + n-dodecane + isopropanol system. Some values do not contain stated uncertainties as these uncertainties were less than 0.000 mole fraction.

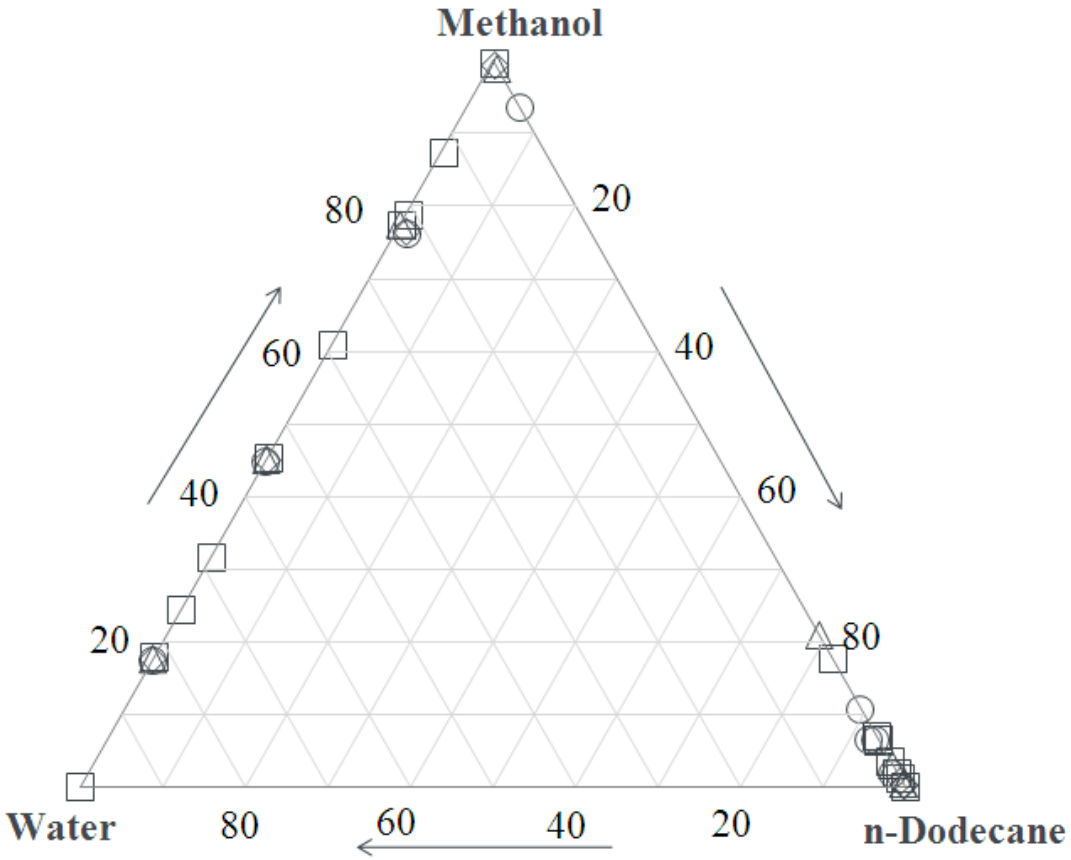

Figure 4-1: Ternary LLE plot of the methanol + water + n-dodecane system. Values are in mole percent. (□) experiments at T = 313.14 K (literature), (◇) simulations at T 313.14 K (this work), (△) simulations at T = 350 K (this work), (○) simulations at T = 400 K (this work). Literature data is from Lasich et al (2011). Tie-lines extend from the data points on the left-hand side to those on the right hand. Tie-lines have not been shown in the figure for the sake of clarity.

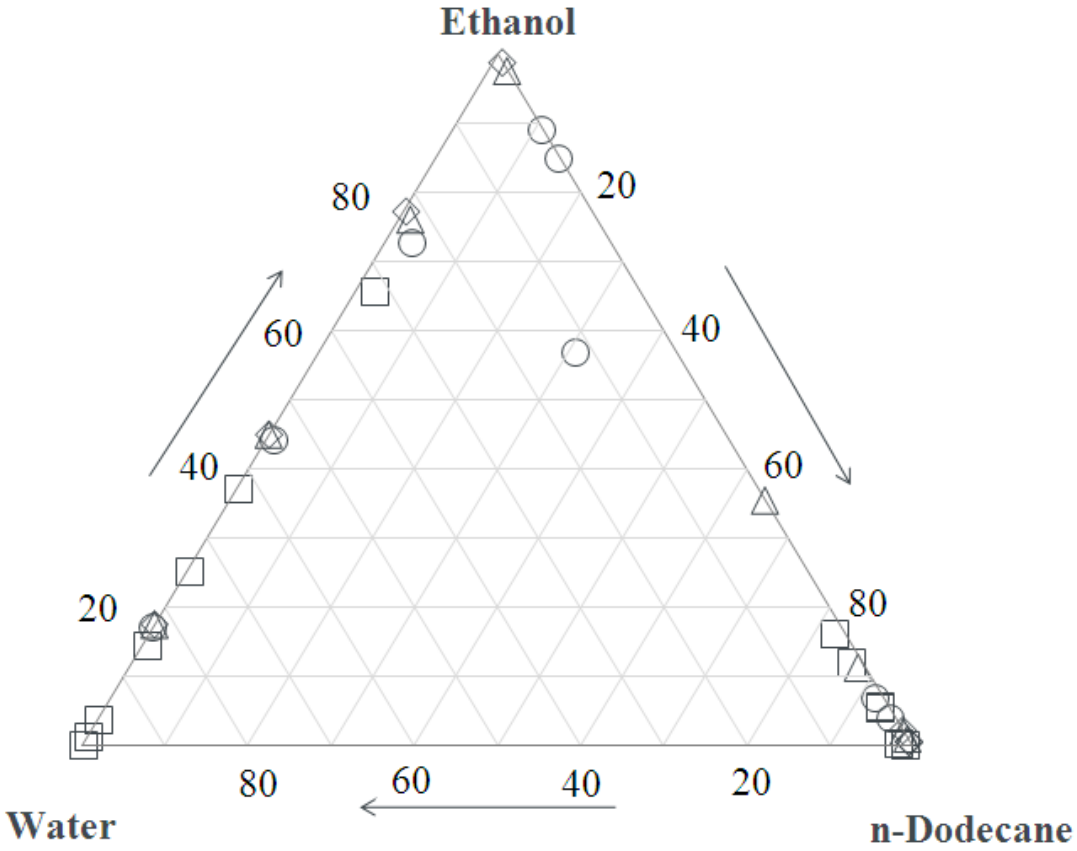

Figure 4-2: Ternary LLE plot of the ethanol + water + n-dodecane system. Values are in mole percent. (□) experiments at T = 333.15 K (literature), (◇) simulations at T = 333.15 K (this work), (△) simulations at T = 350 K (this work), (○) simulations at T = 400 K (this work). Literature data is from Lasich et al (2011). Tie-lines extend from the data points on the left-hand side to those on the right hand. Tie-lines have not been shown in the figure for the sake of clarity.

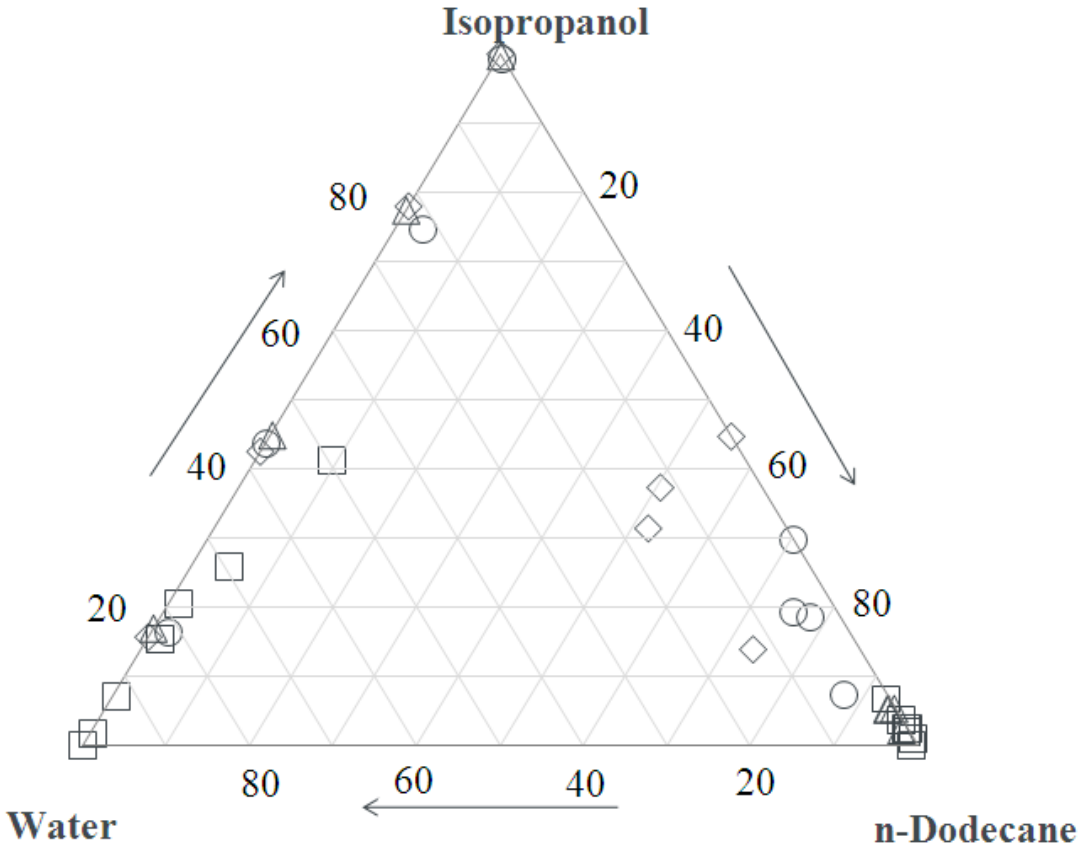

Figure 4-3: Ternary LLE plot of the isopropanol + water + n-dodecane system. Values are in mole percent. (□) experiments at T = 333.15 K (literature), (◇) simulations at T = 333.15 K (this work), (△) simulations at T = 350 K (this work), (○) simulations at T = 400 K (this work). Literature data is from Lasich et al (2011). Tie-lines extend from the data points on the left-hand side to those on the right hand. Tie-lines have not been shown in the figure for the sake of clarity.

4.2 Water solubility in perfluoroalkanes:

The simulations of the non-polymeric perfluoroalkanes were performed using the Gibbs ensemble program previously discussed in chapter 2.1.3, as modified by Johansson (2007). In the context of this work, the term "polymer" refers to molecules with a carbon number greater than or equal to 20. Therefore, all perfluoroalkane simulations would be those simulations involving linear perfluorocarbons up to, but not including a carbon number of 20.

The procedure followed in this work was based upon that of Johansson (2007), which was also used in Johansson & Ahlström (2007) and Johansson et al (2007). This procedure entailed the simulation of the system of alkane + water for a number of different carbon numbers and a number of different temperatures. Initially, each system consisted of 100 perfluoroalkane molecules and 500 water molecules, each contained within a pure phase. The course of the simulations in this chapter was the same as for the test system, which was discussed in chapter 4.1. This procedure entailed a two-step equilibration process, followed by production runs to generate statistics. For a more detailed description, see chapter 4.1. In the course of this chapter's work on perfluoroalkanes, each production period consisted of no less than 60,000,000 Monte Carlo moves, and several runs were used to generate the final results. This was to ensure that adequately representative statistics would be obtained of the system being analyzed.

In this work, the effect of carbon number and temperature on the solubility of water in the perfluoroalkane was examined. This data was compared directly to the literature, namely Johansson (2007). For the full table of the water solubility data for the perfluoroalkane simulations, consult chapter 4.4. An extensive set of tables which includes phase densities and solubility data for both phases can be found in the appendix to this work. The data obtained for the solubility of water in perfluoroalkanes is represented in the following figures;

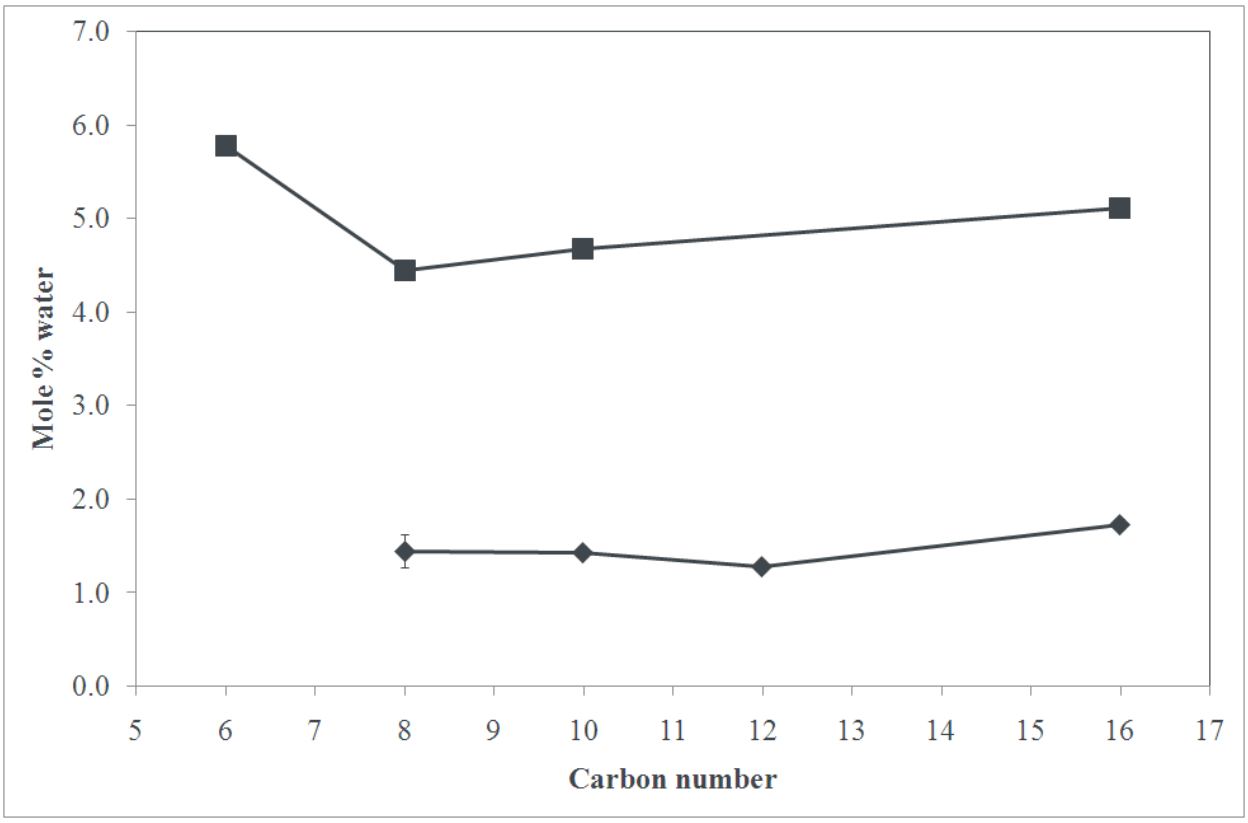

Figure 4-4: Solubility of water in alkanes and perfluoroalkanes versus carbon number at T = 450 K. (■) n-alkanes (literature), (◆) perfluoroalkanes (this work). The literature data is from Johansson (2007).

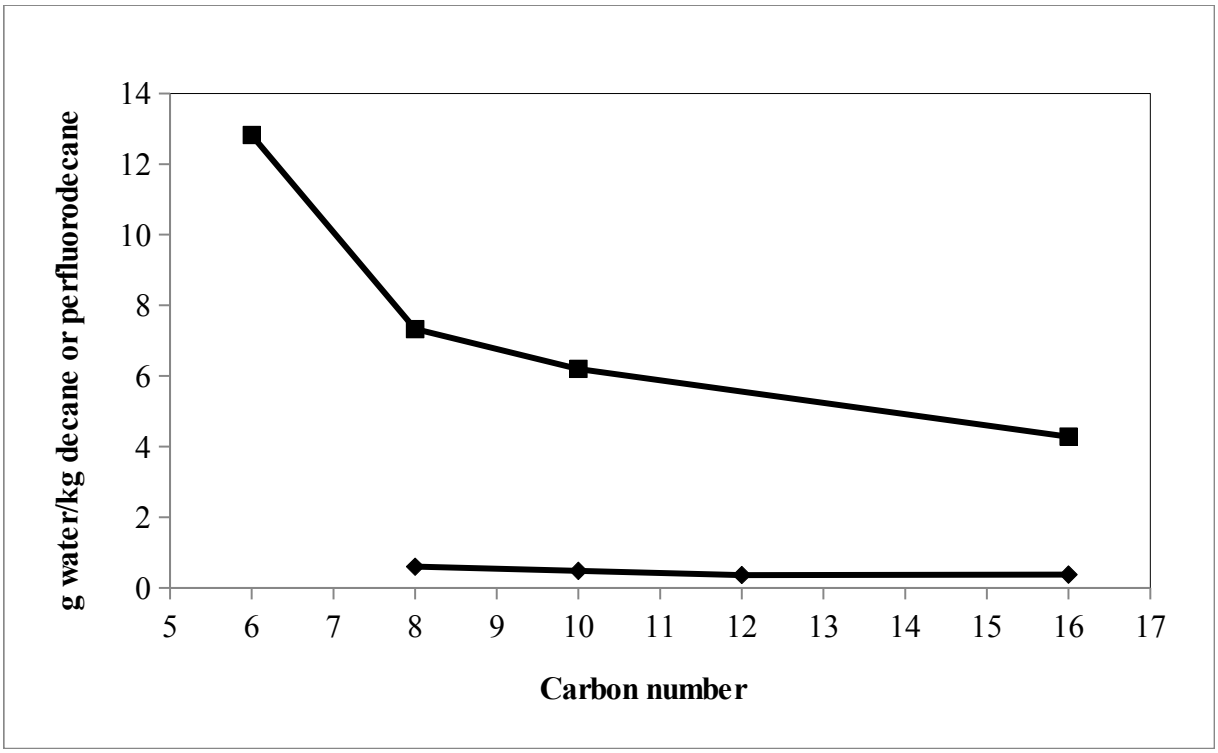

Figure 4-5: Solubility of water in alkanes and perfluoroalkanes versus carbon number at T = 450 K, on a mass basis. (■) n-alkanes (literature), (◆) perfluoroalkanes (this work). The literature data is from Johansson (2007).

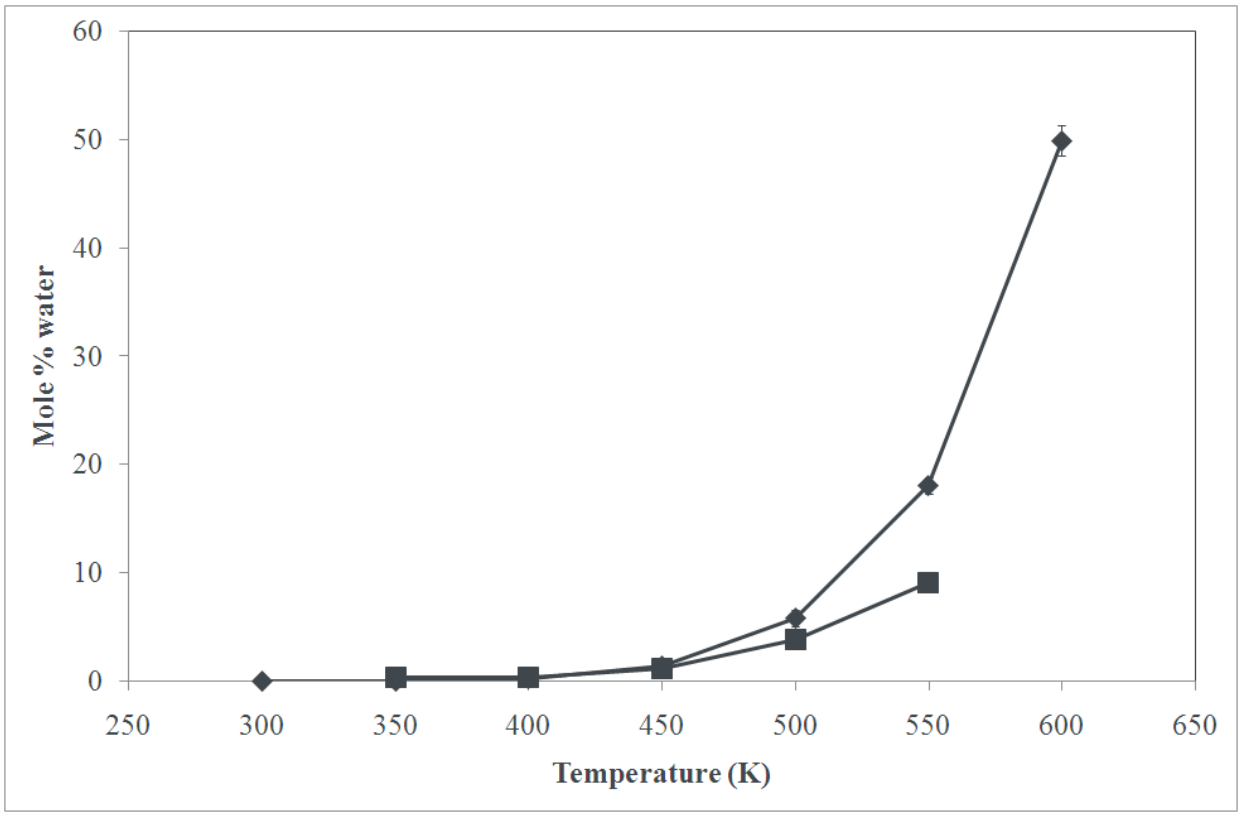

Figure 4-6: Solubility of water in n-decane and perfluorodecane over a temperature range from 300 K to 600 K. (■) n-alkanes (literature), (◆) perfluoroalkanes (this work). The literature data is from Johansson (2007).

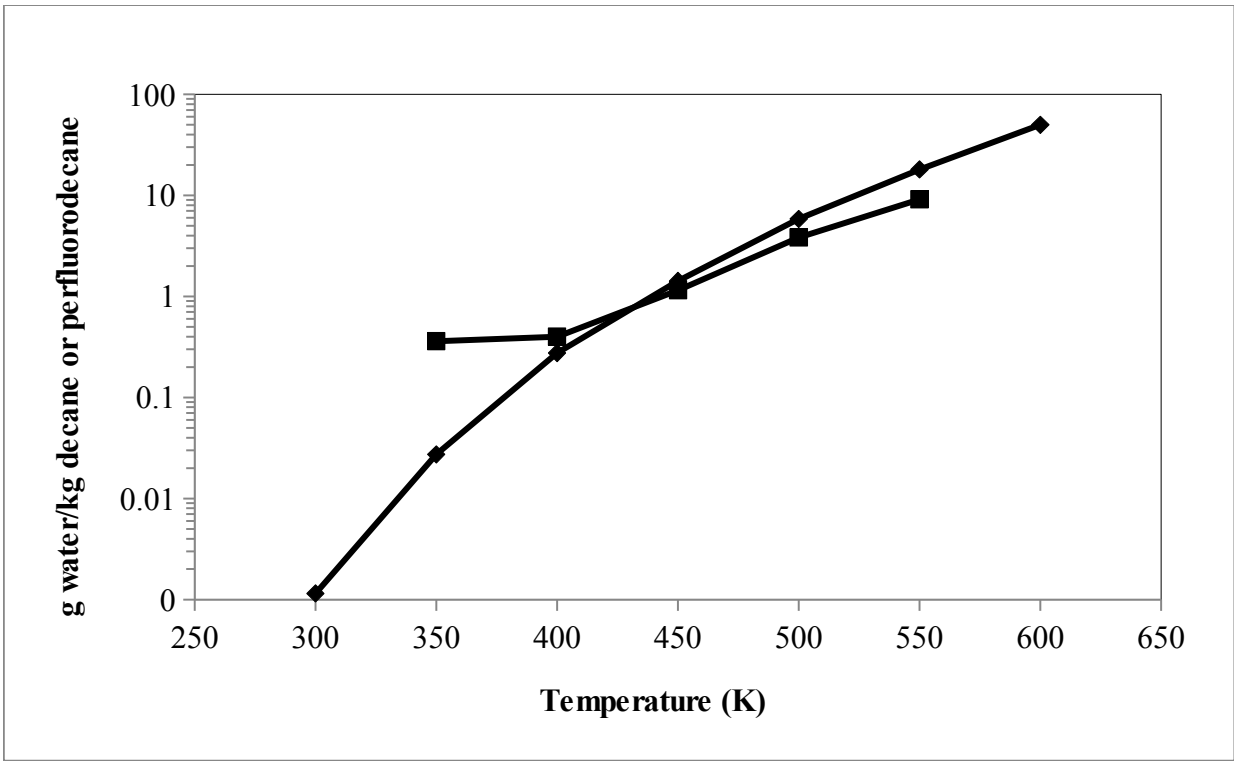

Figure 4-7: Solubility of water in n-decane and perfluorodecane over a temperature range from 300 K to 600 K, on a mass basis. (■) n-alkanes (literature), (◆) perfluoroalkanes (this work). The literature data is from Johansson (2007). The y-axis has been made logarithmic for clarity.

4.3 Polymer generation:

The co-ordinates resulting from the polymer generation algorithm developed in this work were plotted in GNU Plot. This plotting was performed using a scripted routine within the program. An example plot of linear chains of PTFE is presented as follows;

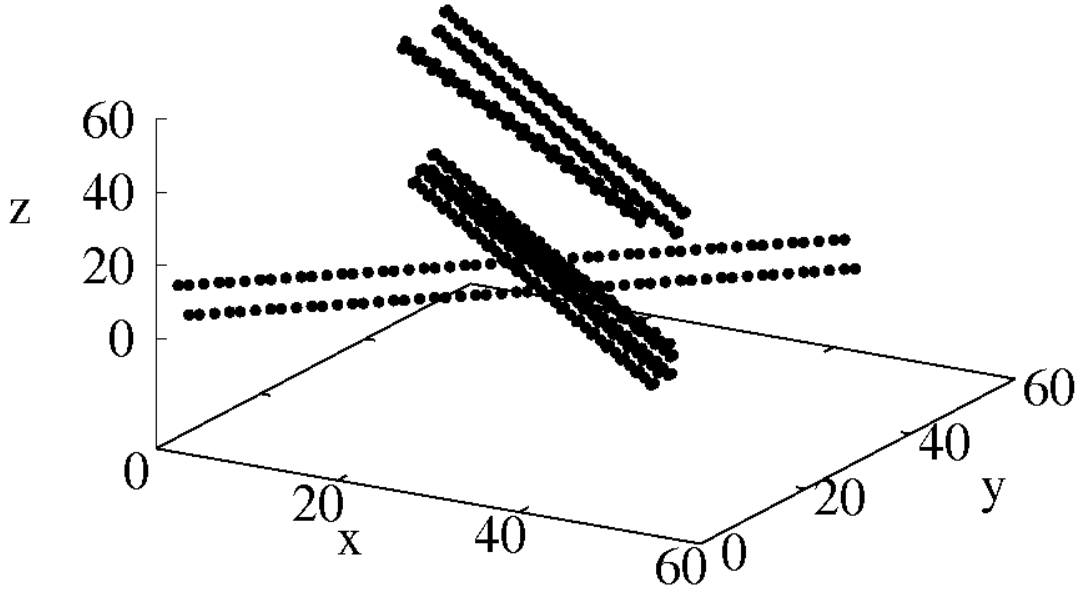

Figure 4-8: Example output graphic of ten PTFE molecules. Each has a carbon number of 50. All dimensions in Ångströms. This plot was one of the outputs of the Linux version of the polymer generation program, and was generated using GNUPlot.

4.4. Water solubility in PTFE:

In this work, the procedure followed for the simulation of the polymers was that of Johansson (2007). The set of tables of data, including the densities of both phases as well as the composition of both phases may be found in the appendix to this work. The results for the solubility analysis for the water + PTFE system can be found in the following tables and figures;

Number of carbon atoms	x_{H2O} (Mole fraction)
8	0.014 ± 0.002
10	0.014
12	0.013
16	0.017 ± 0.001
20	0.037 ± 0.001
30	0.182 ± 0.007
35	0.260 ± 0.004
40	0.458 ± 0.006
45	0.548 ± 0.018
50	0.551 ± 0.015
300	0.980

Table 4-6: Tabulated solubilities of water in PTFE for various carbon numbers at T = 450 K.

Number of carbon atoms	x_{H2O} (Mole fraction)
8	0.054
10	0.058 ± 0.007
12	0.035 ± 0.011
16	0.073 ± 0.005
50	0.799 ± 0.002
100	0.976 ± 0.002
300	0.980

Table 4-7: Solubilities of water in PTFE for various carbon numbers at T = 500 K.

Number of carbon atoms	x_{H2O} (Mole fraction)
8	0.400 ± 0.017
10	0.499 ± 0.014
11	0.400 ± 0.004
12	0.362 ± 0.003
13	0.391
16	0.425 ± 0.006
20	0.467 ± 0.004
40	0.939
50	0.965 ± 0.002
100	0.978 ± 0.029
300	0.980

Table 4-8: Solubilities of water in PTFE for various carbon numbers at T = 600 K.

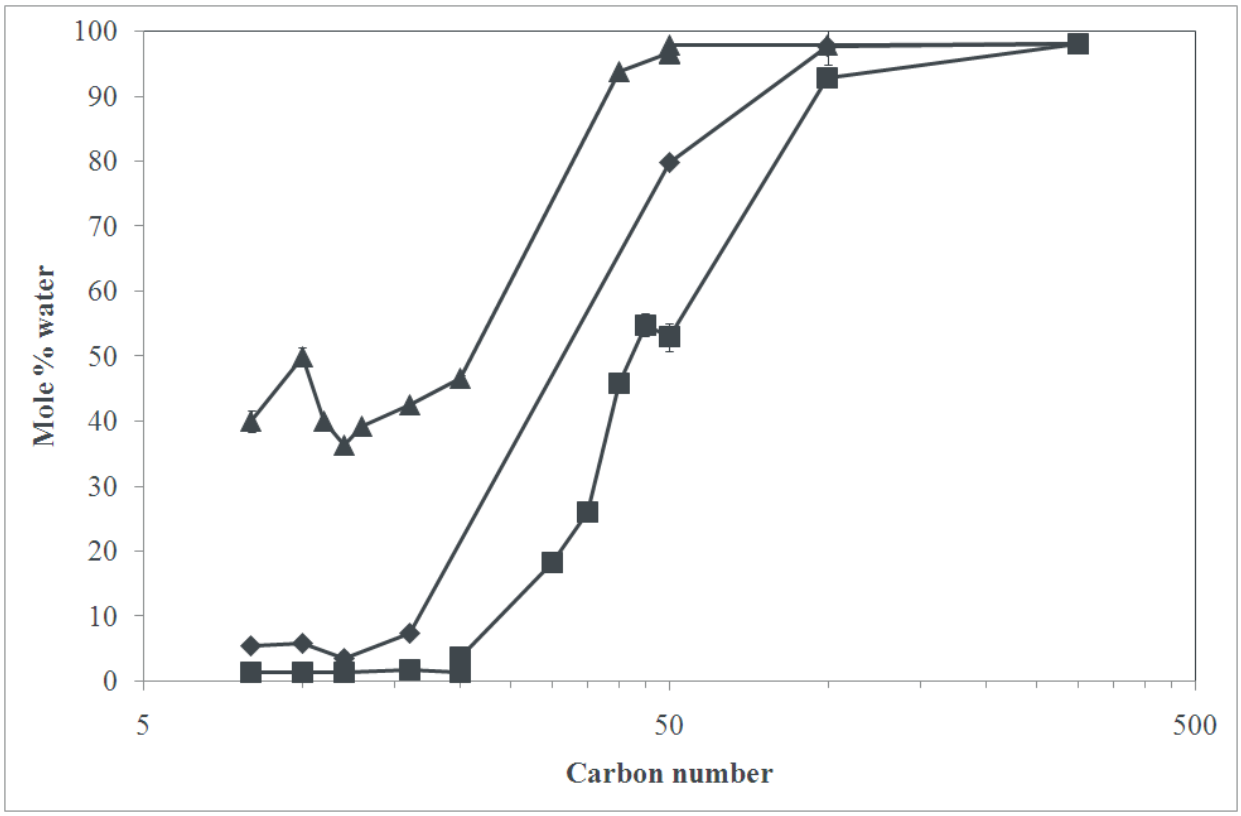

Figure 4-9: Solubility of water in PTFE as a function of carbon number, for three different temperatures, on a molar basis. (■) T = 450 K, (◆) T = 500 K, (▲) T = 600 K. Lines have been added between the points as guides for the eye. The x-axis has been made logarithmic for clarity at the smaller carbon numbers.

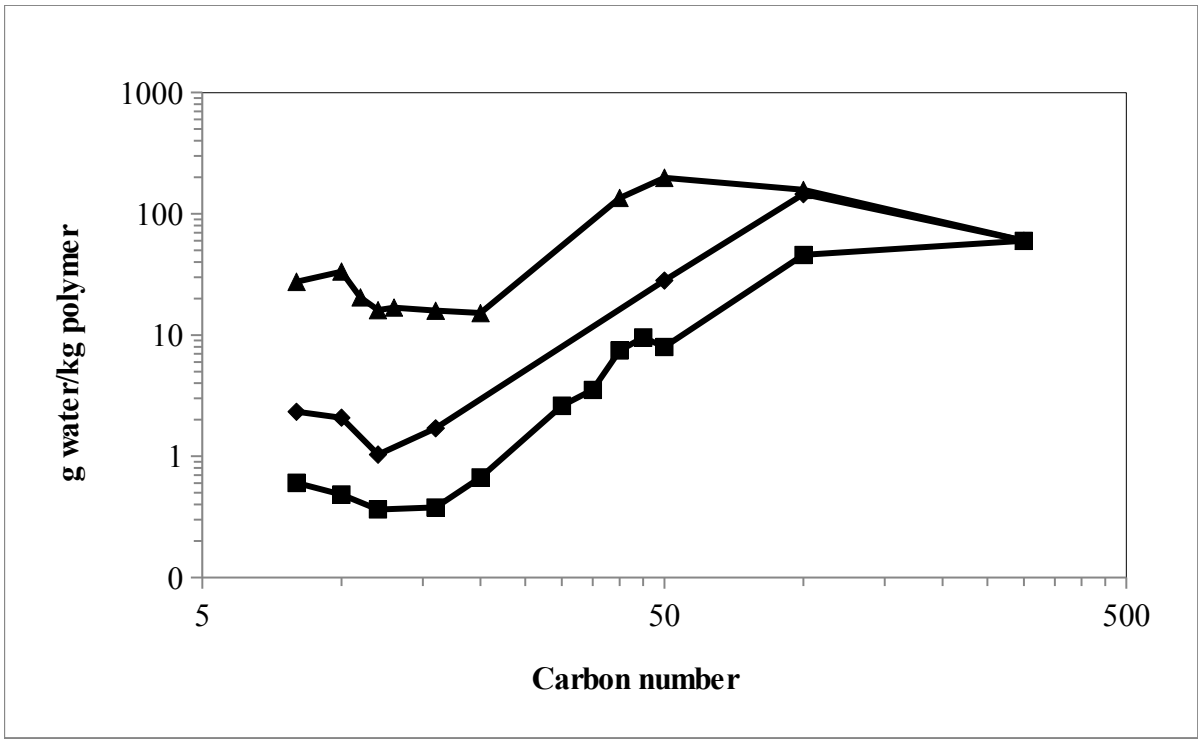

Figure 4-10: Solubility of water in PTFE as a function of carbon number, for three different temperatures, on a mass basis. (■) T = 450 K, (◆) T = 500 K, (▲) T = 600 K. Lines have been added between the points as guides for the eye. The x-axis and y-axis have been made logarithmic for clarity.

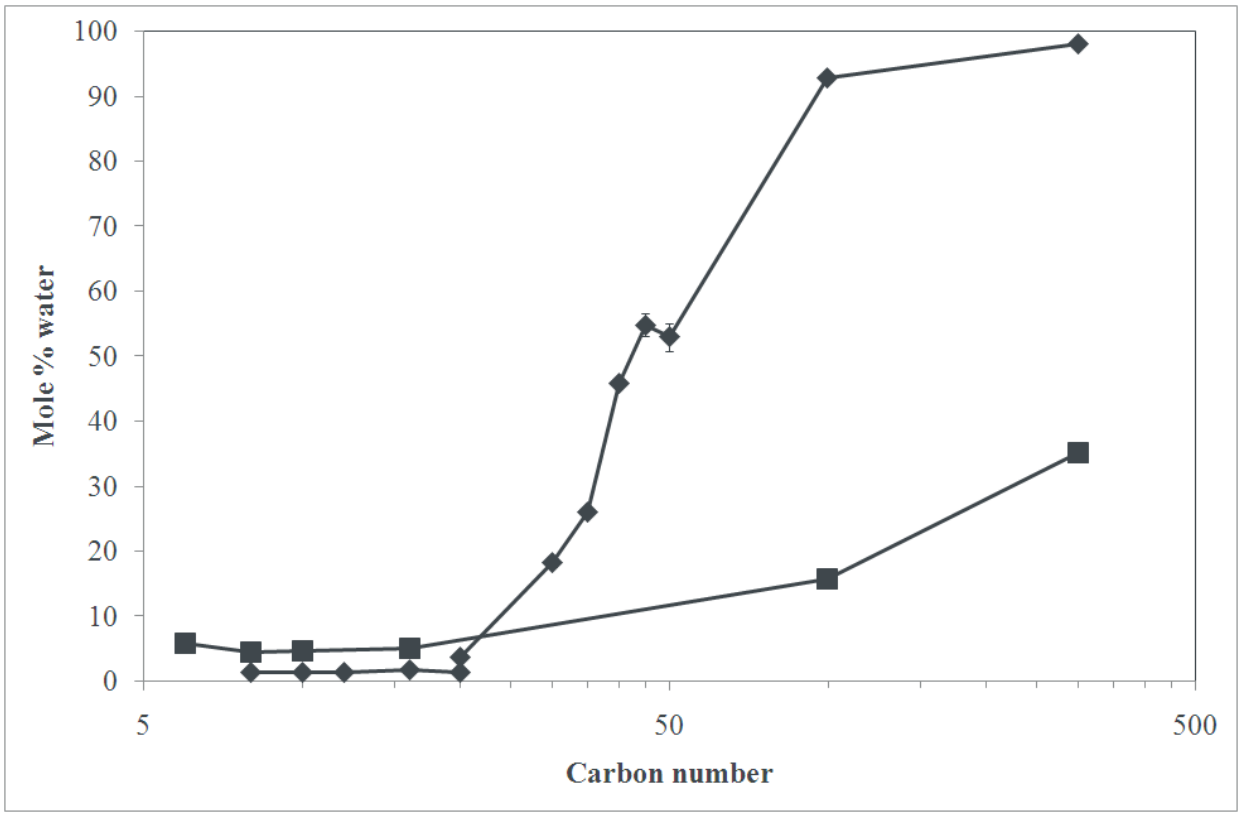

Figure 4-11: Graph of the solubility of water, at T = 450 K, as a function of carbon number in PTFE compared to PE, on a molar basis. (■) PE (literature), (◆) PTFE (this work).The literature data is from Johansson (2007). Lines have been added between the points as guides for the eye. The x-axis has been made logarithmic for clarity at the smaller carbon numbers.

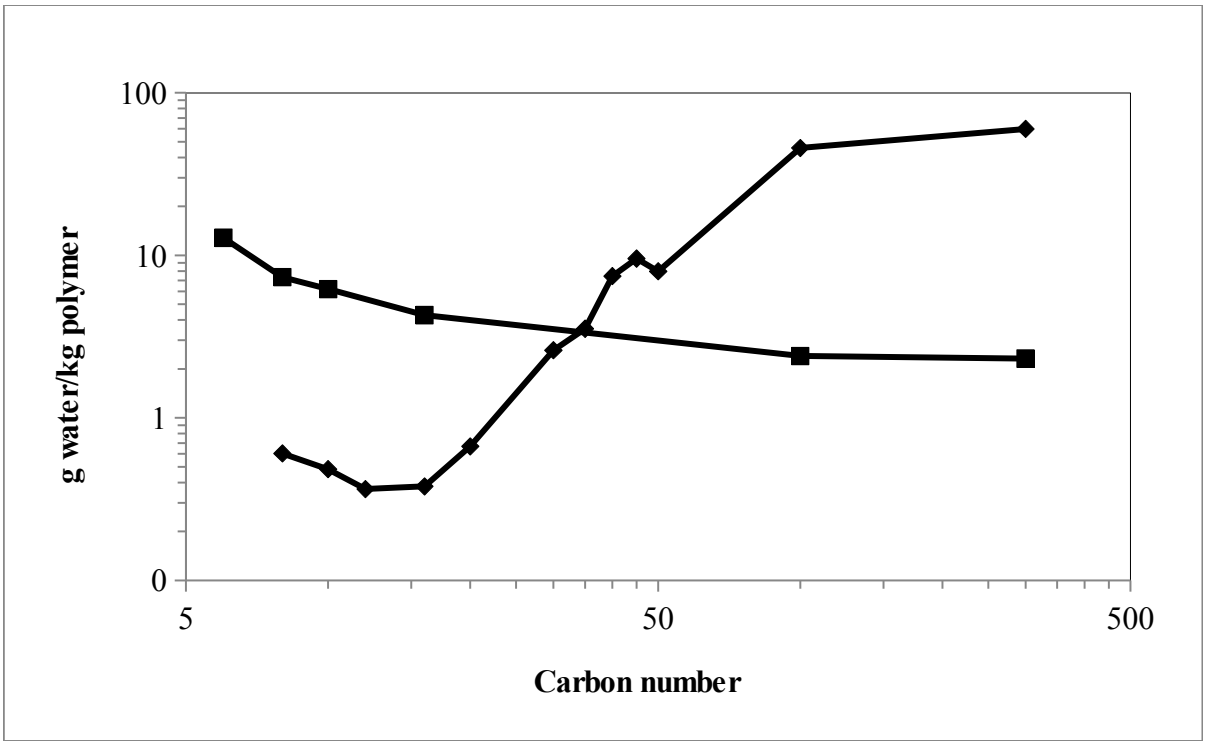

Figure 4-12: Graph of the solubility of water, at T = 450 K, as a function of carbon number in PTFE compared to PE, on a mass basis. (■) PE (literature), (◆) PTFE (this work).The literature data is from Johansson (2007). Lines have been added between the points as guides for the eye. The x-axis and y-axis have been made logarithmic for clarity.

4.5 Cluster analysis of water molecules:

The clustering of water molecules in perfluoroalkanes and PTFE was also analyzed in this work. The influence of carbon number and temperature on the clustering of water molecules in the organic phase was analyzed, so as to compare to the data for water clustering in normal alkanes and polyethylene found in the literature, as reported by Johansson & Ahlström (2007), Johansson (2007) and Johansson et al (2007). This analysis was performed using the algorithm devised by Johansson (2007) for the water + polyethylene system, and implemented in Fotran90. The results are presented graphically as follows;

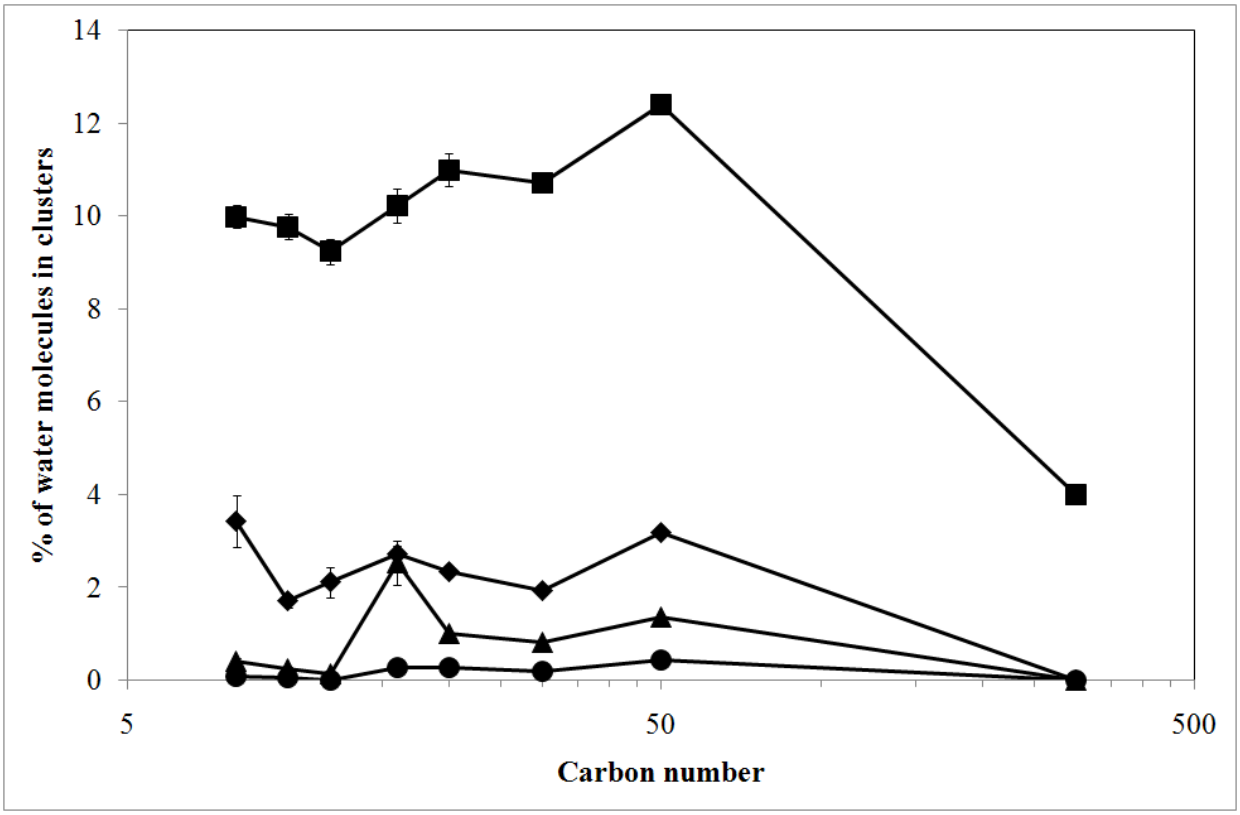

Figure 4-13: Percentage of water molecules included in clusters in the perfluoroalkane phase as a function of carbon number at T = 450 K. (■) n = 2, (◆) n = 3, (▲) n = 4, (●) n = 5. The scale of the x-axis has been made logarithmic for clarity at the smaller carbon numbers. Lines joining the points have been added as guides for the eye.

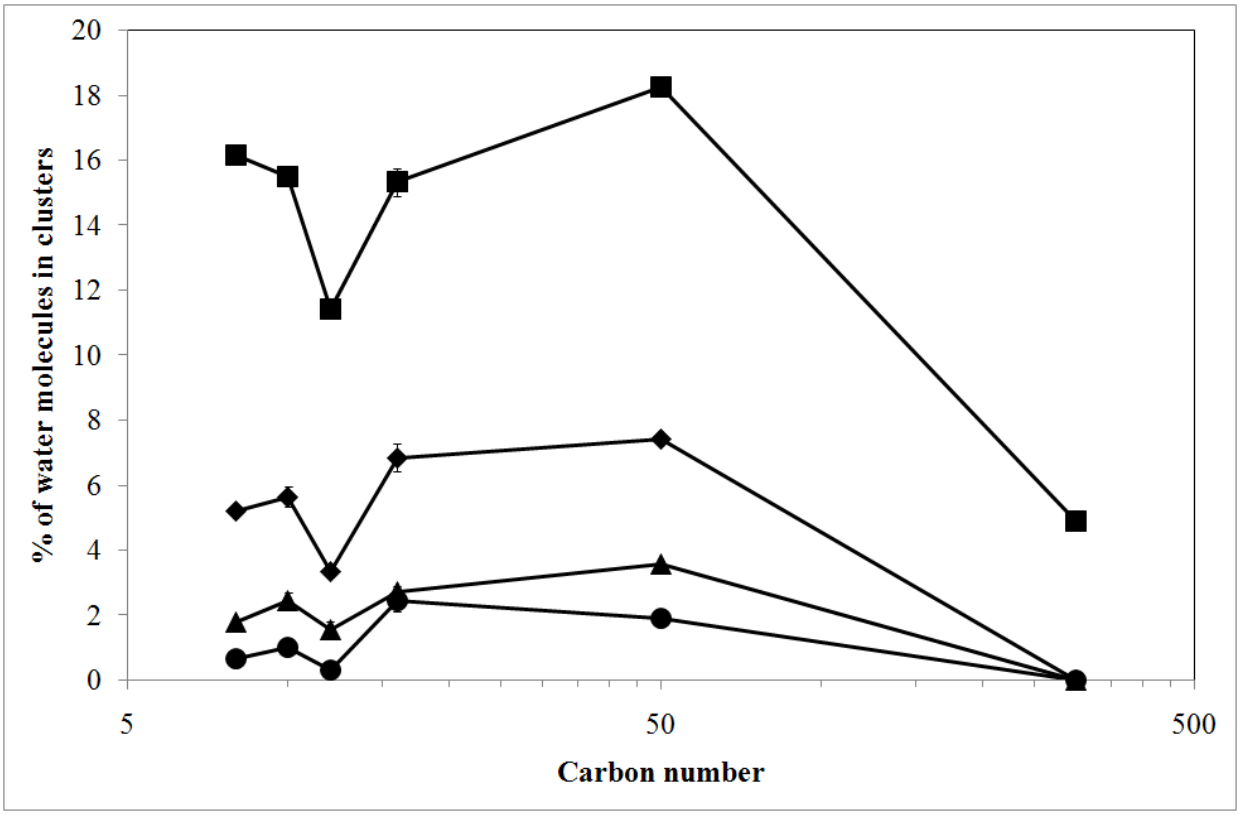

Figure 4-14: Percentage of water molecules included in clusters in the perfluoroalkane phase as a function of carbon number at T = 500 K. (■) n = 2, (◆) n = 3, (▲) n = 4, (●) n = 5. The scale of the x-axis has been made logarithmic for clarity at the smaller carbon numbers. Lines joining the points have been added as guides for the eye.

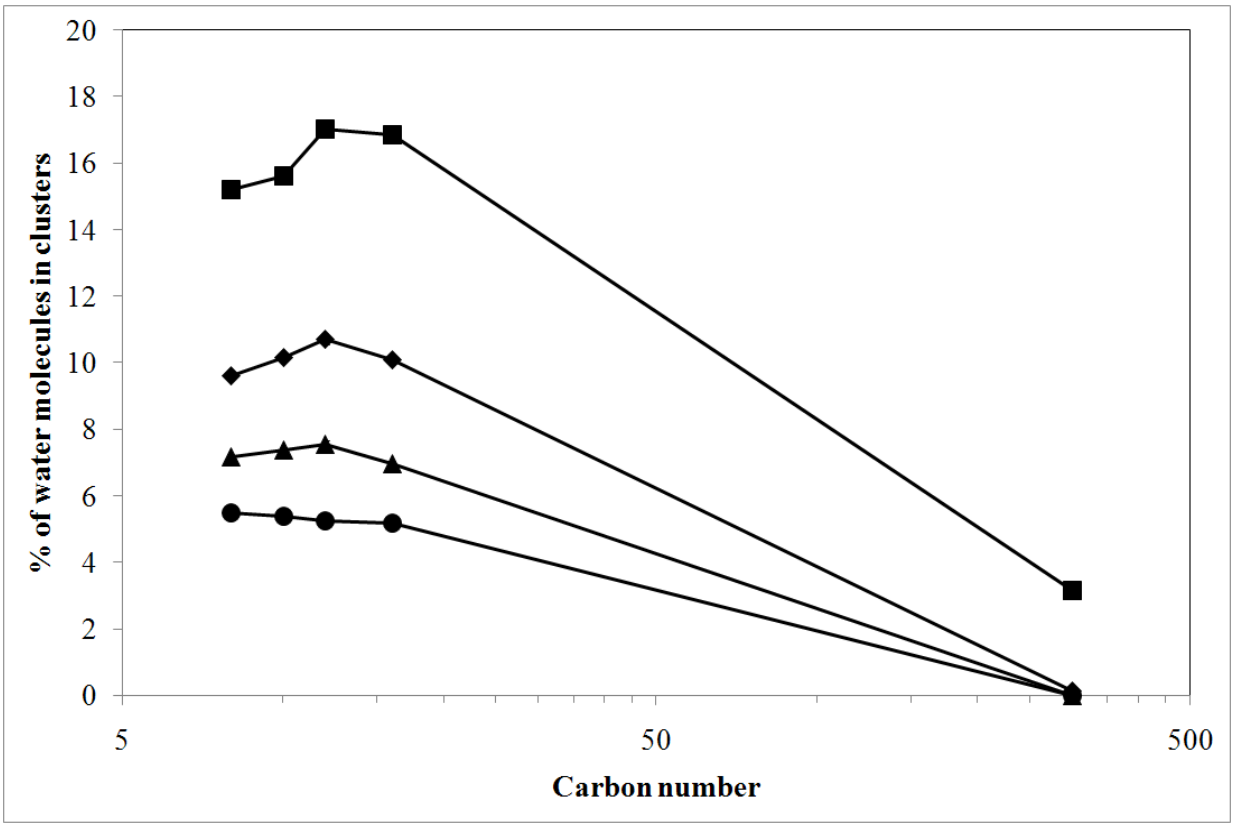

Figure 4-15: Percentage of water molecules included in clusters in the perfluoroalkane phase as a function of carbon number at T = 600 K. (■) n = 2, (◆) n = 3, (▲) n = 4, (●) n = 5. The scale of the x-axis has been made logarithmic for clarity at the smaller carbon numbers. Lines joining the points have been added as guides for the eye.

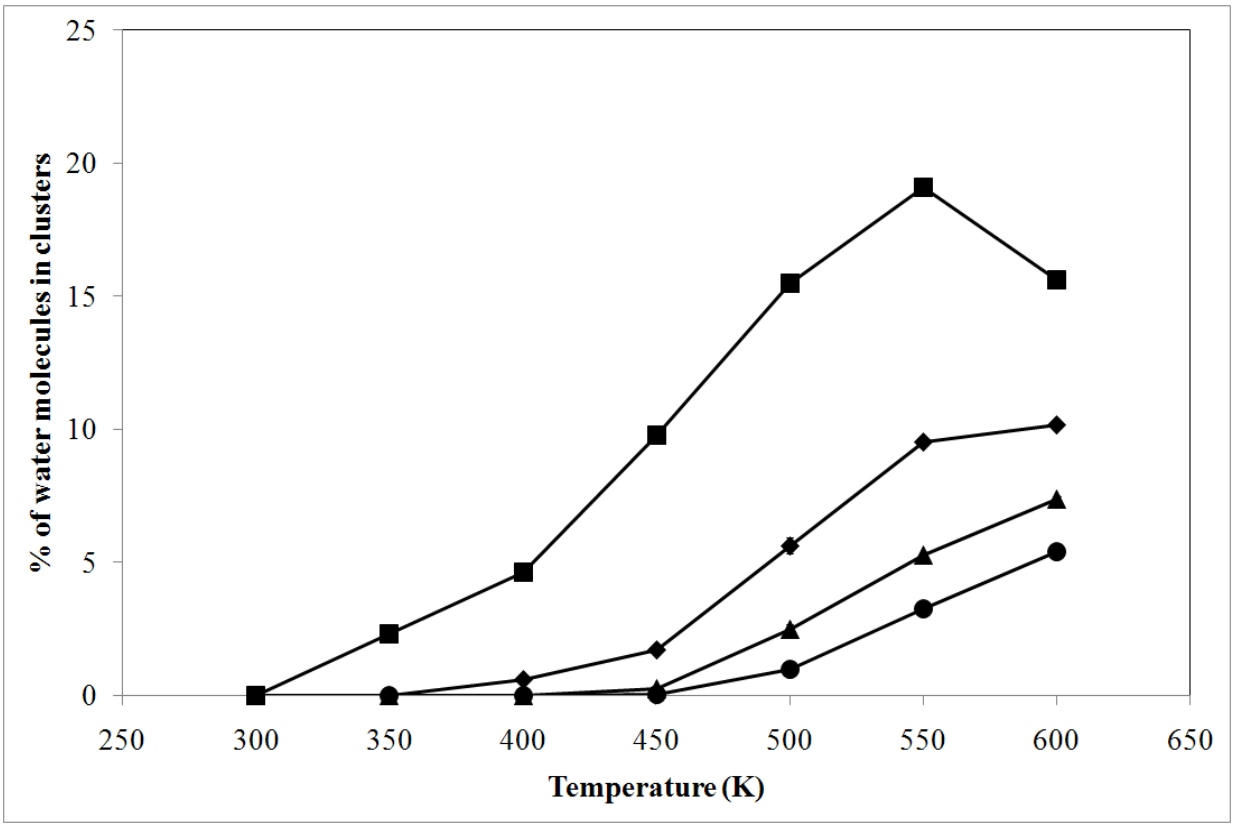

Figure 4-16: Percentage of water molecules included in clusters in the perfluoroalkane phase as a function of temperature at a polymer carbon number of 10. (■) n = 2, (◆) n = 3, (▲) n = 4, (●) n = 5. Lines joining the points have been added as guides for the eye.

The following two figures illustrate the frequency distributions of the most common tetramer and pentamer topologies with respect to temperature for PTFE at a carbon number of 300;

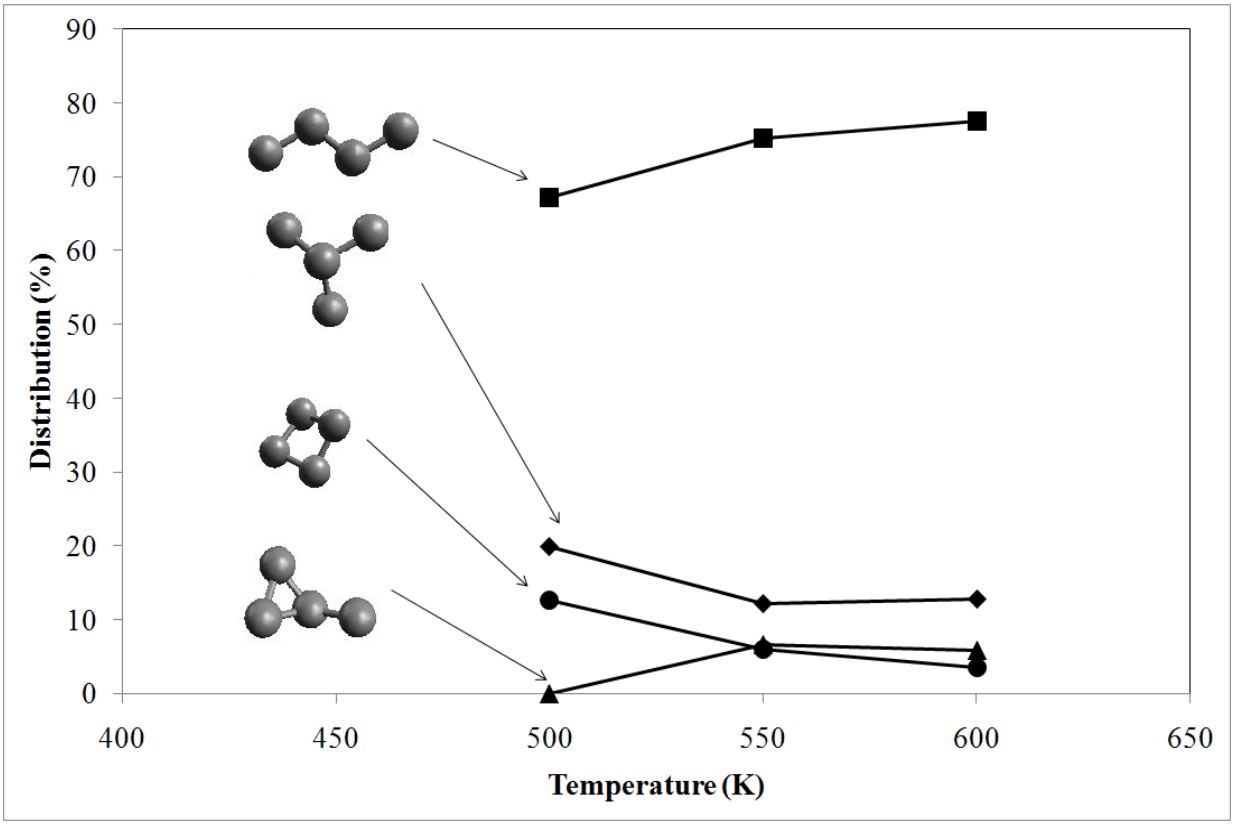

Figure 4-17: Frequency distribution of the four most common tetramer configurations as a function of temperature. Lines joining the points have been added as guides for the eye.

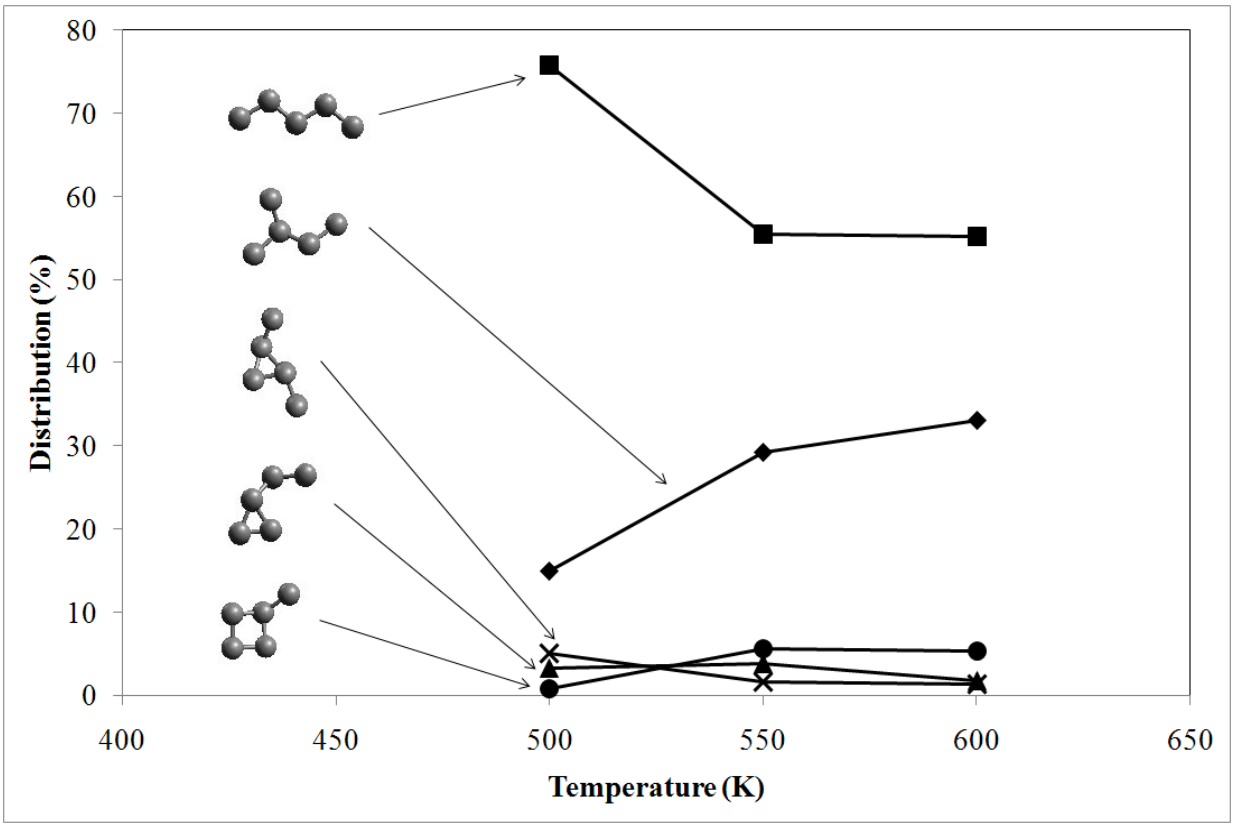

Figure 4-18: Frequency distribution of the five most common pentamer configurations as a function of temperature. Lines joining the points have been added as guides for the eye.

CHAPTER 5: DISCUSSION

5.1 Test system:

The test system(s) of light alcohols + water + n-dodecane was compared to the experimental measurements of Lasich et al (2011). This comparison was conducted in the interests of extrapolation to higher temperatures. The extrapolation simulations were all conducted at a pressure of 400 kPa, to ensure that no vaporization of any species occurred. While this was significantly higher than the pressure in the laboratory experiments being used for comparison (i.e. 101.325 kPa), the work of Tsonopoulos (1999) showed that the influence of pressure on liquid-liquid solubility is insignificant.

As can be seen in the systems containing methanol, the simulations at 313.14 K and 350 K agree closely with the experimental results (see figure 4-1). It should also be noted that the phase envelope did not change significantly between the temperatures encountered in the experimental measurement, and the same was evident regarding the lower of the temperatures encountered in the simulations (i.e. 313.14 K and 350 K). This would suggest that the immiscibility evident in the system is not easily overcome by an increase in temperature. It can be seen that at a temperature of 400 K, the mutual solubility of the system increases, which is just what one might expect for a system exhibiting LLE. This would be due to the existence of multiple phases being restricted to a particular temperature, pressure or composition range, as discussed by Smith et al (2005). At this higher temperature, it can also be seen that the greatest increase in solubility was experienced by n-dodecane in the aqueous phase, but only in the limit where the mole fraction of the methanol tends to unity. The variation in composition with temperature for the organic phase (i.e. the phase dominated by the n-dodecane) was found to be negligible, as evidenced by figure 4-1.

With regard to the systems containing ethanol, a significant deviation from experimental results occurred. This deviation was the absence of a plait point in the ternary LLE data. This suggests that the ethanol and the n-dodecane are not fully miscible together, contradicting the laboratory experiments.

Whilst the experimental measurements over a temperature range from 298.14 K to 333.15 K clearly exhibited a plait point, none of the simulated isotherms for the ethanol systems exhibit this phenomenon. In order to verify that the simulation results could be repeated, a compositional convergence test was conducted. This test entailed selecting a composition in the region in which a single phase was expected, and running simulations to determine if a single-phase or two-phase scenario would result. In the situation encountered in this work, the composition selected was such that both phases were initially fixed at equal compositions, in the region where the plait point was expected. The length of this test was 630,000,000 Monte Carlo moves to ensure that a sufficient number of Monte Carlo moves would be performed for any trends to be observed. This test yielded a result confirming the previous simulations, which can be seen in the following figure;

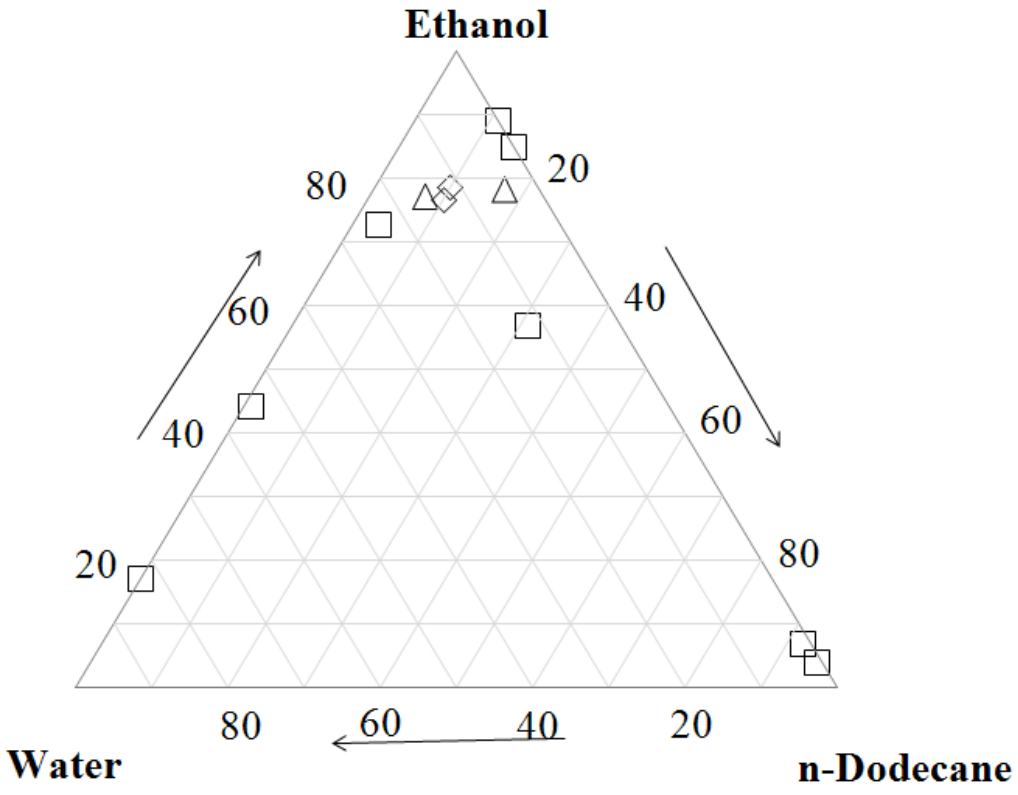

Figure 5-1: Compositional convergence test for the water + ethanol + n-dodecane system at T = 400 K and P = 400 kPa. Values are in mole percent. (□) simulations at T = 400 K, (◇) "starting" compositions at T = 400 K, (△) "final" compositions at T = 400 K. The full results of this test may be found in the appendix to this work.

This test clearly confirmed the results obtained for the simulation, and thus confirms that the simulated results do not compare favourably with the laboratory experiments found in the literature, i.e. Lasich et al (2011). As far as actual values are concerned, the convergence test was initiated at a single phase composition of 75 mole % ethanol, 10 mole % water and 15 mole % n-dodecane, and concluded at two different phase compositions of 73.11 mole % ethanol, 9.96 mole % water, 16.93 mole % n-dodecane and 77.94 mole % ethanol, 9.96 mole % water and 12.1 mole % n-dodecane respectively. This clearly indicated the existence of two distinct phases.

To account for this significant deviation from the experimental data, it was necessary to examine the work from which the force field parameters were derived. In the case of the ethanol, the work of Chen et al (2001) illustrated clear deviations (of the order of 40 %) from experimental VLE data when the n-hexane + methanol and n-hexane + ethanol systems were investigated. This would suggest that the TraPPE parameters for the alcohols and alkanes may not fully describe interactions between these two types of organic compounds. It should be noted that it has been shown by Chen et al (2001) that these parameters were sufficient to describe the pure species properties. Thus, it should be recommended that an adjustment to the Lorentz-Berthelot mixing rules by way of an interaction parameter be undertaken, as in the work of Johansson (2007) when dealing with alkanes and water, in order to allow the TraPPE model to more accurately describe such systems.

With regard to the isopropanol + water + n-dodecane system simulated in this work, the same trends as observed with the simulations of the ethanol + water + n-dodecane system can be observed. A significant observation would then, again, be the absence of a plait point in the ternary LLE data, as presented in figure 4-3. This absence would likely also be due to the same reasons as discussed previously in this chapter for the ethanol + water + n-dodecane system. The main reason for this deviation would thus be the value of the interaction parameter for the Lorentz-Berthelot mixing rules. This interaction parameter would account for the non-ideality in the interaction between the alkane and alcohol species in the system.

As far as general trends regarding the simulations of the systems of light alcohols + water + n-dodecane was concerned, the trend of increased solubility with increased temperature was observed in all cases. This was evident in figures 4-1, through 4-3. The most marked increases in solubility were seen to occur in the systems containing ethanol and isopropanol. In systems containing both of these alcohols, it was observed that the greatest approach to total miscibility occurred in the organic phase, which was dominated by the n-dodecane, in the limit as the mole fraction of the alcohol in the aqueous phase tended to unity. This would likely occur due the interactions between the alkyl constituents of the alcohols and

the purely alkyl n-dodecane. The fact that the n-dodecane is fully alkyl in nature and the alcohols are at least partially alkyl in nature would mean that they are more chemically similar to one another than n-dodecane would be to water. It is this structural similarity that would produce greater interactions between the alcohol-alkane pair as opposed to the water-alkane pair. Thus, the greater mutual solubility between the alcohol-alkane pair encountered in this work would be expected.

Furthermore, the general trends observed in this work correlated with the trends observed for shorter alkanes (n-hexane and n-heptane), as discussed in the literature by Kontogeorgis et al (1999). In this work, a similar disparity in the partitioning of the alcohol (methanol in this case) between the aqueous and organic phases was observed. Additionally, in the aforementioned work of Kontogeorgis et al (1999), the upper limit of the composition of the alcohol in the organic phase was found to be low, which was also observed in this work.

As an additional validation step, a comparison was drawn between the molecules generated in the simulations and those modeled in the open source molecular modeling program, Avogadro (see references), using the Universal Force Field (UFF) for the optimization. When a molecule is constructed in the system using the Gibbs ensemble program, it is built using built-in subroutines and specified parameters. The program's user specifies the parameters for the routines and which routines should be used for each construction step. This process then constructs each molecule pseudo-atom by pseudo-atom. It is not possible to merely provide the Gibbs ensemble program with the identity of the desired molecule which is to be created. Each molecule is user-defined. Therefore, it would be desired to verify that the user has constructed these molecules correctly. This is the reason for undertaking this verification step using an independent method, such as the UFF. The reason for using this force field was that it was applicable to many elements in the periodic table and was not specific to any particular classes of chemicals. Therefore, it could be used consistently to model all of the species encountered in this work. The UFF is derived from the work of Rappé et al (1992). To conduct this comparison, the co-ordinates of a randomly-selected molecule of each species was input into Avogadro (see references), with the appropriate atoms on the relevant sites. The geometric properties of this molecule, i.e. bond lengths and bond angles, were then determined. The reason for not comparing the torsion angles was due to the fact that there are multiple dihedral angles for which the torsional potential energy is at a minimum of some kind (i.e. local or absolute). That this is the case is well documented in the literature, with Cui et al (1998) providing a good example when dealing with perfluoroalkanes in particular. The dihedral angles which may occur in an actual system may also be influenced by neighboring molecules, which would not be the case in an UFF-optimized individual molecule. Since this UFF-optimized individual molecule was the basis of this confirmation step, comparing dihedral angles would thus be irrelevant. These properties were

then compared to a representation of the molecule of interest which was generated from scratch and geometrically optimized in Avogadro (see references). This same procedure was followed throughout the course of this work in order to validate the molecules being generated. A full table of randomly selected molecules compared in this way, using Avogadro (see references), can be found in the appendix 2 to this work. This table covers both the test system(s) and the core PTFE + water simulations in this work. A graphical example of such a geometric validation is presented below, for ethanol;

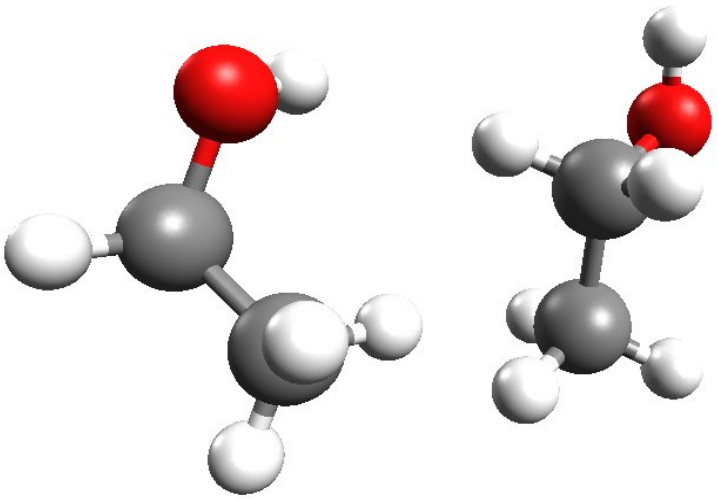

Figure 5-2: Graphical representation of the ethanol modeled in this work (on the left) as compared to ethanol modeled by the UFF (on the right), using Avogadro (see references). It is important to note that the hydrogen atoms shown explicitly in this diagram for the TraPPE ethanol (on the left) do not occur in the model, and instead are accounted for implicitly; they have been included in this diagram for aesthetic reasons.

5.2 Water solubility in perfluoroalkanes:

With regard to the solubility of water in perfluoroalkanes, the intended direct comparison for this work was the previous work on normal alkanes and water performed by Johansson (2007). This comparison was illustrated by figures 4-4 through 4-7. What should be noted about the former pair of these four figures was that the values from the literature represented here were the reported solubility

values using the classical Lorentz-Berthelot mixing rules. What was important to consider for any comparison with such previous work was that, in the case of the work presented here, this mixing rule was not adjusted. The adjustment using an interaction parameter (k_{ij}) can be represented as follows;

$$\varepsilon_{ij} = k_{ij} (\varepsilon_{ii} \varepsilon_{jj})^{0.5} \qquad \text{Eq. (12)}$$

The reason for not adjusting this mixing rule using an interaction parameter was the lack of feasibility. In order to adjust this interaction parameter, the simulated phase compositions or densities would be compared to experimental measurements. This parameter would then be adjusted in order that the simulated values would match the experimental values as closely as possible. The problem encountered in this work was that of the low temperatures at which the available data was measured, along with the limited nature of these data sets. The data in question was that of Freire et al (2006, 2010). The experiments in this prior work were conducted over a temperature range of 288.15 K to 318.15 K, and over a carbon number of 6 to 9 carbon atoms. This low temperature would result in problems with the acceptance of interphase swap moves, especially when the larger fluoroalkane molecules were being dealt with. For example, the percentage of accepted swap moves encountered in the low temperature simulations (i.e. at T = 300 K) for perfluorodecane in this work was of the order of 1 out of every 9,000,000 attempts (i.e. ~$1x10^{-7}$ percent!). This problem with the Gibbs ensemble technique was discussed in chapter 2.1.4 of this work, and more thoroughly by Gubbins (1993) and Johansson (2007). This low probability of swap move acceptance would thus hinder the development of any reliable statistics in the system being analyzed. In addition, the actual values states in the work of Freire et al (2006, 2010) were of the order of 0.01 mole percent, which was below the most precise statement of any compositions possible in this work, due to the size of the systems being analyzed (i.e. ~0.1 mole percent). This precision issue was discussed in greater detail in chapter 4.1 of this work. It was for these reasons that the simulations were conducted without interaction parameter adjustment.

What was evident from the plots of the solubility data presented in figures 4-4 and 4-5 was that similar general trends were present for both normal alkanes and perfluoroalkanes. That is, the solubility of water in the alkane/perfluoroalkane was not significantly dependent on carbon number for carbon numbers from 8 up to 16 carbon atoms at a fixed temperature of 450 K. For alkanes, this approximately constant value was ~4 to ~6 mole percent water, and for perfluoroalkanes it was ~1 to ~2 mole percent water.

With regard to the temperature dependence of the solubility of water in perfluoroalkanes and

alkanes, similar trends were again observed. This trend was that of an exponential-type variation of solubility with increasing temperature. What should be noted here is that the values stated for the alkanes is in reference to the penultimate solubility values taken from the literature, with the appropriately adjusted interaction parameter. As stated in the previous paragraph, some caution should be used when dealing with the simulations conducted at temperatures of ~300 K, since the percentage of accepted swap moves was exceedingly low, although when the compositions of the phases were analyzed as a function of the number of moves applied to the system, the values were seen to be stable. Another important point to note was that the actual values of the solubility of water for temperatures below ~400 K were actually below the threshold of the precision of any stated compositions in this work (i.e. of the order of 0.1 mole percent). This precision issue was discussed in greater detail in chapter 4.1 of this work. Thus, even if the statistics generated were insufficient for these low temperatures, the extremely small values encountered would have precluded their usefulness anyway. Also, as the aim of this portion of the solubility analysis was to determine trends and general temperature- and carbon number-dependence, the results obtained were sufficient.

It is also important to note that the literature data used for the comparison made use of the SPC water model. In contrast, this study used the SPC-E water model. However, a precedent has in fact been set in the literature for direct comparison, namely the work of Bolton et al (2009). In this work, data for the solubility of water in PE generated using the SPC water model was directly compared to data generated using the SPC-E. However, it should be noted that as these are two different water models, perhaps any comparison may provide some indication as to the order of magnitude of the solubility. This approximate, order of magnitude approach would then provide one with a rough idea as to the solubility of water into various polymers using different water models. This important point should also be considered for the systems of water + PTFE.

5.3 Polymer generation:

The polymer co-ordinates which were generated by the Python routine written for this project were used for some of the polymer simulations in this work. The polymer simulations it was used in were those where the carbon number was between and not including 16 and 300. The polymer program ran to completion successfully using the co-ordinates generated by the Python routine. The trends observed for the simulations which used these co-ordinates concurred with those observed for all of the other systems.

Thus, the polymer co-ordinates which were generated by the Python routine have been validated.

A significant shortcoming of the polymer generation routine was found to be in generating large molecules, of the order of ~70 carbon atoms or longer. In generating such large molecules, the simplistic nature of the "straight chain" generation algorithm used in this routine hindered the development of curved chains. This curvature would be dependent not only on the bending energy of the molecule, but also the stretching and torsional potential energies. These energies were modeled using the TraPPE and Cui models in this work, as discussed in chapters 2.1.1 and 6.8 respectively. The lack of such curvature in the PTFE chains would result in the confinement of these chains to within cubic regions of a size directly proportional to the lengths of the chains, since such chains cannot "bend" or twist in any way whatsoever. This arrangement of the molecules would then result in problems when the end-bridging scheme of the polymer program was to be used (this scheme was discussed in chapter 2.1.12), since there would thus be very limited options for the end-bridging scheme to be applied to. To overcome this shortcoming, the initial co-ordinates which were used for the long PTFE chains (i.e. 300 carbon atoms in this work) were those of the polyethylene molecules used in the work of Johansson (2007).

5.4 Water solubility in PTFE:

As in the work of Johansson (2007), it was found that the solubility of the ten carbon chain in water was extremely low. It was found to so low as to be negligible, since it was at least two orders of magnitude below the previously stated precision of the phase compositions in this work. Thus, the ten carbon chain was used as a surrogate for the polymer in the Gibbs ensemble portion of the program. In order to validate this, a 16 carbon chain was used in a simulation of the short polymer molecule. This data point was compared to the previously obtained measurement, and it was found that the solubilities obtained agreed favourably. This raw data may be found in the appendix to this work.

Upon examination of figures 4-9 and 4-10, it was apparent that there was a plateau for the solubility of water into PTFE which was a function of both carbon number and temperature. In order to verify the observation of this plateau region, an additional data point was simulated. This data pointed consisted of a system where the ratio of water molecules to PTFE molecules was doubled. This was conducted due to the observation that the plateau region occurred at close to the maximum possible solubility of water into the PTFE. This maximum may obtained by the observation that the system consisted of 500 water molecules and 10 PTFE molecules. If all of the water molecules are placed into the

polymer phase, a value obtained would be 98.0 mole percent water. It should be noted that the "water-rich" phase contained no polymer molecules whatsoever. This verification step was conducted for a polymer chain length of 50 carbon atoms. This verification step resulted in a system in which there were 500 water molecules and 5 PTFE molecules, as opposed to the usual 500 water molecules to 10 PTFE molecules used in the other data points. The result of this verification step was found to agree closely with the previously-obtained data. This result is to be found in the appendix to this work.

The solubility of water, on a molar basis, observed in the PTFE was found to be vastly greater than that in PE, as evidenced by figure 4-11. This would not be surprising though, if one considers the molar densities of PTFE as compared to PE at comparable polymer carbon numbers. The mass density of high-density polyethylene is ~950 kg/m^3 at 25 ^oC (according to Dynalab Corp – see references), whereas the mass density of PTFE is ~2160 kg/m^3 at 25 ^oC (according to Boedeker Plastics – see references). Using a polymer carbon number of 300 carbon atoms then yields molar densities of ~0.14 $kmol/m^3$ and ~0.23 $kmol/m^3$ for PTFE and PE respectively. Thus it is apparent that there are far fewer PTFE molecules in a given volume than PE molecules, and therefore there would be more free volume in PTFE than in PE. This may be further illustrated by comparing the nature of the Lennard-Jones potential between the constituents of the PTFE molecules as opposed to those of the PE molecules, as illustrated in the following plots;

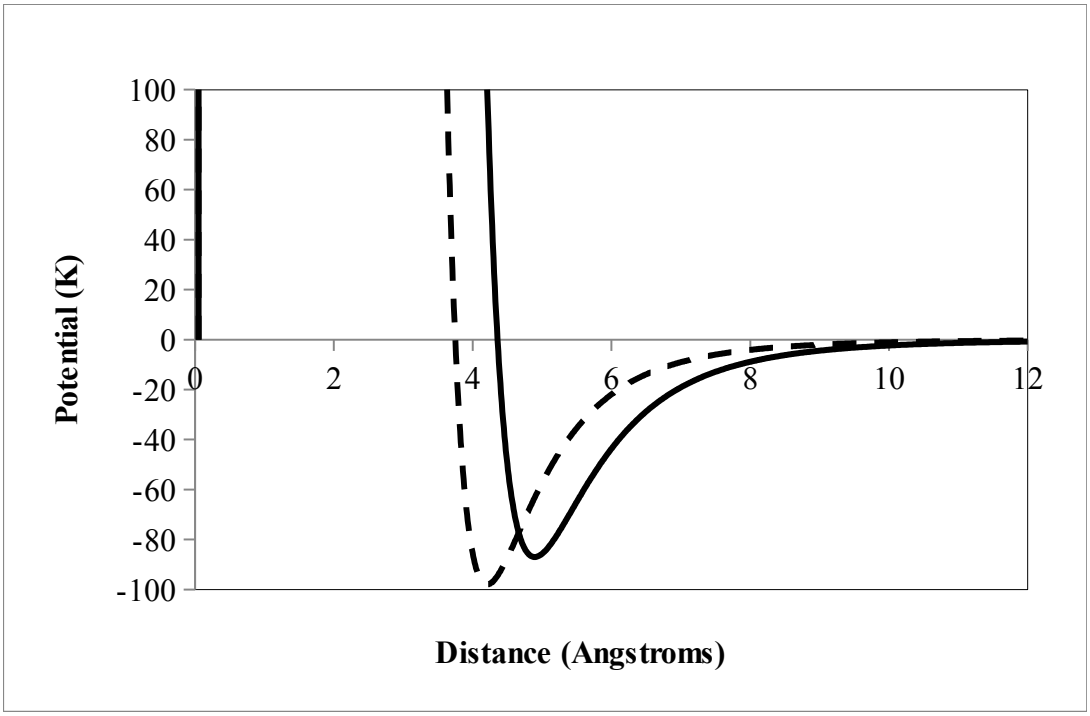

Figure 5-3: Lennard-Jones potential between pairs of atoms at the ends of linear polymer molecules. (-) CF_3-CF_3 pair, (--) CH_3-CH_3 pair. This plot was constructed using a distance resolution of 0.05 Ångströms.

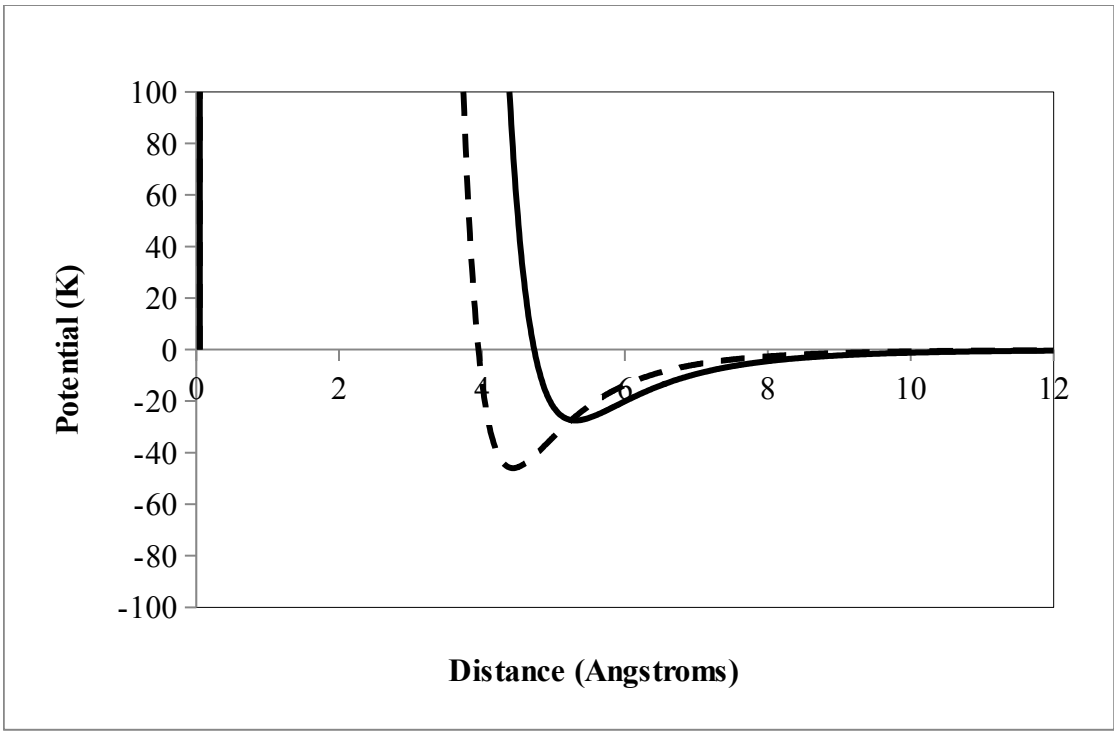

Figure 5-4: Lennard-Jones potential between pairs of atoms along the chain of linear polymer molecules. (-) CF_2-CF_2 pair, (--) CH_2-CH_2 pair. This plot was constructed using a distance resolution of 0.05 Ångströms.

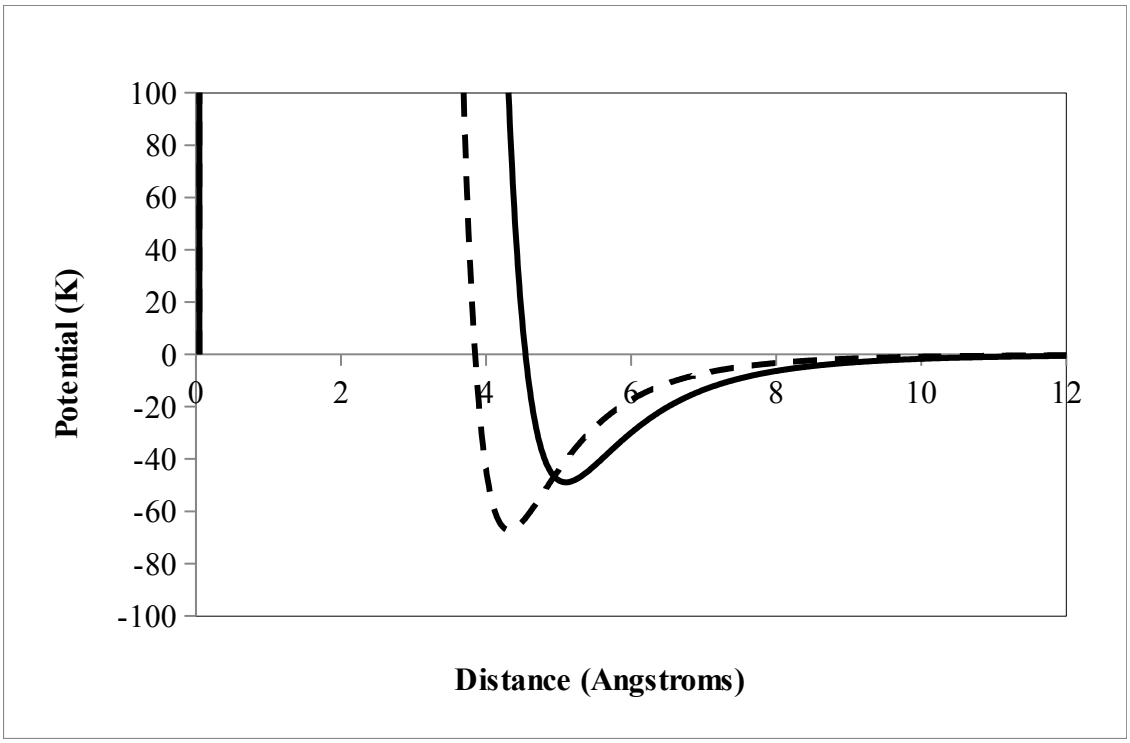

Figure 5-5: Lennard-Jones potential between an atom on the end and an atom along the chain of a linear polymer molecule. (-) CF_3-CF_2 pair, (--) CH_3-CH_2 pair. This plot was constructed using a distance resolution of 0.05 Ångströms.

Figures 5-3 through 5-5 clearly illustrate that the most energy favorable distances between PTFE molecules are greater than between PE molecules, by a margin of ~20 percent (5 Å versus 4 Å). This distance increase may then be translated into a volume increase of ~95 percent for PTFE versus PE.

In order to determine whether the system temperature would result in similarly large water solubilities in the polymer for other polymers, a further simulation was performed for polyethylene + water at 600 K. This would then serve to provide evidence in favour of the acceptability of the high solubility of water in PTFE found in this work. At 600 K it was found that the polymer phase consisted of 88.1 mole percent water. This result then would suggest that similarly high solubilities of water into the polymer are possible for other polymers. This result may be found in the full set of PTFE + water simulation data presented in the appendix to this work.

The increased void size observed by plotting the Lennard-Jones potential concurs qualitatively with the work of Dlubek et al (1998), in which the free volume found in PTFE and PE was compared by way of positron probing. In this work, it was found that the average hole size in PTFE was roughly twice

the size of the average hole in PE at the same temperature, with peak values of ~0.37 nm^3 for PTFE and ~0.18 nm^3 for PE at a temperature of 300 K. Using these void volumes, and using the radius of a water molecule of 1.5828 Å, as stated by Tamai et al (1995) – which yielded a spherical volume of ~0.0166 nm^3 – it becomes apparent that in an average void in PTFE, it would be possible fit a maximum of ~22 water molecules as opposed to ~11 water molecules in an average-sized void in PE (this is, of course, not taking into account the interactions between the water and the PTFE/PE molecules, and so is a purely geometric maximum). Thus, it would be entirely reasonable to expect to find significantly more water inside a body of PTFE as compared to PE. It is important that caution should be used when using this quick calculation to determine quantitative simulation results, as the radius of the water molecule model which is used in any particular simulation is applicable, not the radius of a physical water molecule. Thus, the analysis discussed in this paragraph should be taken qualitatively, in that there may be possibly twice as many water molecules per void in PTFE as compared to PE, not necessarily 22 as compared to 11.

By looking at the Lennard-Jones potential between the water molecules and the polymer constituents of PTFE and PE (i.e. the chain-end molecules and the molecules lying on the middle of the polymer chains), trends regarding intermolecular spacing may also be observed. The relevant plots are as follows;

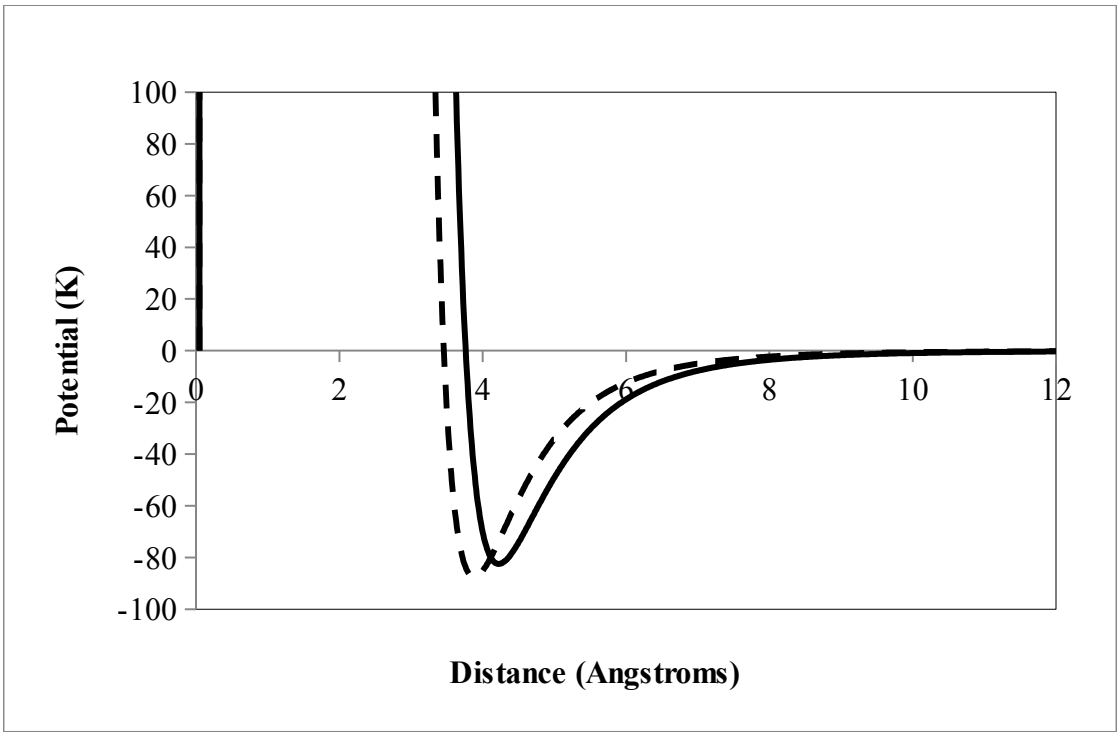

Figure 5-6: Lennard-Jones potential between a water molecule and an atom on the end of a linear polymer molecule. (-) H_2O-CF_3 pair, (--) H_2O-CH_3 pair. This plot was constructed using a distance resolution of 0.05 Ångströms.

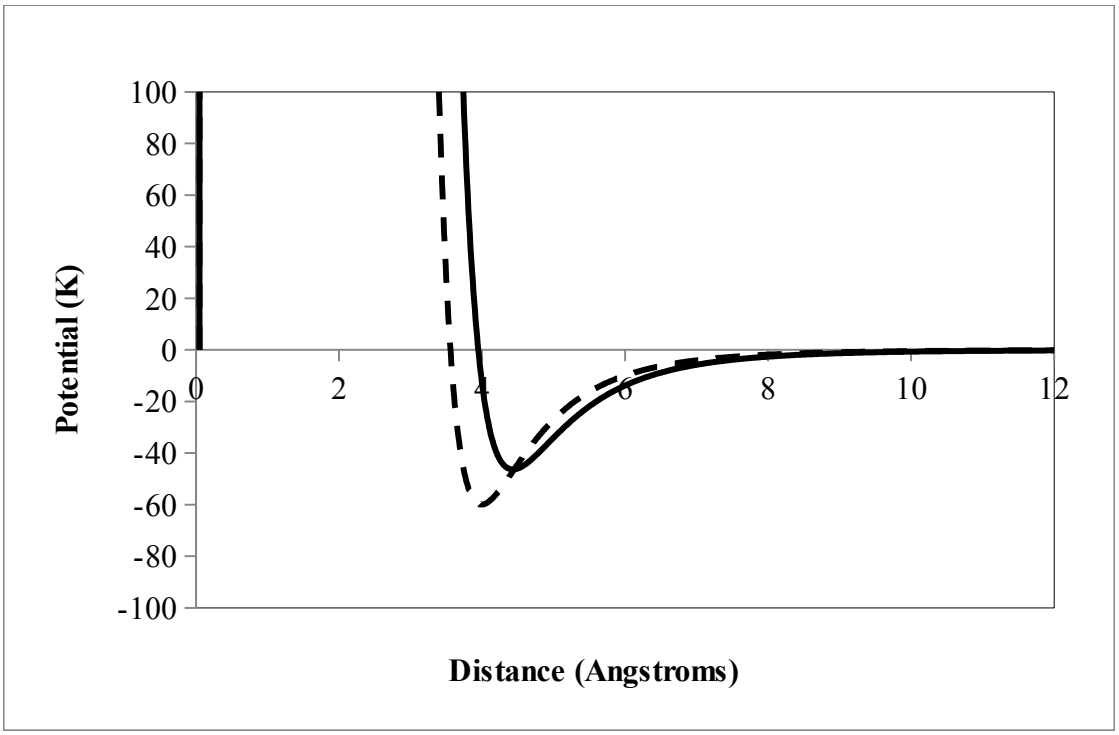

Figure 5-7: Lennard-Jones potential between a water molecule and an atom along the chain of a linear polymer molecule. Solid lines are for the H_2O-CF_2 pair, dashed lines are for the H_2O-CH_2 pair. Plot was constructed using a distance resolution of 0.05 Ångströms.

Figures 5-6 and 5-7 clearly illustrate that the most energy-favorable distance for water molecules to be found at in PTFE matrices is slightly larger than in matrices of PE molecules; by ~13 percent along the carbon numbers (~4.5 Å versus ~4 Å) and by ~8 percent at the chain ends (~4.2 Å versus ~3.9 Å). That this increase from PE to PTFE is not as great as the increase in distance found between polymer molecules (as shown in figures 5-4 and 5-5) would then suggest that a greater number of water molecules would be found in the spaces between PTFE molecules as compared to PE molecules. This concurs with the aforementioned findings of Dlubek et al (1998).

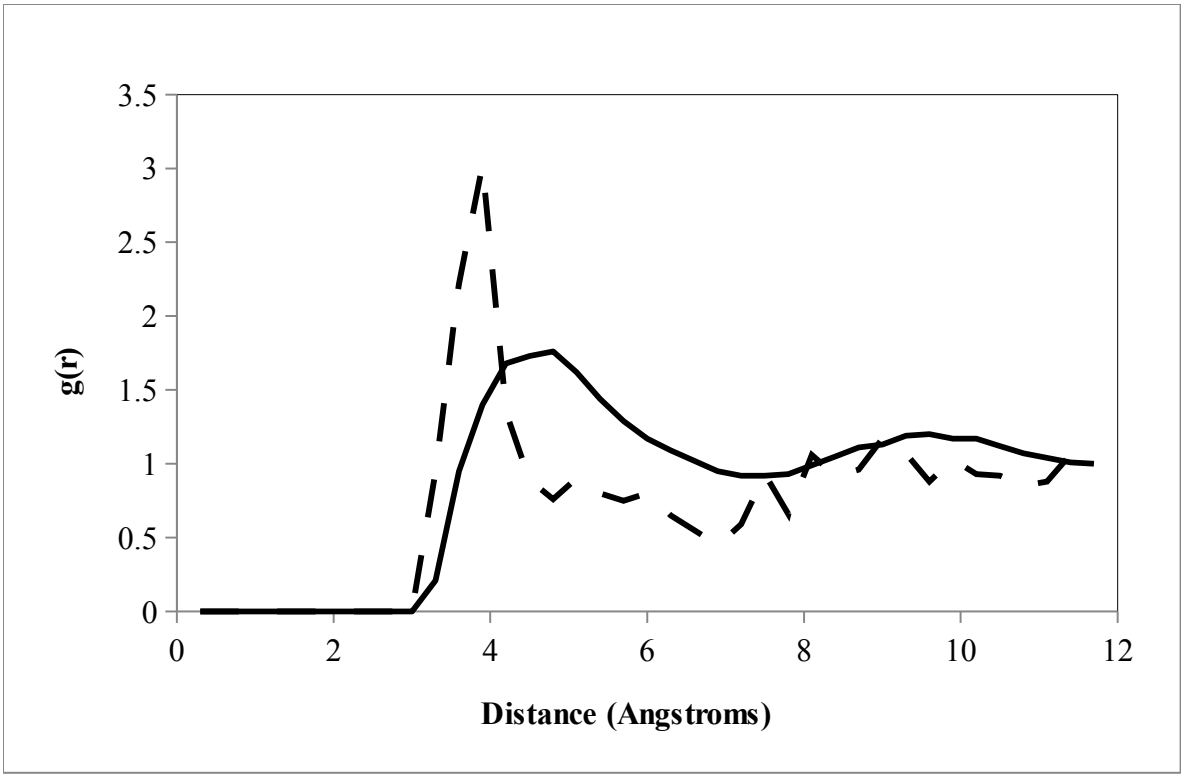

Figure 5-8: Radial distribution function of water in PTFE, for a carbon number of 300 at conditions of T = 450 K and P = 2 MPa. Solid lines are for the H_2O-CF_2 pair, dashed lines are for the H_2O-CF_3 pair.

Further insight into the ordering of the PTFE molecules can be gained by examining the radial distribution functions (RDFs) of the water molecules with relation to the end atoms and atoms along the length of the polymer chain. These RDFs can then be compared to RDFs obtained for the water-PE system, as presented by Johansson et al (2007). The relevant plot, normalized by comparison to the water density in the bulk material, is as follows;

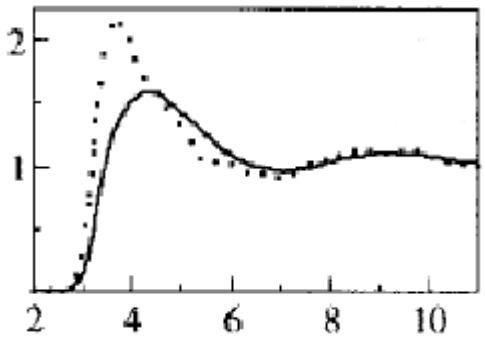

Figure 5-9: Radial distribution function of water in PE, for a carbon number of 300 at conditions of T = 450 K and P = 600 kPa. From Johansson et al (2007). The solid line is for the H_2O-CH_2 pair, the dotted line is for the H_2O-CH_3 pair.

A comparison of the amplitudes of the peaks for the PTFE RDF would suggest a greater degree of ordered supramolecular structuring in the PTFE matrix as compared to the PE matrix. This is evident by the higher amplitudes of the peaks in the RDFs presented in figures 5-8 and 5-9. Such higher amplitudes would suggest that the probability of occurrence of water molecules is more restricted to specific regions in PTFE as compared to PE. Highly ordered supramolecular structure is a feature found most evident in crystalline solids. In these solids, the molecules confined only to certain discrete regions in space. In a n amorphous liquid, it is more usual for the molecules to not be confined to certain discrete regions of space. This increased level of ordering was also found by Friedemann et al (2001) in their investigation into clustering of alkanes and perfluoroalkanes. In their study, Friedemann et al (2001) also found that the perfluorinated forms of the alkanes being investigated were far more rigid than the alkanes themselves. From this it can be inferred that as the polymer chains would be induced to move further apart due to increasing temperatures, the rigid perfluoroalkanes would leave a more free volume between themselves as compared to the alkanes. This greater free volume would this lead to higher water solubilities in the perfluoroalkanes than the alkanes. Another consideration would be the effect of increasing polymer carbon number coupled with this perfluoroalkane rigidity. Since a linear alkane molecule can become more knotted the longer it gets, the difference in supramolecular structure caused by perfluoroalkane rigidity would thus become more apparent at larger polymer carbon numbers. The increasing differences in structure between PTFE and PTFE molecules is apparent upon examination of water solubility data. These differences become more pronounced at longer polymer chain lengths. As the polymer chain length increased, the differences between the PTFE + water and PE + water solubility data became more apparent.

A further point of importance to analyse was the irregular break in the general monotonic trends of the system. This was observed to occur between carbon numbers 10 and 12, as illustrated by figures 4-9 and 4-10, as well as in the results of the cluster analysis (chapter 4.5). In all of these sets of data it would appear that there would be two different smoothed trends, one going up to carbon number 10, and another continuing from carbon number 12. This clearly indicates a change in structure in the perfluoroalkane occurring when the molecule reaches a length of ~12 carbon atoms. If one considers the work of Jang et al (2003), then it becomes apparent as to why this irregularity may be occurring. As discussed in chapter 2.2, it can be inferred from the data of Jang et al (2003) that a change in helical energy contributions between carbon numbers 10 and 12. At carbon numbers less than and equal to 10 carbon atoms, it was found in the aforementioned work that Coulombic forces provided more energy than the total fluorine-fluorine interaction towards the helical to all-trans conformation transformation, whereas the scenario was reversed at carbon numbers larger than or equal to 12 carbon atoms. The aforementioned work did not contain any data for a chain length of 11 carbon atoms. The relevant graph from Jang et al (2003) can be found following;

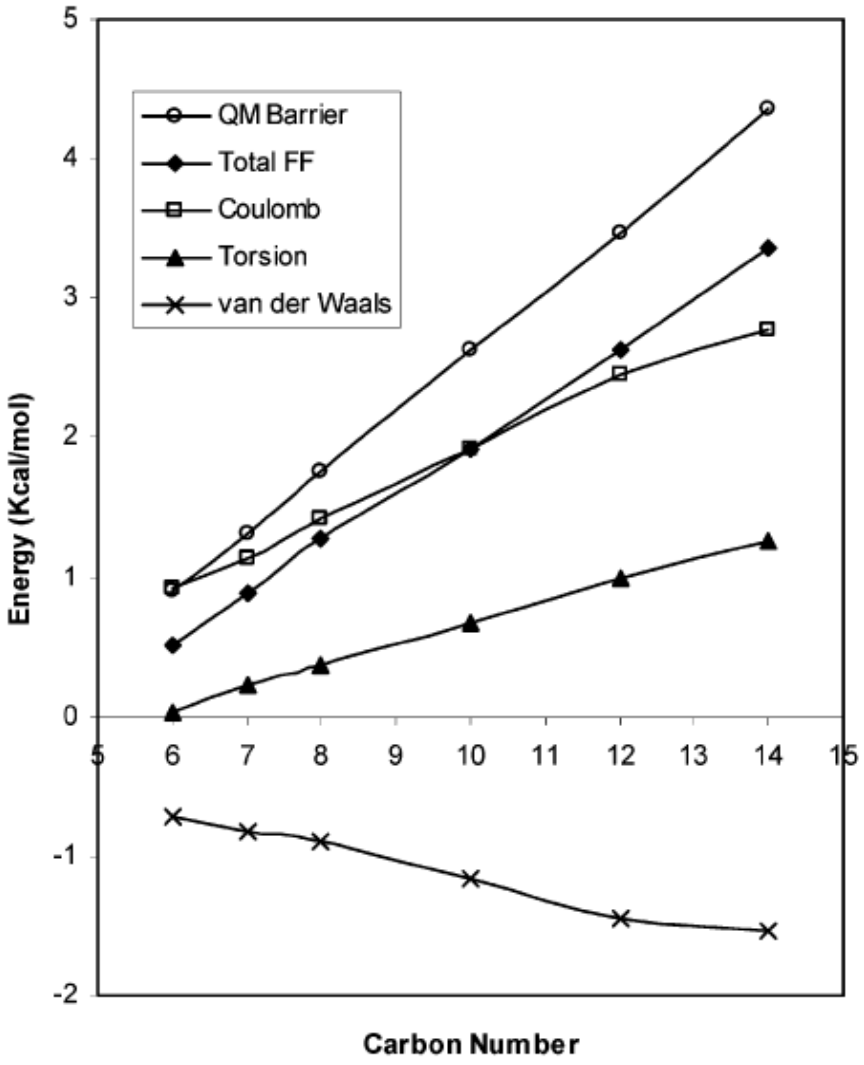

Figure 5-10: Energy components for the helical to all-trans conformation transformation of perfluoroalkanes versus carbon number. From Jang et al (2003).

It is also possible to examine the average total intramolecular energy of each species in the system. Such data may be found among the various output files produced by the Gibbs ensemble program. Following may be found a plot of these intramolecular energies;

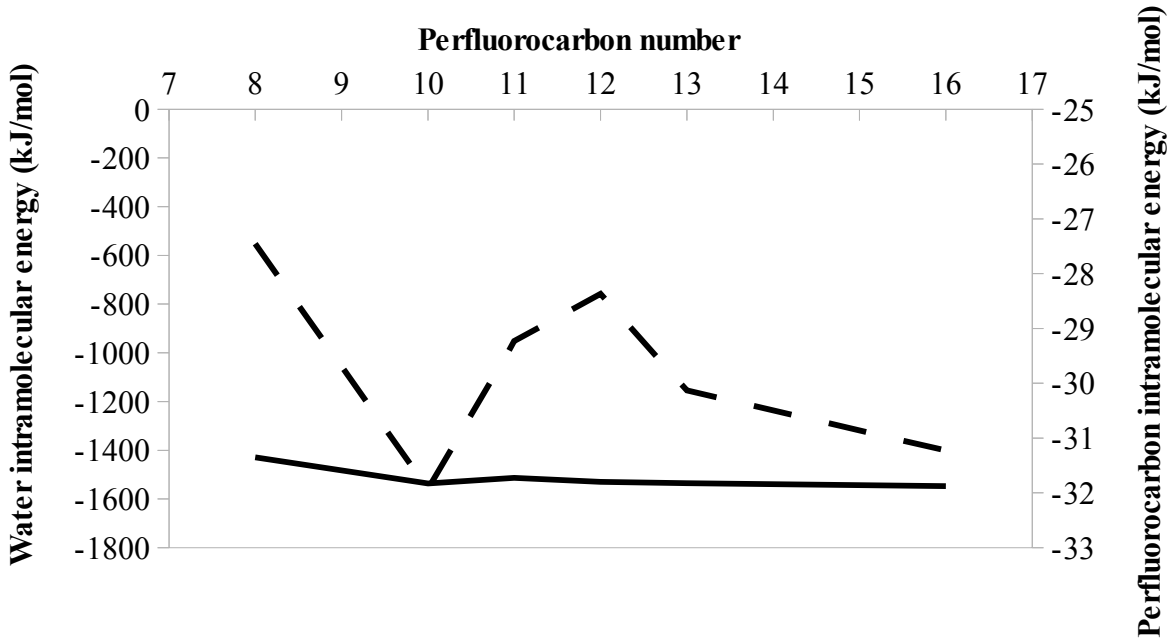

Figure 5-11: Average total intramolecular energy of the linear perfluorocarbon and water molecules as a function of perfluorocarbon carbon number, at T = 600 K. The dashed line is for perfluorocarbons, the solid line is for water.

The analysis presented in figure 5-11 was performed at a temperature of 600 K. This was due to the irregularities in the clustering and solubility data being most pronounced at higher temperatures. Figure 5-11 clearly illustrates a peak in the intramolecular energy of the perfluorocarbon molecules at a carbon number of 12. In contrast, the intramolecular energy of the water molecules remains largely constant across the entire range of carbon numbers. This then concurs with the inference obtained from the literature. However, further investigation on the effects upon the intramolecular structure of perfluorocarbons should be undertaken before any firm conclusions may de drawn.

5.5 Cluster analysis of water molecules:

The water cluster topologies encountered in this work were directly compared to the work of Johansson (2007). The different types of geometric arrangements of the water clusters encountered in this work were defined along the same lines as Johansson (2007).

Upon examination of figures 4-13 through 4-15 it was apparent that as a function of carbon number, the size of the water clusters would decrease significantly, to the point that there were negligible fractions of water molecules in clusters of larger than two molecules at a carbon number of 300. It was also found, in figure 4-16, as well as in the aforementioned three figures, that as a function of temperature, the fraction of water molecules in each of the cluster sizes increased, thus indicating that as the temperature increased, there were more water molecules in all clusters. This concurs with the observations from the figures 4-9 and 4-10, and figure 4-16, since in these figures the solubility of water increases with temperature, and thus it would be reasonable to assume that with this greater number of water molecules in the perfluoroalkane phase, more water molecules would be found in clusters at higher temperatures.

A further point to note would be the appearance of the curves for each of the different cluster sizes illustrated in figure 4-16. In this figure, it is apparent that there is a peak at ~550 K for bimolecular which then decreases at higher temperatures. It can also be seen that for trimolecular clusters, there may be some sort of leveling-off behavior occurring, whilst the frequency of tetramolecular clusters seems to increase more rapidly at the highest temperatures encountered in this study. This trend concurs with the work of Johansson (2007) and Johansson et al (2005), in which it was seen that for each cluster size, there was a particular temperature at which maximal frequency was to be found. For pure water vapour, it was found by Johansson et al (2005) that the temperature for maximal dimer frequency was between 550 K and 600 K, using the SPC-E water model. For water in PTFE, it can then be concluded from this work that the temperature for maximal dimer frequency would be ~550 K. This value is somewhat different to that found by Johansson et al (2005) due to the differences in the water models being used; SPC-E - this work - versus SPC – Johansson et al (2005). The determination of the temperature at which this maximal frequency of larger clusters may occur is inherently limited by the critical conditions of the water model being used, as well as the critical conditions of any other species in the system. This is due to the requirement that the system being studied should be subcritical, in order for phase separation to occur.

In chapter 5.4, the nature of the arrangement of water molecules within the PTFE matrix was discussed, which may also shed light onto the observed clustering behavior of water in PTFE as compared to PE. In PE, it was found by Johansson et al (2007) that there were significantly more water molecules at the chain ends in PE than along the length of the PE molecules (see figure 5-9). In this work, as evidenced by figure 5-8, the same was found to be true, with more water molecules being found at the polymer chain ends than along the length of the polymer chain. This should be expected, though, due to steric effects, as discussed by Johansson (2007).

A further factor contributing to the decreased water clustering observed in PTFE as compared to PE would be the observation of the spacing of water molecules inferred from figures 5-8 and 5-9. The larger ratio of the second peak to the first peak found in PTFE as opposed to PE would suggest that the water molecules are not as densely-packed around the PTFE molecules as they are around PE molecules. This lower density of water molecules around the PTFE molecules would then also result in fewer water clusters forming, as there are fewer water molecules in close proximity which could interact with each other through, for example, Hydrogen bonding.

Upon examination of figures 4-4 and 4-5, and figures 4-9 and 4-10, it can be seen that there is an irregularity at a polymer carbon number of ~12 carbon atoms. This ties in with the details discussed in chapter 5.4. Essentially, it can be inferred from the data of Jang et al (2003) that there is a change in the regime of the energy contributions towards the helical to all-trans conformation transformation from a polymer carbon number of 10 upwards. Therefore, it may be expected that the clustering behavior of water molecules would differ at polymer carbon numbers greater than 10.

It can also be seen that the irregularity at carbon number 12 becomes increasingly less apparent at higher temperatures for the smaller water clusters. However, it becomes increasingly apparent for the larger water clusters at the higher temperatures. This may be expected if one considers that the free volume increases greatly at the higher temperatures. This is due to the rigidity of the perfluoroalkane chains. At these higher temperatures then, there will be voids of increasing size in which water clusters may be found. Therefore, the probability of small water clusters to encounter a perfluoroalkane chain decreases significantly with increasing temperature. Meanwhile, increasing void size may lead to larger and larger water clusters forming. These clusters will in turn be in contact with the perfluoroalkane chains. This will continue until thevoid sizes increase further so as to drastically decrease the probability of this occurring too. Essentially, the influence of the helical structure of PTFE will decrease for a given water cluster size with increasing temperature. This is due to the decreasing proportion of the free volume within the PTFE matrix being adjacent to the PTFE molecules themselves.

Further insight into the clustering of water molecules within the PTFE can be gained from detailed examination of the frequency of occurrence of particular arrangements of the water molecules as a function of temperature, as well as an examination of the binding energy of the clusters as a function of temperature. A similar analysis was conducted for water clustering in PE by Johansson et al (2007). The results of this type of analysis can be found in figures 4-17 and 4-18. What was apparent in these figures was that at higher temperatures, the formation of linear tetramers and pentamers was increasingly favorable. With regard to tetramers, it was evident from figure 4-17 that the vast majority of clusters were

linear, whilst for pentamers a branched linear structure (see the second series in figure 4-18) was most prevalent. In figure 4-18 it was also seen that at from a temperature of 500 K to 550 K there was a significant shift in frequency distribution, with the aforementioned branched structure dropping in frequency from ~75 % to ~55 %, whilst the linear pentamer increased in frequency from ~15 % to ~30 %. Previous computational and experimental work has shown that for water structures up to pentamers, the minimum energy structures are cyclic, according to Kabrede & Hentschke (2003). However, it was found by Johansson et al (2005) that at higher temperatures, open (i.e. linear) water structures tend to dominate, due to entropic effects. These entropic effects are due to the entropies of the cyclic water structures as compared to the linear water structures. These effects have also been observed experimentally by Mhin et al (1993). Therefore, the trends observed in this work concur with the observations of Johansson et al (2005), in that linear structures are seen to be increasingly prevalent at higher temperatures.

In order to further examine the supramolecular structuring of the perfluoroalkane matrix in comparison to the alkane matrix, the binding energy of the water clusters may also be examined. This "binding energy" refers to the energy that keeps the water molecules bound together in the cluster. This "binding energy" is more commonly known as the Hydrogen bond energy. The binding energy for the water molecules found in this work can be found following;

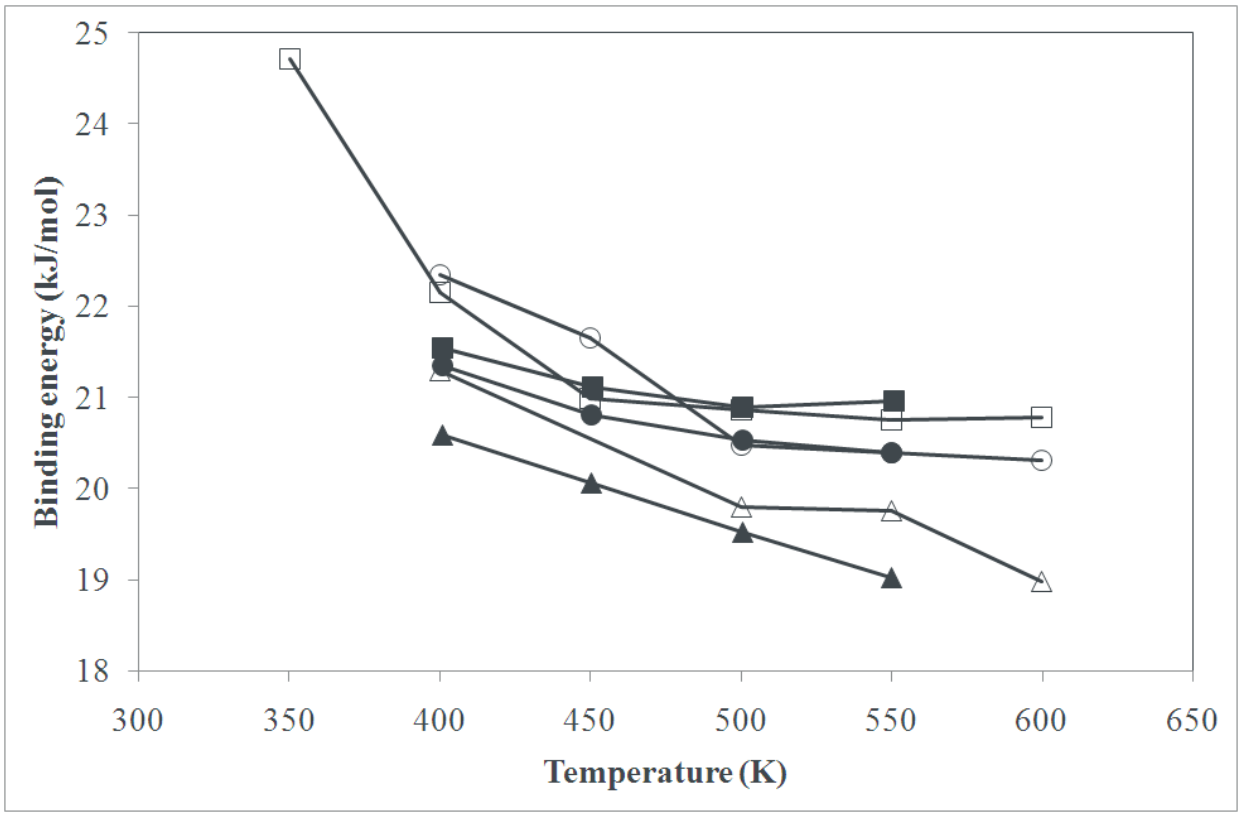

Figure 5-12: Dimer and trimer water cluster binding energy versus temperature in perfluorodecane and decane. (■) dimers in decane, (□) dimers in perfluorodecane, (●) linear trimers in decane, (○) linear trimers in perfluorodecane, (▲) cyclic trimers in decane, (△) cyclic trimers in perfluorodecane. Lines have been added between the points as guides for the eye. The data for the decane is from Johansson et al (2007).

What can be observed in figure 5-12 is that at the lower temperatures, the binding energies of the water clusters are higher in perfluorodecane than in decane, whilst the binding energies are fairly similar for perfluorodecane and decane as the temperature increases. At the lower temperatures, this higher binding energy, which is noticeable for all of the topologies in figure 5-12, suggests that there may be denser packing of the perfluorodecane molecules at lower temperatures than occurs in the decane. At the lower temperatures, the denser packing does not appear to be totally in evidence, as only the cyclic trimers have higher binding energies in perfluorodecane than in decane. This suggests that it is simply more difficult and less probable for water molecules to form cyclic structures in perfluorodecane than in decane, whilst the reverse appears to be true of the linear water clusters, both in the case of dimers and trimers. In this regard, it is possible that future study into the geometry of the free volume in

perfluoroalkanes as compared to alkanes may shed further light on the matter.

Another topic to examine is the extent to which perfluoroalkane molecules influence the configuration of water molecules. This may be achieved by comparison to pure, saturated water vapour. The comparison to pure saturated water vapor was undertaken as this possessed a similar density to the water found in the polymer matrix. A similar study for the polyethylene/alkane + water system was undertaken by Johansson (2007), which illustrated that the alkane molecules themselves did not play a significant role in affecting the clustering behavior of the water molecules, except at temperatures lower than ~ 450 K.

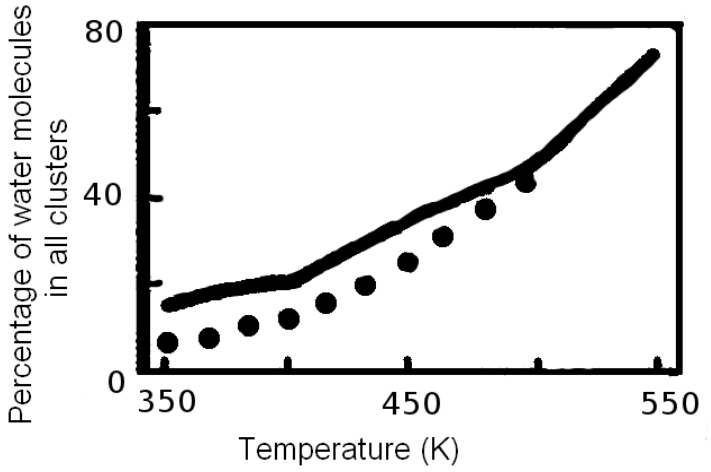

Figure 5-13: Percentage of water molecules in all clusters versus temperature for the decane + water system compared to pure saturated water vapor. (-) water in decane, (··) pure saturated water vapor. From Johansson (2007).

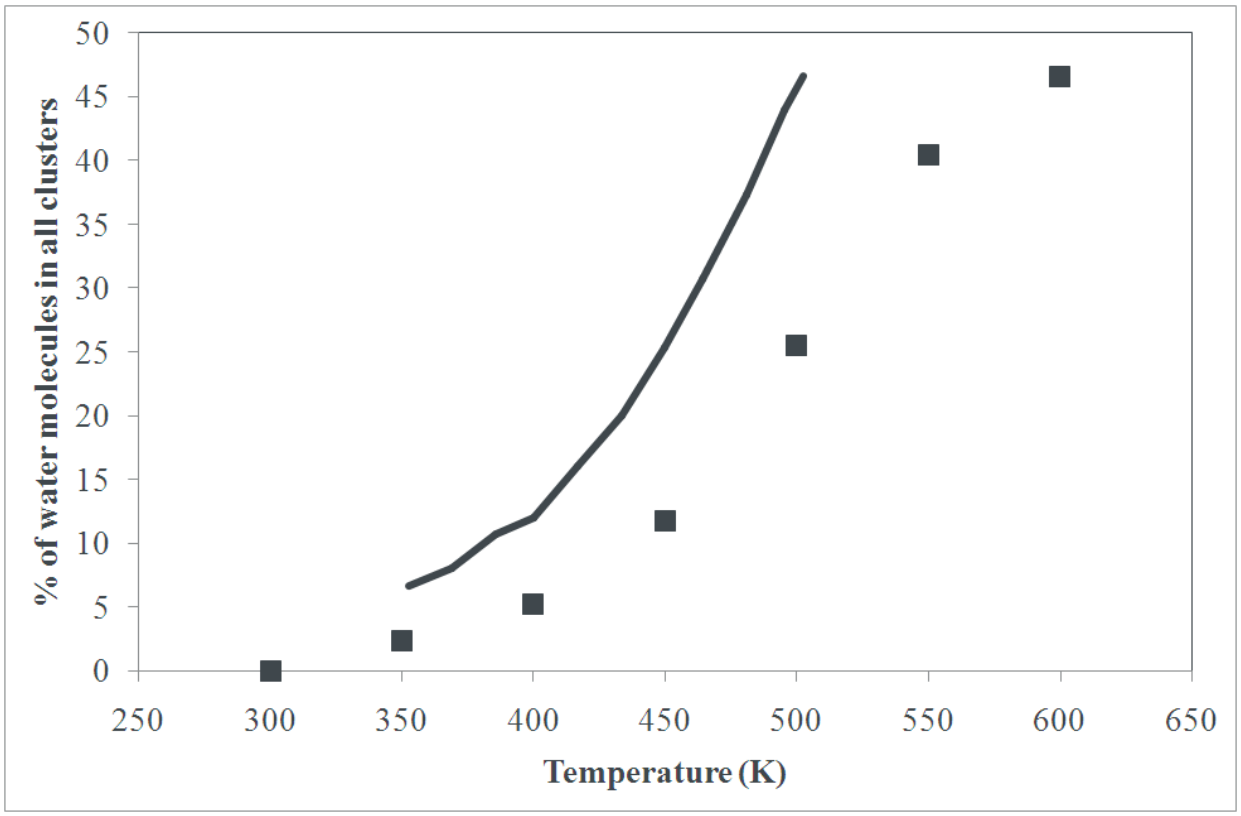

Figure 5-14: Percentage of water molecules in all clusters as a function of temperature for the perfluorodecane + water system compared to pure saturated water vapor. (■) water in perfluorodecane, (-) pure saturated water vapor (literature data). The literature data is from Johansson (2007).

Figures 5-13 and 5-14 illustrate a contrast in trends between the two different systems. For the system of decane + water, there is a more similar trend in the clustering behavior at the higher temperatures, whereas for the perfluorodecane + water system, the reverse is observed. This may indicate that although there appears to be significantly more free volume with increasing temperature for systems of perfluoroalkanes as compared to alkanes, this extra free volume is still significantly affected by the fluorine atoms along the perfluoroalkane molecules. Further study of the strength and nature of these water-fluorine interactions should be undertaken in future work in order to more accurately assess this phenomenon.

CHAPTER 6: CONCLUSIONS

For the test system of the light alcohols + water + n-dodecane, it was found that the simulations agreed closely with the laboratory experiments only for the smallest of the three alcohols being studied, i.e. methanol. This was found to be due to shortcomings in the TraPPE parameters when accounting for the interactions of the alcohol + n-dodecane pair. This shortcoming was evident in the literature by which these parameters were developed. This deviation from laboratory experiments was found to increase from ethanol to isopropanol; thus increasing with increasing carbon number in the alcohol.

The application of MC simulations towards extrapolation of laboratory experiments at conditions which were infeasible in the laboratory was successfully demonstrated for the methanol + water + n-dodecane system. The shortcomings of molecular models, i.e. the TraPPE model, were illustrated for the ethanol + water + n-dodecane and isopropanol + water + n-dodecane systems.

The influence of temperature and polymer carbon number was successfully determined for the system of PTFE + water. This investigation was carried out for a wide range of temperatures and polymer carbon numbers.

It was found that the solubility of water into the perfluoroalkane phase was exponentially increased with increasing temperature. For perfluoroalkane carbon numbers of 8 to 16 carbons at 450 K, it was found that carbon number did not have a significant influence, which was also observed by Johansson (2007) for water in alkanes.

The solubility of water in PTFE was found to have an asymptotic value of 98.0 mole percent, or 59.6 g/kg polymer, which was significantly larger than the value of 2.5 g/kg polymer obtained for polyethylene by Johansson et al (2007). This may have been due to the greater rigidity of the perfluoroalkane chains as compared to alkanes, which was described by Friedemann et al (2001). This greater rigidity would lead to greater supramolecular order for perfluoroalkanes as compared to alkanes. Cluster analysis showed there was greater supramolecular ordering of the PTFE than was found in PE by Johansson (2007), which concurred with the work of Friedemann et al (2001).

Previous experimental work on the mean hole size in PTFE and PE by Dlubek et al (1998) determined that the individual voids in the PTFE were approximately double the size of the voids in PE. This greater specific free volume may also help to explain the high solubility of water in PTFE found in this work.

An irregularity was observed in the solubility of water in the perfluoroalkane phase and in the clustering behavior of water in the perfluoroalkane phase between carbon numbers of 10 and 12. This may have been due to a change in the regime of the energy contributions towards the transformation from an all-helical to an all-trans configuration inferred from the data of Jang et al (2003) for a carbon number of 10 in perfluoroalkanes.

Linear water clusters were found to occur far more frequently than cyclic clusters in PTFE, which was also found by Johansson (2007) for the case of water in PE. In both systems, linear water clusters were found to account for approximately 90 percent of the total water clusters. Increasing temperature was found to lead to an increasing frequency of linear water clusters over cyclic water clusters, which was also found by Johansson (2007) to be the case for water in PE.

CHAPTER 7: RECOMMENDATIONS

Several recommendations for future work have arisen from this project. For the systems of light alcohols + water + n-dodecane it should be recommended that the TraPPE parameters for the alcohols and n-dodecane are refined using laboratory experiments, or that further work be done on the mixing rules applied to the existing TraPPE parameters. This would be undertaken iteratively, with each adjustment of the parameters being compared to the experimental data, until a satisfactory agreement with the experimental data is obtained. This was not undertaken as it did not fall within the scope of this project, as the system of light alcohols + water + n-dodecane was a test system, used only to gain familiarity and expertiseTransactions of the Connecticut Academy of Arts and Sciences in the field of molecular simulations.

In order to confirm the results of the simulations of water solubility into the PTFE, laboratory experiments of the molten polymer with water should be undertaken. Such measurements were not undertaken as they did not fall within the scope of this project, as this project concerned the computer simulation, at a molecular level, of the system of PTFE + water.

In order to gain further insight into the clustering of water into the PTFE matrix, a comprehensive study of the spatial geometry of the free volume of the PTFE matrix should be undertaken. In addition, a more detailed analysis of the PTFE polymer chains themselves may be undertaken in the future in order to determine the behavior of the molecular structure of these chains over varying carbon numbers and temperatures. This analysis would provide further insight into the variance of the geometry of the perfluoroalkane chains under different conditions. This would then enable more solid conclusions to be drawn as to the geometric effects of the perfluoroalkane chains upon the neighbouring water molecules. Such an analysis fell beyond the scope of this project which was concerned solely with the effects of temperature and polymer carbon number on the solubility and structuring of water within the PTFE matrix. Such an analysis should be seriously considered for future work.

REFERENCES

- ASTM standard D5229/D5229M-92 (1992) "Standard Test Methodology for Moisture Absorption Properties and Equilibrium Conditioning of Polymer Matrix Composite Materials," American Society for Testing and Materials.
- Adams, J. (2007) "Microwulf: A Personal, Portable Beowulf Cluster" available online: http://www.calvin.edu/~adams/research/microwulf/ (date accessed: 12/05/2010).
- Allen, M.P. and Tildesley, D.J. (1987) "Computer Simulation of Liquids" 2nd Edition, Claredon Press: Oxford.
- Avogadro: an Open-Source Molecular Builder and Visualization Tool. Version 0.9.7. http://avogadro.openmolecules.net/
- Berendsen, H.J.C., Grigera, J.R. and Straatsma, T.P. (1987) "The Missing Term in Effective Pair Potentials" *J. Phys. Chem.* **91**, 6269.
- Berendsen, H.J.C., Postma, J.P.M., van Gunsteren, W.F. and Hermans, J. (1981) "Interaction Models for Water in Relation to Protein Hydration" In: Pullman, B. (Editor) *Intermolecular Forces*, Reidel, Dordrecht, the Netherlands, 331.
- Berthelot, D.C. (1898) "Sur le Mélange des Gaz" *Compt. Rendus* **126**, 1703.
- Bhownath, R. (2008) "The Use of n-Dodecane as a Solvent in the Extraction of Light Alcohols from Water" MSc Thesis, University of KwaZulu-Natal: Durban, South Africa.
- Boedeker Plastics (2011) "PTFE Specifications" available online: http://www.boedeker.com/ptfe_p.htm (date accessed: 04/03/2011).
- Bolton, K., Johansson, E., Jönsson, L. and Ahlström, P. (2009) "Simulation of Water Clusters in Vapour, Alkanes and Polyethylenes" *Molecular Simulation* **35(10-11)**, 888.
- Boulougouris, C., Economou, I.G. and Theodorou, D.N. (1998) "Engineering a Molecular Model for Water Phase Equilibrium over a Wide Temperature Range" *J. Phys. Chem. B* **102**, 1029.
- Boulougouris, G.C., Errington, J.R., Economou, I.G., Panagiotopoulos, A.Z. and Theodorou, D.N. (2000) "Molecular Simulation of Phase Equilibria for Water – n-Butane and – n-Hexane

Mixtures" *J. Phys. Chem. B* **104**, 4958.

- Buckingham, R.A. (1938) "The Classical Equation of State of Gaseous Helium Neon and Argon" *Proc. R. Soc. London* **Ser. A 168**, 264.
- Camel, V. (2003) "Review: Solid Phase Extraction of Trace Elements" *Spectrochimica Acta Part B* **58**, 1177.
- Castro, B.D. and Aznar, M. (2005) "Liquid-Liquid Equilibrium of PEG 8000 + Magnesium Sulfate or Sodium Sulfate Aqueous Two-Phase Systems at 35°C: Experimental Determination and Thermodynamic Modeling" *Brazilian Journal of Chemical Engineering*, Vol. 22, No. 03, 463.
- ChemBlink: Online Database of Chemicals from Around the World "Dodecane" available online: http://www.chemblink.com/products/112-40-3.htm (date accessed: 22/11/2010).
- Chen, B., Xing, J. and Siepmann, J.I. (2000) "Development of polarizable water force fields for phase equilibrium calculations", *J. Phys. Chem. B* **104**, 2391.
- Chen, B., Potoff, J.J. and Siepmann, J.I. (2001) "Monte Carlo Calculations for Alcohols and Their Mixtures with Alkanes. Transferable Potentials for Phase Equilibria. 5. United-Atom Description of Primary, Secondary, and Tertiary Alcohols" *J. Phys. Chem. B* **105**, 3093.
- Clifford, S.L. (2006) "Molecular Simulation and Modeling of the Phase Equilibria of Polar Compounds" PhD Thesis, University of KwaZulu-Natal: Durban, South Africa.
- Courel, M., Dornier, M., Rios, G.M. and Reynes, M. (2000) "Modeling of Water Transport in Osmotic Distillation Using Asymmetric Membrane" *Journal of Membrane Science* **173**, 107.
- Cui, S.T., Siepmann, J.I., Cochran, H.D. and Cummings, P.T. (1998) "Intermolecular Potentials and Vapor-Liquid Phase Equilibria of Perfluorinated Alkanes" *Fluid Phase Equilibria* **146**, 51.
- de Leeuw, S.W., Perram, J.W. and Smith, E.R. (1980a) "Simulation of Electronic Systems in Periodic Boundary Conditions. I. Lattice Sums and Dielectric Constants" *Proceedings of the Royal Society of London. Series A, Mathematical and Physical Sciences* **373(1752)**, 27.
- de Leeuw, S.W., Perram, J.W. and Smith, E.R. (1980b) "Simulation of Electronic Systems in Periodic Boundary Conditions. II. Equivalence of Boundary Conditions" *Proceedings of the Royal Society of London. Series A, Mathematical and Physical Sciences* **373(1752)**, 57.
- de Leeuw, S.W., Perram, J.W. and Smith, E.R. (1980c) "Simulation of Electronic Systems in Periodic Boundary Conditions. III. Further Theory and Applications" *Proceedings of*

the Royal Society of London. Series A, Mathematical and Physical Sciences **388(1794),** 177.

- Dlubek, G., Saarinen, K. and Fretwell, H.M. (1998) "The Temperature Dependence of the Local Free Volume in Polyethylene and Polytetrafluoroethylene: A Positron Lifetime Study" *Journal of Polymer Science: Part B: Polymer Physics* **36**, 1513.
- DuPont de Nemours (Nederland) B.V. (2006) "Safety Data Sheet: Teflon® PTFE" **a**vailable online: http://msds.dupont.com/msds/pdfs/EN/PEN_09004a358023be41.pdf (date accessed: 23/03/2010).
- DuPont de Nemours (Nederland) B.V. (2007) "Safety Data Sheet: Teflon™ AF Amorphous Fluoropolymer" available online: http://msds.dupont.com/msds/pdfs/EN/PEN_09004a35803537ac.pdf (date accessed: 23/03/2010).
- Du Preez, N.B. (2005) "Determination of Phase Equilibria for Long-Chain Linear Hydrocarbons by Monte Carlo Simulation" MSc Thesis, University of KwaZulu-Natal: Durban, South Africa.
- Dynalab Corp "Plastic Properties of High Density Polyethylene (HDPE)" available online: http://www.dynalabcorp.com/technical_info_hd_polyethylene.asp (date accessed: 04/03/2011).
- ElringKlinger Kunststofftechnik GmbH "PTFE: Properties and Applications of an Exceptional Compound" available online: http://www.elringklinger-kunststoff.de/pages/e_werkst_elring_ptfe.html (date accessed: 17/09/2010).
- Errington, J. and Panagiotopoulos, A.Z. (2000) "Gibbs Ensemble Monte Carlo" Computer program, available online: http://kea.princeton.edu/jerring/gibbs/index.html (date accessed: 01/06/2010).
- Ewald, P.P. (1921) "Die Berechnung Optischer und Elektrostatischer Gitterpotentiale" *Ann. Phys*. **64**, 253.
- Fraleigh, J.B. and Beauregard, R.A. (1995) "Linear Algebra" 3rd Edition, Addison-Wesley: Reading, Massachusetts.
- Freire, M.G., Gomes, L., Santos, L.M.N.B.F., Marrucho, I.M. and Coutinho, J.A.P. (2006) "Water Solubility in Linear Fluoroalkanes Used in Blood Substitute Formulations" *J. Phys. Chem. B* **110**, 22923.
- Freire, M.G., Carvalho, P.J., Santos, L.M.N.B.F., Gomes, L.R., Marrucho, I.M. and Coutinho, J.A.P. (2010) "Solubility of Water in Fluorocarbons" Experimental and COSMO-RS

Prediction Results" *J. Chemical Thermodynamics* **42**, 213.

- Frenkel, D. and Smit, B. (2001) "Understanding Molecular Simulation: From Algorithms to Applications" 2nd Edition, Academic Press: San Diego, California.
- Friedemann, R., Naumann, S. and Brickmann, J. (2001) "Aggregation of Alkane and Fluoroalkane Clusters: Molecular Dynamics Simulation Results" *Phys. Chem. Chem. Phys.* **3**, 4195.
- Gedde, U.W. (1995) "Polymer Physics" 1st Edition, Chapman & Hall: London.
- Gibbs, J.W. (1873) "Graphical methods in the thermodynamics of fluids" *Transactions of the Connecticut Academy of Arts and Sciences* **2**, 309.
- Gubbins, K.E. (1993) "Applications of Molecular Simulation" *Fluid Phase Equilibria* **83**, 1.
- Haile, J.M. and Mansoori, G.A., editors (1983) "Molecular-Based Study of Fluids. (Advances in Chemistry Series; 204)" Based on a symposium jointly sponsored by the ACS divisions of industrial and engineering chemistry, and physical chemistry at the 182nd ACS national meeting, New York, New York, August 26, 1981; American Chemical Society: New York, New York.
- Huang, S.H. and Radosz, M. (1990) "Equation of State for Small, Large, Polydisperse, and Associating Molecules" *Ind. Eng. Chem. Res.* **29**, 2284.
- Hurst, N. (2000) "How to Build an Ultra Cheap Beowulf Cluster" available online: http://www.clustercompute.com/ (date accessed: 12/05/2010).
- Jain, A. (2006) "Beowulf Cluster Design and Setup" available online: http://cs.boisestate.edu/~amit/research/beowulf/beowulf-setup.pdf (date accessed: 12/05/2010).
- Jang, S.S., Blanco, M., Goddard, W.A. III, Caldwell, G. and Ross, R.B. (2003) "The Source of Helicity in Perfluorinated N-Alkanes" *Macromolecules* **36**, 5331.
- Johansson, E. and Ahlström, P. (2007) "Atomistic Simulation Studies of Polymers and Water" Springer Lecture Notes in Computer Science **4966/2007**, 59.
- Johansson, E.L. (2007) "Simulations of Water Clustering in Vapour, Hydrocarbons and Polymers" Thesis for the Degree of Doctor of Philosophy, Chalmers University of Technology: Göteborg, Sweden.
- Johansson, E., Bolton, K. and Ahlström, P. (2005) "Simulations of Vapor Water Clusters at Vapor-Liquid Equilibrium" *J. Chem. Phys.* **123**, 024504.
- Johansson, E.L., Bolton, K., Theodorou, D.N. and Ahlström, P. (2007) "Monte Carlo Simulations of Equilibrium Solubilities and Structure of Water in *n*-Alkanes and

Polyethylene" *J. Chem. Phys.* **126**, 224902.

- Kabrede, H. and Hentschke, R. (2003) "Global Minima of Water Clusters $(H_2)_N$, $N \leq 25$, Described by Three Empirical Potentials" *J. Phys. Chem. B* **107**, 3914.
- Kalinichev, A.G. and Bass, J.D. (1997) "Hydrogen Bonding in Supercritical Water 2: Computer Simulations" *J. Phys. Chem. A* **101**, 9720.
- Karayiannis, N.C., Giannousaki, A.E., Mavrantzas, V.G. and Theodorou, D.N. (2002) "Atomistic Monte Carlo Simulation of Strictly Monodisperse Long Polyethylene Melts Through a Generalized Chain Bridging Algorithm" *J. Chem. Phys.* **117**, 5465.
- Karayiannis, N.C., Mavrantzas, V.G. and Theodorou, D.N. (2002) "A Novel Monte Carlo Scheme for the Rapid Equilibriation of Atomistic Polymer Systems of Precisely Defined Molecular Architecture" *Phys. Rev. Lett.* **88,** 105503.
- Kontogeorgis, G.M., Yakoumis, I.V., Meijer, H., Hendricks, E. and Moorwood, T. (1999) "Multicomponent Phase Equilibrium Calculations for Water-Methanol-Alkanes Mixtures" *Fluid Phase Equilbria* **158-160**, 201.
- Kontogeorgis, G.M. and Folas, G.K. (2010) "Thermodynamic Models for Industrial Applications: From Classical and Advanced Mixing Rules to Association Theories" John Wiley & Sons Ltd.: Chichester, West Sussex.
- Landau, L.D. and Lifshitz, E.M. (1980) "Course of Theoretical Physics Volume 5: Statistical Physics Part 1" 3rd Edition, translated from Russian by Sykes, K.B. and Kearsley, M.J., Pergamon Press Ltd.: Oxford.
- Landau, L.D. and Lifshitz, E.M. (1980) "Course of Theoretical Physics Volume 9: Statistical Physics Part 2" 3rd Edition, translated from Russian by Sykes, K.B. and Kearsley, M.J., Pergamon Press Ltd.: Oxford.
- Lappan, U., Geißler, U., Häußler, L., Pompe, G. and Scheler, U., (2004) "The Estimation of the Molecular Weight of Polytetrafluoroethylene Based on the Heat of Crystallisation. A Comment on Suwa's Equation " *Macromol. Mater. Eng.* **289**, 420-425.
- Lasich, M., Bhownath, R., Naidoo, P., Ramjugernath, D. and Moodley, T. (2011) "Liquid-Liquid Equilibria of Light Alcohols with Water and n-Dodecane" *J. Chem. Eng. Data*, in press.
- Lennard-Jones, J.E. (1931) "Cohesion" *Proceedings of the Physical Society* **43**, 461.
- Lennert, T.J., Hendra, P.J., Everall, N. and Clayden, N.J. (1996) "Comparative Quantitative Study on the Crystallinity of Poly(tetrafluoroethylene) including Raman, Infra-red and ^{19}F Nuclear Magnetic Resonance Spectroscopy" *Polymer* **38(7)**, 1521.

- Lin, H.L., Yu, T.L., Huang, L.N., Chen, L.C., Shen, K.S. and Jung, G.B. (2005) "Nafion/PTFE Composite Membranes for Direct Methanol Fuel Cell Applications" *Journal of Power Sources* **150**, 11.
- Lorentz, H.A. (1881) "Ueber die Anwendung des Satzes vom Virial in der kinetischen Theorie der Gase" *Ann. Phys.* **12**, 127.
- Martin, M.G. and Siepmann, J.I .(1998) "Transferable Potentials for Phase Equilibria. 1. United-Atom Description of n-Alkanes" *J. Phys. Chem. B* **102**, 2569.
- Martin, M.G. and Siepmann, J.I. (1999) "Novel Configurational-Bias Monte Carlo for Branched Molecules. Transferable Potentials for Phase Equilibria. 2. United-Atom Description of Branched Alkanes" *J. Phys. Chem. B* **103**, 4508.
- Mavrantzas, V.G., Boone, T.D., Zervopoulou, E. and Theodorou, D.N. (1999) "End-Bridging Monte Carlo: A Fast Algorithm for Atomistic Simulation of Condensed Phases of Long Polymer Chains" *Macromolecules* **32**, 5072.
- McCall, D.W., Douglass, D.C., Blyler, L.L. Jr., Johnson, G.E., Jelinski, L.W. and Bair, H.E. "(1984) "Solubility and Diffusion of Water in Low-Density Polyethylene" *Macromolecules* **17**, 1644.
- McKnight, T. (2006) "Molecular Simulation of Vapour-Liquid Equilibrium using Beowulf Clusters" PhD Thesis, University of KwaZulu-Natal: Durban, South Africa.
- Metropolis, N., Rosenbluth, A.W., Rosenbluth, M., Teller, A.H. and Teller, E. (1953) "Equation of State Calculations by Fast Computing Machines" *J. Chem. Phys.* **21**, 1087.
- Micro-Coax "Application Notes #27: Understanding Phase Versus Temperature Behavior 'The Teflon™ Knee' " available online: http://www.micro-coax.com/pages/technicalinfo/applications/27.asp (date accessed: 31/03/2010), Micro-Coax: Pottstown, Pennsylvania.
- Moodley, S. (2008) "Molecular Simulation of Vapour-Liquid-Liquid Equilibrium" MSc Thesis, University of KwaZulu-Natal: Durban, South Africa.
- Omega Engineering (2010) "Technical Selection Guide: PFA Fluorocarbon Information" available online: http://www.omega.com/techref/fluoro.html (date accessed: 02/06/2010), Omega Engineering: Bridgeport, New Jersey.
- Pal, S., Weiss, H., Keller, H. and Müller-Plathe, F. (2005) "The Hydrophobicity of Nanostructured Alkane and Perfluoroalkane Surfaces: A Comparison by Molecular Dynamics Simulation" *Phys. Chem. Chem. Phys*. **7**, 3191.
- Panagiotopoulos, A.Z. (1987) "Direct Determination of Phase Coexistence Properties of

Fluids by Monte Carlo Simulation in a New Ensemble" *Mol. Phys*. **61**, 813.

- Pant, P.V.K. and Theodorou, D.N. (1995) "Variable Connectivity Method for the Atomistic Monte Carlo Simulation of Polydisperse Polymer Melts" *Macromolecules* **28**, 7224.
- Rae, P.J. and Dattelbaum, D.M. (2004) "The Properties of Poly(tetrafluoroethylene) (PTFE) in Compression" *Polymer* **45**, 7615.
- Rappé, A.K., Casewit, C.J., Colwell, K.S., Goddard, W.A. III and Skiff, W.M. (1992) "UFF, a Full Periodic Table Force Field for Molecular Mechanics and Molecular Dynamics Simulations" *J. Am. Chem. Soc. Vol. 114, No. 25,* 10024.
- Rivas, B.L., Maureira, A.E. and Mondaca, M.A. (2008) "Aminodiacetic Water-Soluble Polymer-Metal Ion Interactions" *European Polymer Journal* **44**, 2330.
- Rivas, B.L., Pereira, E.D. and Moreno-Villoslada, I. (2003) "Water-Soluble Polymer-Metal Ion Interactions" *Prog. Polym. Sci.* **28**, 173.
- Rosenbluth, M.N. and Rosenbluth, A.W. (1955) "Monte Carlo Calculation of the Average Extension of Molecular Chains" *J. Chem. Phys.* **23**(2), 356.
- Ryckaert, J.P. and Bellemans, A. (1975) **"**Molecular Dynamics of Liquid Normal-Butane near its Boiling Point" *Chem. Phys. Lett.* **30**, 23.
- Siepmann, J.I. (1990) "A Method for the Direct Calculation of Chemical Potentials for Dense Chain Molecules" *J. Chem. Phys.* **97**, 2817.
- Siepmann, J.I. and Frenkel, D. (1992) "Configurational-Bias Monte Carlo - A New Sampling Scheme for Flexible Chains" *Mol. Phys.* **75**, 59.
- Smith, J.M., Van Ness, H.C. and Abbott, M.M. (2005) "Introduction to Chemical Engineering Thermodynamics" 7th Edition, McGraw-Hill: New York.
- Stillinger, F.H. (1963) "Rigorous Basis of the Frenkel-Band Theory of Association Equilibrium" *J. Chem. Phys.* **38**, 1486.
- Swendson, K. (2004) "The Beowulf HowTo" available online: http://tldp.org/HOWTO/html_single/Beowulf-HOWTO/ (date accessed: 12/05/2010).
- Tamai, Y., Tanaka, H. and Nakanishi, K. (1994) "Molecular Simulation of Permeation of Small Penetrants through Membranes. 1. Diffusion Coefficients" *Macromolecules* **27**, 4498.
- Tamai, Y., Tanaka, H. and Nakanishi, K. (1995) "Molecular Simulation of Permeation of Small Penetrants through Membranes. 2. Solubilities" *Macromolecules* **28**, 2544.
- Terra Nitrogen Corporation "Material Safety Data Sheet: Methanol" available online: http://www.methanol.org/pdf/MethanolMSDS.pdf (date accessed: 22/11/2010).
- Thomas, G.B. Jr., as revised by Weir, M.D., Hass, J. and Giordano, F.R. (2005) "Thomas'

Calculus" 11th Edition (International Edition), Pearson Education Inc.: Boston, Massachusetts.

- Tsonopoulos, C. (1999) "Thermodynamic Analysis of the Mutual Solubilities of Normal Alkanes and Water" *Fluid Phase Equilibria* **156**, 21.
- Weber, T.A. (1978) "Simulation of Normal Butane Using a Skeletal Alkane Model" *J. Chem. Phys.* **69**, 2347.
- Widom, B. (2002) "Statistical mechanics: a concise introduction for chemists" 1st Edition, Cambridge University Press: Cambridge, UK.
- Zhang, L. and Siepmann, J.I. (2005) "Pressure Dependence of the Vapor-Liquid-Liquid Phase Behavior in Ternary Mixtures Consisting of n-Alkanes, n-Perfluoroalkanes, and Carbon Dioxide" *J. Phys. Chem. B* **109**, 2911.

APPENDIX 1: Model Parameters

Bond length	Non-bonded interactions (Lennard-Jones)	Bond bending $V_{bend}(A)/k_B = k_A(A - A_0)^2 / 2$	Charge
O-H = 1.0 Å, fixed	ε_O/k_B = 78.21 K	A_0(H-O-H) = 109.5 °, fixed	q_O = -0.82e
	σ_O = 3.166 Å		q_H = 0.41e

Table A-1-1: SPC water model parameters used in this work.

Bond length	Non-bonded interactions (Lennard-Jones)	Bond bending $V_{bend}(A)/k_B = k_A(A - A_0)^2 / 2$	Charge
O-H = 1.0 Å, fixed	ε_O/k_B = 78.21 K	A_0(H-O-H) = 109.5 °, fixed	q_O = -0.8476e
	σ_O = 3.166 Å		q_H = 0.4238e

Table A-1-2: SPC-E water model parameters used in this work.

Bond length	Non-bonded interactions (Lennard-Jones)	Bond bending $V_{bend}(A)/k_B = k_A(A - A_0)^2 / 2$	Charge
CH3-O = 1.43 Å, fixed	ε_{CH3}/k_B = 98 K	k_A(CH3-O-H) = 55,400 rad^{-2}	q_O = -0.7e
O-H = 0.95 Å, fixed	ε_O/k_B = 93 K	A_0(CH3-O-H) = 108.5 ^{o}	q_H = 0.435e
	σ_{CH3} = 3.75 Å		
	σ_O = 3.02 Å		

Table A-1-3: TraPPE methanol parameters used in this work.

Bond length	Non-bonded interactions (Lennard-Jones)	Bond bending $V_{bend}(A)/k_B = k_A(A - A_0)^2 / 2$	Torsion $V_{torsion}(D)/k_B = c_0 + c_1[1 + \cos(D)] + c_2[1 - \cos(2D) + c_3[1 + \cos(3D)]$	Charge
CH_3-CH_2 = 1.54 Å, fixed	ε_{CH3}/k_B = 98 K	$k_A(CH_3\text{-}CH_2\text{-}O)$ = 50,400 rad^{-2}	c_0 = 0 K	q_{CH2} = 0.265e
CH_2-O = 1.43 Å, fixed	ε_{CH2}/k_B = 46 K	$A_0(CH_3\text{-}CH_2\text{-}O)$ = 109.47 °	c_1 = 209.82 K	q_O = -0.7e
O-H = 0.95 Å, fixed	ε_O/k_B = 93 K	$k_A(CH_2\text{-}O\text{-}H)$ = 55,400 rad^{-2}	c_2 = -29.17 K	q_H = 0.435e
	σ_{CH3} = 3.75 Å	$A_0(CH_2\text{-}O\text{-}H)$ = 108.5 °	c_3 = 187.93 K	
	σ_{CH2} = 3.95 Å			
	σ_O = 3.02 Å			

Table A-1-4: TraPPE ethanol parameters used in this work.

Bond length	Non-bonded interactions (Lennard-Jones)	Bond bending $V_{bend}(A)/k_B = k_A(A - A_0)^2 / 2$	Torsion $V_{torsion}(D)/k_B = c_0 + c_1[1 + \cos(D)] + c_2[1 - \cos(2D) + c_3[1 + \cos(3D)]$	Charge
CH_3-CH = 1.54 Å, fixed	ε_{CH3}/k_B = 98 K	$k_A(CH_3\text{-}CH\text{-}CH_3)$ = 62,500 rad^{-2}	c_0 = 215.96 K	q_{CH} = 0.265e
CH-O = 1.43 Å, fixed	ε_{CH}/k_B = 10 K	$A_0(CH_3\text{-}CH\text{-}CH_3)$ = 112 °	c_1 = 197.33 K	q_O = -0.7e
O-H = 0.95 Å, fixed	ε_O/k_B = 93 K	$k_A(CH_3\text{-}CH\text{-}O)$ = 50,400 rad^{-2}	c_2 = 31.46 K	q_H = 0.435e
	σ_{CH3} = 3.75 Å	$A_0(CH_3\text{-}CH\text{-}O)$ = 109.47 °	c_3 = -173.92 K	
	σ_{CH} = 4.33 Å	$k_A(CH\text{-}O\text{-}H)$ = 55,400 rad^{-2}		
	σ_O = 3.02 Å	$A_0(CH\text{-}O\text{-}H)$ = 108.5 °		

Table A-1-5: TraPPE isopropanol parameters used in this work.

Bond length	Non-bonded interactions (Lennard-Jones)	Bond bending $V_{bend}(A)/k_B = k_A(A - A_0)^2 / 2$	Torsion $V_{torsion}(D)/k_B = c_0 + c_1[1 + \cos(D)] + c_2[1 - \cos(2D) + c_3[1 + \cos(3D)]$
CH_i-CH_j = 1.54 Å, fixed	ε_{CH2}/k_B = 46 K	$k_A(CH_i\text{-}CH_j\text{-}CH_k)$ = 62,500 rad^{-2}	c_0 = 0 K
	ε_{CH3}/k_B = 98 K	$A_0(CH_i\text{-}CH_j\text{-}CH_k)$ = 114 °	c_1 = -335.03 K
	σ_{CH2} = 3.95 Å		c_2 = 68.19 K
	σ_{CH3} = 3.75 Å		c_3 = -791.32 K

Table A-1-6: TraPPE alkane parameters used in this work.

Bond length	Non-bonded interactions (Lennard-Jones)	Bond bending $V_{bend}(A)/k_B = k_A(A - A_0)^2 / 2$	Torsion $V_{torsion}(D)/k_B = \Sigma_i[c_i\cos^i(D)]$ for i = [0,7]
CF_i-CF_j = 1.54 Å, fixed	ε_{CF3}/k_B = 87 K	$k_A(CF_i\text{-}CF_j\text{-}CF_k)$ = 62,500 rad^{-2}	c_0 = 940.1 K
	ε_{CF2}/k_B = 27.5 K	$A_0(CF_i\text{-}CF_j\text{-}CF_k)$ = 114 ^{o}	c_1 = -282.7 K
	σ_{CF3} = 4.36 Å		c_2 = 1,355.2 K
	σ_{CF2} = 4.73 Å		c_3 = 6,800 K
			c_4 = -7875.3 K
			c_5 = -14,168 K
			c_6 = 9,213.7 K
			c_7 = 4,123.7 K

Table A-1-7: TraPPE perfluoroalkane parameters used in this work. This includes the modified torsional potential.

APPENDIX 2: Molecular validation

This work		Reference		Deviation from ref. (%)
Bond no.	Length (Å)	Bond no.	Length (Å)	
1	1	1	0.951	5.164
2	1	2	0.951	5.164
Angle no.	Angle (°)	Angle no.	Angle (°)	
1	109.5	1	107.69	1.68

Table A-2-1: Results of the validation testing of the SPC water molecules generated in this work. The reference values are those which have been optimized using the UFF in Avogadro (see references).

This work		Reference		Deviation from ref. (%)
Bond no.	Length (Å)	Bond no.	Length (Å)	
1	1	1	0.951	5.164
2	1	2	0.951	5.164
Angle no.	Angle (°)	Angle no.	Angle (°)	
1	109.5	1	107.69	1.68

Table A-2-2: Results of the validation testing of the SPC-E water molecules generated in this work. The reference values are those which have been optimized using the UFF in Avogadro (see references).

This work		Reference		Deviation from ref. (%)
Bond no.	Length (Å)	Bond no.	Length (Å)	
1	1.43	1	1.395	2.524
2	0.95	2	0.949	0.137
Angle no.	Angle (°)	Angle no.	Angle (°)	
1	111.181	1	107.451	3.471

Table A-2-3: Results of the validation testing of the methanol molecules generated in this work. The reference values are those which have been optimized using the UFF in Avogadro (see references).

This work		Reference		Deviation from ref. (%)
Bond no.	Length (Å)	Bond no.	Length (Å)	
1	0.95	1	0.95	0.285
2	1.43	2	1.41	1.454
3	1.54	3	1.52	1.456
Angle no.	Angle (°)	Angle no.	Angle (°)	
1	113.7	1	108	5.473
2	106.5	2	107	0.14

Table A-2-4: Results of the validation testing of the ethanol molecules generated in this work. The reference values are those which have been optimized using the UFF in Avogadro (see references).

This work		Reference		Deviation from ref. (%)
Bond no.	Length (Å)	Bond no.	Length (Å)	
1	1.54	1	1.525	0.997
2	1.54	2	1.528	0.799
3	1.43	3	1.417	0.903
4	0.95	4	0.948	0.243
Angle no.	Angle (°)	Angle no.	Angle (°)	
1	114.2691	1	110.8609	3.074
2	138.4024	2	111.9646	23.613
3	106.5354	3	106.7103	0.164
4	109.8865	4	106.6491	3.036

Table A-2-5: Results of the validation testing of the isopropanol molecules generated in this work. The reference values are those which have been optimized using the UFF in Avogadro (see references).

Length (Å)		Reference		Deviation from ref. (%)
Bond no.	This work	Bond no.	Length (Å)	
1	1.54	1	1.538	0.143
2	1.54	2	1.536	0.247
3	1.54	3	1.538	0.13
4	1.54	4	1.537	0.215
5	1.54	5	1.534	0.385
6	1.54	6	1.537	0.215
7	1.54	7	1.54	0.026
8	1.54	8	1.526	0.904
9	1.54	9	1.536	0.241
10	1.54	10	1.526	0.904
11	1.54	11	1.538	0.137
Angle no.	Angle (°)	Angle no.	Angle (°)	
1	114.18	1	113.36	0.724
2	117.22	2	113.33	3.436
3	109.67	3	110.89	1.108
4	110.5	4	113.18	2.367
5	111.48	5	110.9	0.524
6	112.24	6	111.01	1.116
7	109.11	7	113.37	3.759
8	116.4	8	111	4.859
9	103.26	9	113.16	8.747
10	116.3	10	113.3	2.652

Table A-2-6: Results of the validation testing of the n-dodecane molecules generated in this work. The reference values are those which have been optimized using the UFF in Avogadro (see references).

This work		Reference		Deviation from ref. (%)
Bond no.	Length (Å)	Bond no.	Length (Å)	
1	1.54	1	1.541	0.058
2	1.54	2	1.559	1.212
3	1.54	3	1.558	1.155
4	1.54	4	1.563	1.472
5	1.54	5	1.541	0.058
6	1.54	6	1.558	1.155
7	1.54	7	1.559	1.212
Angle no.	Angle (°)	Angle no.	Angle (°)	
1	115.381	1	117.213	1.563
2	110.094	2	117.047	5.941
3	111.059	3	117.047	5.116
4	111.604	4	116.066	3.845
5	105.343	5	117.213	10.127
6	111.211	6	116.066	4.183

Table A-2-7: Results of the validation testing of the perfluoroalkane molecules generated in this work. perfluorooctane was used for this test. The reference values are those which have been optimized using the UFF in Avogadro (see references).

APPENDIX 3: Compositional convergence testing

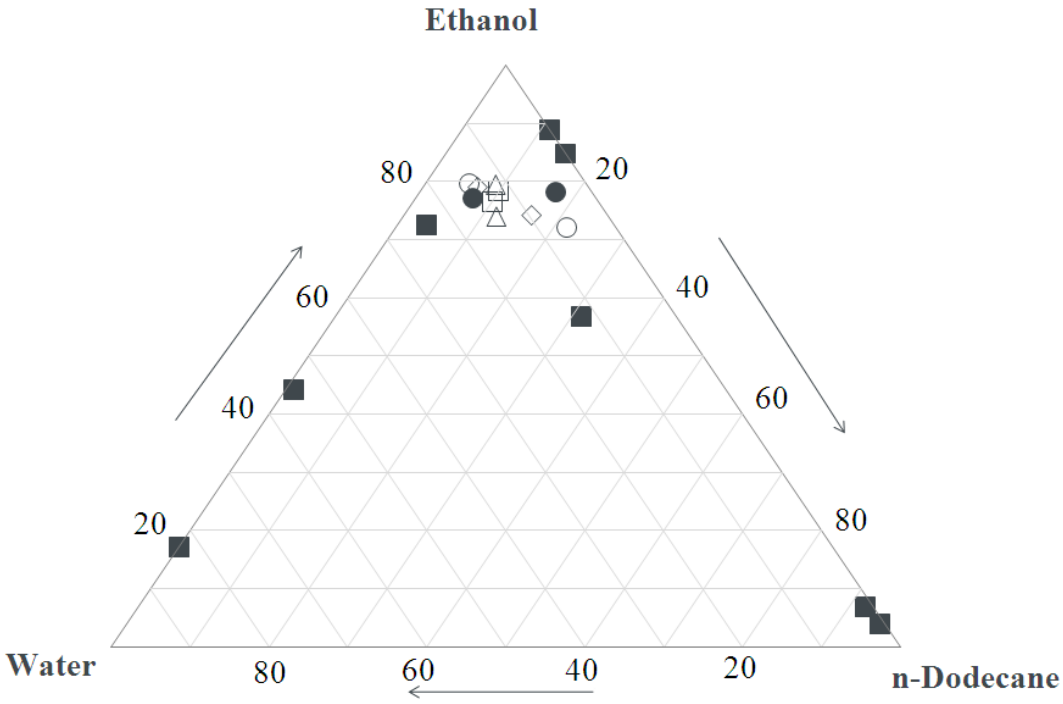

Figure A-3-1: Ternary LLE plot of the compositional convergence test. Values are in mole percent. (■) simulations at T = 400 K (this work), (□) after 0 MC moves, (◇) after 6x106 MC moves, (△) after 12x106 MC moves, (○) after 18x106 MC moves, (●) after 24x106 MC moves.

		Compositions (mole fractions)				
	MC moves (10^6)	0	6	12	18	24
Phase I	x_{Water}	0.134	0.095	0.142	0.063	0.045
	$x_{n\text{-}Dodecane}$	0.101	0.161	0.119	0.216	0.172
	$x_{Ethanol}$	0.765	0.743	0.739	0.721	0.783
Phase II	x_{Water}	0.116	0.140	0.115	0.149	0.156
	$x_{n\text{-}Dodecane}$	0.099	0.068	0.090	0.055	0.073
	$x_{Ethanol}$	0.785	0.791	0.795	0.796	0.772

Table A-3-1: Results of the compositional convergence test for the ethanol + water + n-dodecane system at T = 400 K.

APPENDIX 4: Perfluoroalkane + water raw data

With regard to the column labeled "Program used"; "GEMC" here refers to the Gibbs Ensemble Monte Carlo program of Errington & Panagiotopoulos (2000), while "Polymer" here refers to the combined Gibbs ensemble and end-bridging program developed by Johansson (2007) using the algorithms of Mavrantzas et al (1999).

N	x_{water}	σ	Program used	Configuration	Comments
8	0.014	0.002	GEMC	500 H_2O, 100 PTFE	
10	0.014	0.000	GEMC	500 H_2O, 100 PTFE	
12	0.013	0.000	GEMC	500 H_2O, 100 PTFE	
16	0.017	0.001	GEMC	500 H_2O, 100 PTFE	
20	0.014	0.000	GEMC	500 H_2O, 100 PTFE	The same point was compared for the 2 programs
20	0.037	0.001	Polymer	500 H_2O, 10 PTFE	
30	0.182	0.007	Polymer	500 H_2O, 10 PTFE	
35	0.260	0.004	Polymer	500 H_2O, 10 PTFE	
40	0.458	0.006	Polymer	500 H_2O, 10 PTFE	
45	0.548	0.018	Polymer	500 H_2O, 10 PTFE	
50	0.529	0.021	Polymer	500 H_2O, 10 PTFE	
100	0.927	0.005	Polymer	500 H_2O, 10 PTFE	
300	0.980	0.000	Polymer	500 H_2O, 10 PTFE	
300	0.980	0.000	Polymer	500 H_2O, 10 PTFE	P = 600 kPa was used instead of 2 MPa to directly compare to data for PE

Table A-4-1: Composition data (in mole fractions) for the perfluoroalkane/PTFE + water systems at T = 450 K.

	Organic box		Water box	
N	ρ	σ	ρ	σ
8	1596.50	0.47	867.00	0.32
10	1670.80	2.28	862.22	1.51
12	1727.20	1.20	922.43	0.29
16	1803.40	8.41	866.49	0.10
50	31.13	6.96	436.42	97.59
300	0.02	0.01	531.43	118.83

Table A-4-2: Density data (in kg/m^3) for the perfluoroalkane/PTFE + water systems at T = 450 K.

N	x_{water}	σ	Program used	Configuration	Comments
8	0.054	0.000	GEMC	500 H_2O, 100 C8F18	
10	0.058	0.007	GEMC	500 H_2O, 100 C8F18	
12	0.035	0.011	GEMC	500 H_2O, 100 C8F18	
16	0.073	0.005	GEMC	500 H_2O, 100 C8F18	
50	0.799	0.002	Polymer	500 H_2O, 10 C8F18	
100	0.976	0.002	Polymer	500 H_2O, 10 C8F18	
300	0.980	0.000	Polymer	500 H_2O, 10 C8F18	

Table A-4-3: Composition data (in mole fractions) for the perfluoroalkane/PTFE + water systems at T = 500 K.

	Organic box		Water box	
N	ρ	σ	ρ	σ
8	1473.30	0.73	812.56	2.45
10	1568.50	7.28	819.88	0.74
12	1628.90	3.51	716.83	2.36
16	1703.40	0.54	815.91	6.48
50	72.17	0.09	819.35	2.20
300	0.06	0.01	898.21	24.32

Table A-4-4: Density data (in kg/m^3) for the perfluoroalkane/PTFE + water systems at T = 500 K.

N	x_{water}	σ	Program used	Configuration	Comments
8	0.400	0.017	GEMC	500 H_2O, 100 PTFE	
10	0.499	0.014	GEMC	500 H_2O, 100 PTFE	
11	0.400	0.004	GEMC	500 H_2O, 100 PTFE	
12	0.362	0.003	GEMC	500 H_2O, 100 PTFE	
13	0.391	0.000	GEMC	500 H_2O, 100 PTFE	
16	0.425	0.006	GEMC	500 H_2O, 100 PTFE	
20	0.467	0.004	Polymer	500 H_2O, 10 PTFE	
40	0.939	0.000	Polymer	500 H_2O, 10 PTFE	
50	0.968	0.001	Polymer	500 H_2O, 10 PTFE	C_{16} used instead of C_{10}
50	0.965	0.002	Polymer	500 H_2O, 10 PTFE	
50	0.980	0.001	Polymer	500 H_2O, 5 PTFE	Water:polymer ratio doubled
100	0.978	0.029	Polymer	500 H_2O, 10 PTFE	
300	0.980	0.000	Polymer	500 H_2O, 10 PTFE	
300	0.881	0.001	Polymer	500 H_2O, 10 PE	PE instead of PTFE

Table A-4-5: Composition data (in mole fractions) for the perfluoroalkane/PTFE + water systems at T = 600 K.

	Organic box		Water box	
N	ρ	σ	ρ	σ
8	1068.70	7.18	590.38	3.28
10	1117.10	15.23	644.53	1.54
12	1305.60	3.26	587.13	5.57
16	1391.70	2.42	643.55	5.94
40	273.21	0.31	626.72	4.40
50	120.01	4.30	564.02	15.02
300	0.26	0.07	696.19	15.06

Table A-4-6: Density data (in kg/m^3) for the perfluoroalkane/PTFE + water systems at T = 600 K.

T (K)	x_{water}	σ	Program used	Configuration	Comments
300	0.000	0.000	GEMC	500 H_2O, 100 PTFE	
350	0.000	0.000	GEMC	500 H_2O, 100 PTFE	
400	0.003	0.000	GEMC	500 H_2O, 100 PTFE	
450	0.014	0.000	GEMC	500 H_2O, 100 PTFE	
500	0.058	0.007	GEMC	500 H_2O, 100 PTFE	
550	0.180	0.007	GEMC	500 H_2O, 100 PTFE	
600	0.499	0.014	GEMC	500 H_2O, 100 PTFE	

Table A-4-7: Composition data (in mole fractions) for the perfluorodecane + water system from T = 300 K to T = 600 K.

APPENDIX 5: Paper I (manuscript to be submitted to *Molecular Simulation*)

Monte Carlo Simulations of Liquid-Liquid Equilibria of Light Alcohols with Water and n-Dodecane

Matthew Lasich[a,*], *Erik L. Johansson*[a] *and Deresh Ramjugernath*[a]

[a]Thermodynamics Research Unit, University of KwaZulu-Natal, King George V Avenue, Durban, 4041, South Africa

[*]Corresponding author. Office: +27 31 260 2187. Fax: +27 31 260 1118. Email: matt.lasich@gmail.com.

Abstract

The light alcohols methanol, ethanol and isopropanol are frequently encountered in aqueous solution in industry. Their removal from the water is achieved via extractive distillation with n-dodecane as the solvent. These alcohols may then be removed from the n-dodecane via a further extraction step. The thermodynamic state of interest encountered in these procedures is that of liquid-liquid equilibrium. Data has previously been measured for these systems at temperatures ranging from 298.14 K to 333.15 K. In this work, Monte Carlo simulations were performed to compare to the earlier experimental data. These simulations used the Gibbs ensemble with the Transferrable Potentials for Phase Equilibrium (TraPPE) coupled with the classical Lorentz-Berthelot combining rules. Simulations were then performed to extrapolate the phase diagrams to 350 K and 400 K. The simulations for the systems containing methanol agreed favorably with the experimental data. The simulations for the ethanol and isopropanol systems failed to reproduce the plait point encountered in the experiments, even at the extrapolated temperatures. The deviations of the simulations from the experimental data were found to increase with increasing carbon number in the alcohol.

Keywords: molecular simulation, alcohol, water, alkane

1. Introduction

In the removal of light alcohols such as ethanol and methanol from water, extractive distillation is employed in industry. The solvent used in this process is n-dodecane, and after this extraction step, the alcohols may be removed in turn from the n-dodecane. Sasol Ltd of South Africa uses this procedure when handling the aforementioned chemicals in this way. The non-ideal nature of the interactions between the water and the n-dodecane, and to a lesser extent between the alcohols and the n-dodecane, results in a system of two liquid phases in contact with each other. One of these two liquid phases is dominated by the n-dodecane, whilst the other is dominated by the alcohol-water mixture. To this end, liquid-liquid equilibrium (LLE) data are necessary to accurately model such systems in industry.

Frequently, LLE data for such systems was measured by laboratory experiments, often conducted at atmospheric pressure. A major drawback associated with LLE measurements is that the boiling points of the species under investigation often result in a limited temperature range for analysis. To overcome this, one option is to engage in the use of molecular simulations to predict LLE data, as computer simulations are not restricted by any such feasibility issues.

The systems studied in this work have been measured previously [1] in the laboratory. This study would then serve to extrapolate the measurements for these systems to higher temperatures which would be difficult to obtain in the laboratory due to the aforementioned constraints. A further use of this current study would be to test the accuracy of the TraPPE model for describing such a system. This may then be for compared with work on liquid-liquid equilibria of alcohols with n-alkanes [2].

2. Theory and methods

The TraPPE model was used to simulate the alcohols and the n-dodecane in this work. The model which was used for the water molecules in this work was the Simple Point Charge (SPC) model. This model was selected due to its agreeable fit to experimental data for water + alkane systems [3]. The water + alkane pair should be more non-ideal than the water + alcohol pair due to there being no hydrogen bonding between the alkanes and water, and the fact that the alkanes are completely non-polar whilst water is a

polar molecule. Therefore, a water model which more accurately described this interaction would be preferred.

The software used in the simulations in this work was the Gibbs ensemble program of Errington and Panagiotopoulos [4], which made use of the Gibbs ensemble method [5]. A potential source of error in molecular simulations is the influence of surface effects due to the ratio of "surface" molecules to "interior" molecules in a system, which increases rapidly with decreasing system size. To overcome this hurdle, the Gibbs ensemble makes use of interconnected "boxes" linked by the possibility of transfer of molecules as a surrogate for the interior space of separate phases.

The bulk of the simulations (~80 percent) in this work were computed on the Beowulf cluster belonging to the Thermodynamics Research Unit at the University of KwaZulu-Natal. In the case of an overflow of simulation jobs in the job queue, a Beowulf cluster at University College of Borås in Sweden was also used.

All of the simulations used for comparison to the literature were conducted at the same temperatures and pressures as the literature. The extrapolations were, in all cases, conducted at P = 60 bara, in order to prevent the vaporization of the water and the alcohols. The constant moles-pressure-temperature (NPT) ensemble of the Gibbs ensemble program was used for the simulations in this work, in order to account for the degrees of freedom of the system according to the Gibbs phase rule [6].

In addition, the NPT ensemble is most analogous to laboratory experimentation, whereby the temperature and pressure are monitored and controlled to manipulate a closed system in which the number of molecules is held constant.

The simulations consisted of runs in two overall portions; equilbriation to ensure that both phases were in internal equilibrium and in equilibrium with each other, and production in order to generate data to reduce statistical uncertainty. Each equilibriation period consisted of between 45×10^6 and 90×10^6 Monte Carlo moves, whilst each production period was between 90×10^6 and 135×10^6 Monte Carlo moves.

The initial compositions of the phases used in the simulations were those of the highest temperatures for each type of alcohol. The size of each system was determined such that there would be between 300 and 500 molecules per system. This lower limit was determined from previous work on water + n-alkanes [7]. The upper limit was determined by memory constraints on the computers being used, in order to avoid excessive computational time for the simulations.

The fractions (expressed as percentages) of the total number of Monte Carlo moves for

translation/rotation, volume change, interphase transfer (swapping) and regrowth were 54.0 %, 0.3 %, 50.0 % and 15.7 % respectively. This was done in order to focus the simulations on the more statistically significant moves (translation/rotation and swapping) as opposed to volume change, which have been described as disproportionately computationally costly [8].

The TraPPE model used in this work made use of the united atom approach. This approach entailed the treatment of individual functional groups as pseudo-atoms. This approach thus results in the hydrogen atoms in the CH_3 and CH_2 functional groups being handled implicitly, for computational expediency. The TraPPE model parametrized the various intra- and intermolecular interactions, namely: Stretching, bending, torsion, the electrostatic potential, and the van der Waals forces. The van der Waals forces were handled by means of a Lennard-Jones potential [9] for computational expediency. The parameters for these interactions were taken from various literature sources [2,10,11,12,13]. The Lennard-Jones interactions between unlike pairs were accounted for using the classical Lorentz-Berthelot combining rules [14,15]

The fairly standard MC moves which were considered in the Gibbs Ensemble were of 3 basic types: volume change, translation/rotation and particle exchange. As has been discussed in the literature [16], the first of these moves attains mechanical equilibrium, the second internal equilibrium, and the third chemical equilibrium. Additionally, configurational bias was also employed in these simulations. This approach entailed the construction of each molecule, atom by atom, followed by spatial testing of the newly-constructed molecule in order to determine the most energy-favorable arrangement. The acceptance or rejection of this arrangement is then determined by using the usual MC Boltzmann weighting criterion. This method has previously been used for alkanes [17] in order to overcome difficulties with particle insertion into dense phases, and for water [18], in which it was found that configurational bias lent itself to rapidly determining favorable orientations of the water molecules by functioning as a combined translation-rotation move.

4. Results

Presented below are ternary LLE diagrams of all of the systems concerned, along with tables of the LLE data.

x_{Water}	$x_{n\text{-}Dodecane}$	$x_{Methanol}$
	T = 313.14 K	
	Phase I	
0.000	0.991 ± 0.013	0.009 ± 0.013
0.000	0.997 ± 0.005	0.003 ± 0.005
0.000	0.998 ± 0.003	0.002 ± 0.003
0.000	0.998 ± 0.004	0.002 ± 0.004
	Phase II	
0.000	0.006	0.994
0.221	0.013	0.765
0.547	0.002	0.450
0.824	0.000	0.176
	T = 350 K	
	Phase I	
0.000	0.791 ± 0.022	0.209 ± 0.022
0.001 ± 0.001	0.969 ± 0.014	0.030 ± 0.014
0.001 ± 0.001	0.995 ± 0.003	0.004 ± 0.003
0.001 ± 0.001	0.996 ± 0.004	0.004 ± 0.004
	Phase II	
0.000	0.010	0.990
0.225 ± 0.001	0.000	0.775 ± 0.001
0.549	0.000	0.451
0.824	0.000	0.176
	T = 400 K	
	Phase I	
0.000	0.893 ± 0.064	0.107 ± 0.064
0.004 ± 0.004	0.931 ± 0.028	0.065 ± 0.027
0.011 ± 0.008	0.923 ± 0.028	0.066 ± 0.023
0.006 ± 0.004	0.975 ± 0.011	0.019 ± 0.010
	Phase II	
0.000	0.065 ± 0.003	0.935 ± 0.003
0.223 ± 0.001	0.015 ± 0.002	0.762 ± 0.002
0.552 ± 0.002	0.001 ± 0.001	0.447 ± 0.002
0.826 ± 0.001	0.000	0.174 ± 0.001

Table 1. Simulated LLE data for the water + n-dodecane + methanol system.

x_{Water}	$x_{n\text{-}Dodecane}$	$x_{Ethanol}$
	T = 333.15 K	
	Phase I	
0.000	0.977 ± 0.020	0.023 ± 0.020
0.000 ± 0.001	0.993 ± 0.008	0.006 ± 0.008
0.000 ± 0.001	0.992 ± 0.008	0.007 ± 0.008
0.000 ± 0.001	0.993 ± 0.009	0.006 ± 0.009
	Phase II	
0.000	0.013	0.987
0.223	0.005	0.772
0.548 ± 0.001	0.001 ± 0.001	0.450 ± 0.001
0.824 ± 0.001	0.000	0.176 ± 0.001
	T = 350 K	
	Phase I	
0.000	0.645 ± 0.023	0.355 ± 0.023
0.009 ± 0.012	0.878 ± 0.021	0.113 ± 0.020
0.001 ± 0.001	0.979 ± 0.015	0.020 ± 0.015
0.001 ± 0.002	0.989 ± 0.012	0.010 ± 0.011
	Phase II	
0.000	0.024	0.976
0.224 ± 0.002	0.015 ± 0.001	0.761 ± 0.002
0.550 ± 0.001	0.000	0.450 ± 0.001
0.825 ± 0.001	0.000	0.175 ± 0.001
	T = 400 K	
	Phase I	
0.000	0.110 ± 0.029	0.890 ± 0.029
0.120 ± 0.017	0.311 ± 0.013	0.568 ± 0.019
0.011 ± 0.011	0.920 ± 0.045	0.069 ± 0.038
0.007 ± 0.007	0.954 ± 0.033	0.039 ± 0.029
	Phase II	
0.000	0.151 ± 0.019	0.849 ± 0.019
0.238 ± 0.012	0.036 ± 0.004	0.726 ± 0.011
0.547 ± 0.003	0.011 ± 0.003	0.442 ± 0.003
0.828 ± 0.005	0.001 ± 0.002	0.171 ± 0.004

Table 2. Simulated LLE data for the water + n-dodecane + ethanol system.

x_{Water}	$x_{n\text{-}Dodecane}$	$x_{Isopropanol}$
	T = 333.15 K	
	Phase I	
0.000	0.553 ± 0.026	0.447 ± 0.026
0.122 ± 0.018	0.505 ± 0.013	0.373 ± 0.018
0.166 ± 0.029	0.520 ± 0.020	0.314 ± 0.024
0.128 ± 0.030	0.733 ± 0.028	0.139 ± 0.022
	Phase II	
0.000	0.000	1.000
0.219 ± 0.007	0.000	0.780 ± 0.007
0.575 ± 0.006	0.000	0.425 ± 0.006
0.843 ± 0.005	0.000	0.157 ± 0.005
	T = 350 K	
	Phase I	
0.000	0.946 ± 0.021	0.054 ± 0.021
0.006 ± 0.004	0.939 ± 0.022	0.054 ± 0.021
0.007 ± 0.006	0.970 ± 0.013	0.023 ± 0.012
0.008 ± 0.006	0.938 ± 0.023	0.053 ± 0.022
	Phase II	
0.000	0.003 ± 0.002	0.997 ± 0.002
0.225 ± 0.001	0.001 ± 0.002	0.774 ± 0.002
0.548 ± 0.001	0.003 ± 0.001	0.449 ± 0.001
0.830 ± 0.003	0.000	0.170 ± 0.003
	T = 400 K	
	Phase I	
0.000	0.702 ± 0.055	0.298 ± 0.055
0.034 ± 0.015	0.779 ± 0.054	0.187 ± 0.047
0.052 ± 0.013	0.754 ± 0.031	0.194 ± 0.027
0.051 ± 0.019	0.875 ± 0.033	0.074 ± 0.021
	Phase II	
0.000	0.007 ± 0.004	0.993 ± 0.004
0.219 ± 0.003	0.035 ± 0.006	0.746 ± 0.005
0.562 ± 0.003	0.001 ± 0.001	0.437 ± 0.003
0.813 ± 0.003	0.021 ± 0.003	0.165 ± 0.003

Table 3. Simulated LLE data for the water + n-dodecane + isopropanol system.

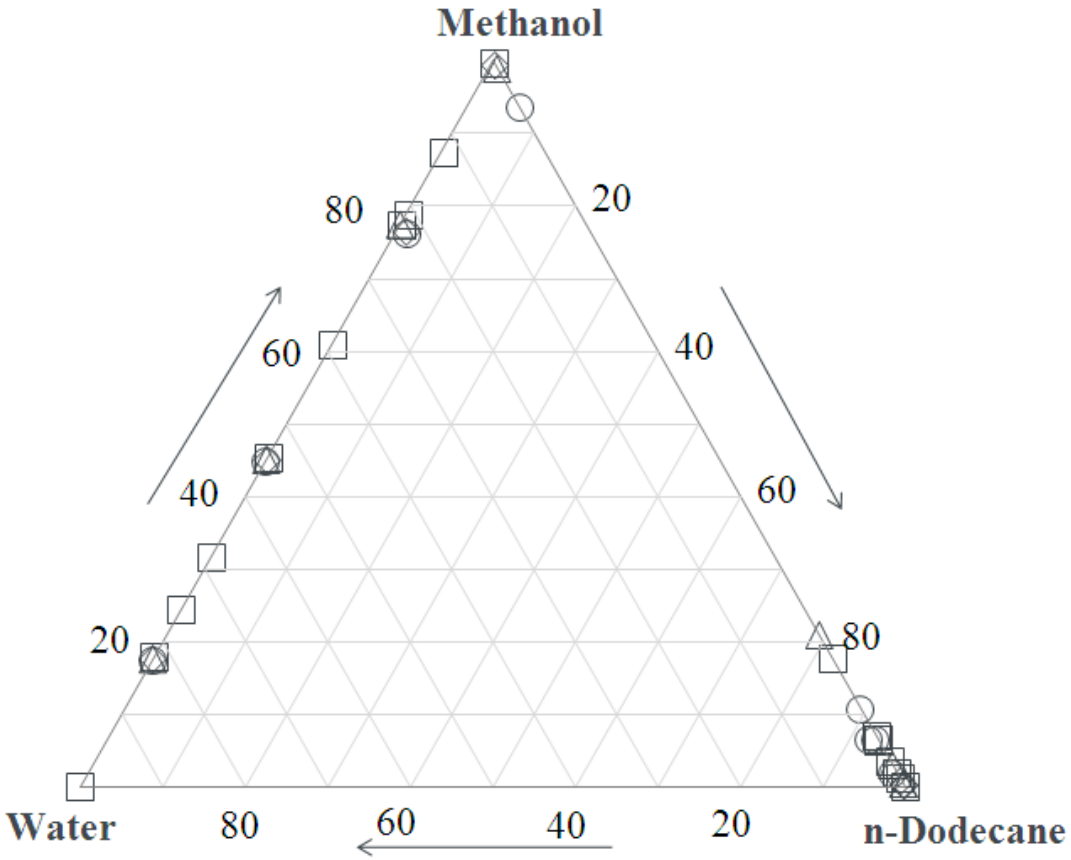

Figure 1. Ternary LLE plot of the methanol + water + n-dodecane system; comparison of simulations with experimental results. (□) experiments at T = 313.14 K (literature), (◇) simulations at T = 313.14 K (this work), (△) simulations at T = 350 K (this work), (◯) simulations at T = 400 K (this work). Literature data is from [1].

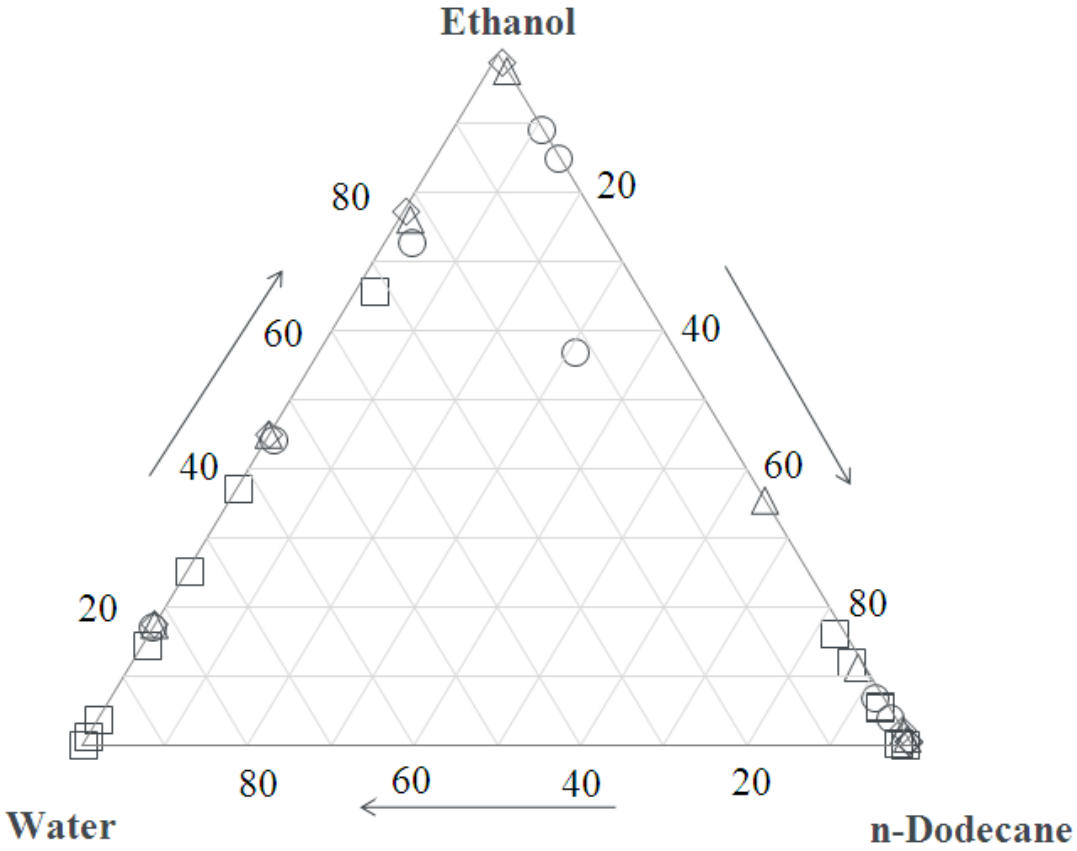

Figure 2. Ternary LLE plot of the ethanol + water + n-dodecane system; comparison of simulations with experimental results. (□) experiments at T = 333.15 K (literature), (◇) simulations at T 313.14 K (this work), (△) simulations at T = 350 K (this work), (○) simulations at T = 400 K (this work). Literature data is from [1].

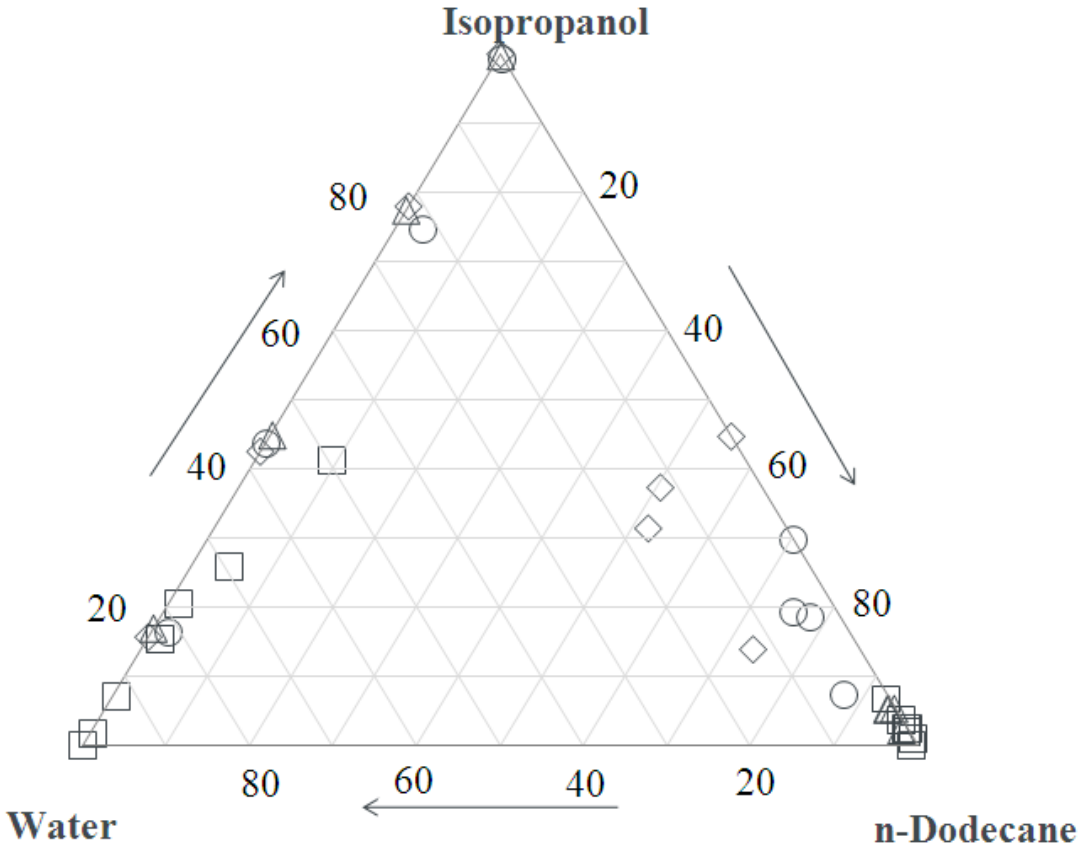

Figure 3. Ternary LLE plot of the isopropanol + water + n-dodecane system; comparison of simulations with experimental results. (□) experiments at T = 333.15 K (literature), (◇) simulations at T 313.14 K (this work), (△) simulations at T = 350 K (this work), (○) simulations at T = 400 K (this work). Literature data is from [1].

5. Discussion

It can be seen in figure 1 that the simulations at T = 313.14 K for the methanol + water + n-dodecane system agreed favourably with the literature. The extrapolations of the methanol + water + n-dodecane

system to T = 350 K and T = 400 K (see figure 1) also yielded only marginal increases in the mutual solubilities between the aqueous and organic phases. It should be noted that the system of methanol + water + n-dodecane did not exhibit a plait point in either the simulations or the laboratory experiments (i.e. the literature data).

The simulations for the ethanol + water + n-dodecane system at T =333.15 K (see figure 2) did not agree favourably with the literature in the region where the $x_{ethanol} > 70$ mole percent in the aqueous phase. In this region, it was observed that the simulations deviated increasingly with increasing ethanol composition in both phases. The most extreme deviation to be found in this region was the absence of a plait point, which occurred not just at T = 333.15 K, but also at T = 350 K and T = 400 K (see figure 2). In contrast to this though, the simulated LLE curve for systems containing less than 70 mole percent ethanol (in the aqueous phase) agreed favourably with the laboratory measurements (i.e. the literature data). This may then suggest that the TraPPE ethanol + SPC water + TraPPE n-dodecane system approximates the real ethanol + water + n-dodecane system in the region where $x_{ethanol}$ in the aqueous phase < 70 mole percent only.

Upon examination of the isopropanol + water + n-dodecane system (see figure 3), similar trends to the ethanol + water + n-dodecane system were observed. In this case (i.e. for the isopropanol + water + n-dodecane system), the simulations did not yield a plait point either, and increasing deviations from the literature data were also observed for concentrations of the alcohol in the aqueous phase exceeding a certain value. It was also observed that the simulations at the extrapolated temperatures (i.e. T = 350 K and T = 400 K) did not yield a plait point. In the case of the isopropanol + water + n-dodecane system, this threshold was observed to be $x_{isopropanol} \sim 20$ mole percent in the aqueous phase. For concentrations of the alcohol in the aqueous phase less than this value, the simulated LLE curves agreed favourably with the laboratory experiments.

The observations for the systems of methanol/ethanol/isopropanol + water + n-dodecane illustrated a trend of increasing deviation from laboratory measurements with increasing carbon number in the alcohol. This was apparent from the threshold concentration of alcohol in the aqueous phase above which significant deviations from the laboratory measurements occurred. Explicitly, this may be represented as follows;

Alcohol carbon number	$x_{alcohol,aqueous}$ range (mole fraction)
1	0.0 – 1.0
2	0.0 – 0.7
3	0.0 – 0.2

Table 4. Approximate ranges of alcohol concentration in the aqueous phase for which the simulations approximated the laboratory experiments favourably.

Table 4 then illustrates that the TraPPE alcohol model does not adequately describe the interactions between alcohol + water + n-dodecane, except possibly within certain phase concentration limits. These limits may become more and more restricted with increasing carbon number in the alcohol (see table 4), although a more exhaustive study should be conducted before any firm conclusions may be drawn in this regard. All that may stated with certainty thus far is that the TraPPE model for alcohols possesses serious shortcomings in systems containing alcohol + water + n-dodecane, using the classical non-bonded interaction combining rules (i.e. the Lorentz-Berthelot combining rules).

Upon examination of the literature from whence the TraPPE parameters for the alcohols were derived [2], it was to be seen that there were significant deviations from laboratory experiments involving interactions of the alcohol-alkane pair. In the case of the methanol + hexane system, for example, it was found in these simulations [2] that there were deviations of up to 40 percent from laboratory measurements of the vapour-liquid equilibrium of the methanol + hexane system. Therefore, it may then be expected that as the interactions between the alcohol-alkane pair become increasingly dominant (i.e. as the proportion of alcohol + alkane to water molecules increases) there may be increasing deviations from laboratory experiments.

6. Conclusions

It was observed that the simulations for the LLE of the methanol + water + n-dodecane system agreed favourably with previous laboratory experiments. Extrapolations of this system to T = 350 K and T = 400 K yielded only marginal increases in the mutual solubility between the aqueous and organic phases.

For the simulated ethanol/isopropanol + water + n-dodecane systems, there were observed to be significant deviations from labortaory experiments. In no cases was there observed to be a plait point, which was found to occur in the laboratory experiments for both of these systems. It was found there was

a threshold of alcohol concentration in the aqueous phase below which the simulations agreed favourably with the laboratory experiments. These thresholds were found to be 70 mole percent and 20 mole percent for ethanol and isopropanol respectively.

The TraPPE description of alcohols, in conjunction with the classical Lorentz-Berthelot combining rules for the non-bonded interactions, was found to be inadequate to describe the interactions between alcohols + water + n-dodecane. It was also observed that there may be a trend of increasing deviations from laboratory experiments with increasing carbon number in the alcohol.

Acknowledgements

We would like to thank the National Research Foundation (NRF) for their generous funding and the School of Engineering at University College of Borås in Sweden for allowing the use of their computing facilities, through which some of the simulations in this work were conducted.

References

[1] M. Lasich, R. Bhownath, P. Naidoo, D. Ramjugernath and T. Moodley, *Liquid-Liquid Equilibria of Light Alcohols with Water and n-Dodecane*, J. Chem. Eng. Data (2011) submitted for review.

[2] B. Chen, J.J. Potoff and J.I. Siepmann, *Monte Carlo Calculations for Alcohols and Their Mixtures with Alkanes. Transferable Potentials for Phase Equilibria. 5. United-Atom Description of Primary, Secondary, and Tertiary Alcohols*, J. Phys. Chem. B 105 (2001) pp. 3093-3104.

[3] E. Johansson and P. Ahlström, *Atomistic Simulation Studies of Polymers and Water*, Springer Lecture Notes in Computer Science 4966/2007 (2007) pp. 59-65.

[4] J. Errington and A.Z. Panagiotopoulous, *Gibbs Ensemble Monte Carlo*; software available at http://kea.princeton.edu/jerring/gibbs/index.html.

[5] A.Z. Panagiotopoulos, *Direct Determination of Phase Coexistence Properties of Fluids by Monte Carlo Simulation in a New Ensemble*, Mol. Phys. 61 (1987) pp. 813-826.

[6] J.W. Gibbs, *Graphical methods in the thermodynamics of fluids*, Transactions of the Connecticut Academy ii (1873) pp. 309-342.

[7] E.L. Johansson, *Simulations of Water Clustering in Vapour, Hydrocarbons and Polymers*, Ph.D. thesis, Chalmers University of Technology, 2007.

[8] S. Moodley, *Molecular Simulation of Vapour-Liquid-Liquid Equilibrium*, Msc diss., University of KwaZulu-Natal, 2008.

[9] J.E. Lennard-Jones, *Cohesion*, Proceedings of the Physical Society 43 (1931) pp. 461-482.

[10] M.G. Martin and J.I. Siepmann, *Transferable Potentials for Phase Equilibria. 1. United-Atom Description of n-Alkanes*, J. Phys. Chem. B 102 (1998) pp. 2569-2577.

[11] M.G. Martin and J.I. Siepmann, *Novel Configurational-Bias Monte Carlo for Branched Molecules. Transferable Potentials for Phase Equilibria. 2. United-Atom Description of Branched Alkanes*, J. Phys. Chem. B 103 (1999) pp. 4508-4517.

[12] H.J.C. Berendsen, J.P.M. Postma, W.F. van Gunsteren and J. Hermans, *Interaction Models for Water in Relation to Protein Hydration*, in *Intermolecular Forces*, B. Pullman, ed., Reidel, Dordrecht, 1981, pp. 331-342.

[13] H.J.C. Berendsen, J.R. Grigera and T.P. Straatsma, *The Missing Term in Effective Pair Potentials* ,Phys. Chem. 91, (1987) pp. 6269-6271.

[14] H.A. Lorentz, *Ueber die Anwendung des Satzes vom Virial in der kinetischen Theorie der Gase*, Ann. Phys. 12 (1881) pp. 127-136.

[15] D.C. Berthelot, *Sur le Mélange des Gaz*, Compt. Rendus 126 (1898) pp. 1703-1706.

[16] K.E. Gubbins, *Applications of Molecular Simulation*, Fluid Phase Equilibria 83 (1993) pp. 1-14.

[17] J.I. Siepmann and D. Frenkel, *Configurational-Bias Monte Carlo - A New Sampling Scheme for Flexible Chains*, Mol. Phys. 75 (1992) pp. 59-70.

[18] E. Johansson, K. Bolton and P. Ahlström, *Simulations of Vapor Water Clusters at Vapor-Liquid Equilibrium*, J. Chem. Phys. 123 (2005) pp. 024504(1-7).

APPENDIX 6: Paper II (manuscript to be submitted to *Molecular Simulation*)

Monte Carlo Simulations of Water Solubility in Polytetrafluoroethylene

Matthew Lasich[a,*], *Erik L. Johansson*[a] *and Deresh Ramjugernath*[a]

[a]Thermodynamics Research Unit, University of KwaZulu-Natal, King George V Avenue, Durban, 4041, South Africa

[*]Corresponding author. Office: +27 31 260 2187. Fax: +27 31 260 1118. Email: matt.lasich@gmail.com.

Abstract

Polytetrafluoroethylene (Teflon®) is encountered in many different environments, yet the solubility behavior of the common solvent water was not to be found in the open literature. Such data may be useful in applications such as textiles, osmotic distillation and membrane fuel cells, where polytetrafluoroethylene may frequently interact with water. Gibbs ensemble Monte Carlo simulations were performed for systems of perfluoroalkanes + water for temperatures from 300 K to 600 K and for perfluoroalkane chain lengths of 8 to 300 carbon atoms. The Transferrable Potentials for Phase Equilibrium (TraPPE) model was used to represent the perfluoroalkane molecules. The Simple Point Charge-Extended (SPC-E) model was selected to represent the water due its high critical temperature of 630 – 640 K. This was important due to the impermeable nature of polymer crystals resulting in the scenario of liquid-liquid equilibrium having to be investigated. High temperatures, up to 600 K, would be required to ensure that the simulated polymer molecules would not crystallize. This methodology was used in the past for systems of alkanes + water. This solubility data was then compared to data for systems of alkanes + water found in the open literature. It was found that increasing the temperature had an exponential-type increase on the solubility of water into the perfluoroalkane phase, similar to the result found for alkanes. It was found that increasing the perfluoroalkane chain length increased the solubility of

water into the perfluoroalkane phase, to an asymptotic maximum of 98.0 mole percent. An irregularity was observed at carbon number 12, which may be ascribed to a change in the energy contribution regime for the helical to all-trans conformation, as inferred from data in the open literature.

Keywords: molecular simulation, water, polymer, polytetrafluoroethylene

1. Introduction

Polytetrafluoroethylene (PTFE), more commonly known as Teflon®, is frequently encountered in many scenarios; sealing tape, frying pans, clothing, fuel cells [1] and osmotic distillation [2], to name a few. However, the solubility behavior of water with this material was not found to have been widely studied in the open literature. Prior measurements in industry, using standards such ASTM D570, have yielded a value of < 0.01 wt% water absorption into the polymer [3,4]. Previous simulations of systems of perfluoroalkanes [5] have illustrated that there is greater supramolecular ordering and greatly increased molecular rigidity in perfluoroalkanes than in alkanes. Previous experiments [6] have found that the average volume of a hole in a PTFE matrix may be roughly twice as large as in polyethylene (PE).

The purpose of this study was to determine the influence, if any, of temperature and perfluoroalkane chain length on the solubility of water in the perfluoroalkane phase. The Transferrable Potentials for Phase Equilibrium (TraPPE) model would be used to model the perfluoroalkane molecules [7,8], whilst the Simple Point Charge-Extended (SPC-E) model was used to model the water molecules [9,10].

2. Theory and methods

Gibbs Ensemble Monte Carlo (GEMC) simulations were performed on the Beowulf cluster belonging to the Thermodynamics Research Unit at the University of KwaZulu-Natal. The software which was used for carbon numbers less than 20 was that of Errington and Panagiotopoulos [11], using the Gibbs ensemble method developed by Panagiotopoulos [12]. For molecules longer than 20, a modified GEMC program was used, in which an end-bridging algorithm [13] had been incorporated.

The Gibbs ensemble is an approach whereby the limitations due to surface effects on small systems of molecules is overcome by the possibility of transfer between “boxes” located within the bulk

material of a particular phase. The GEMC program used in this work also made use of configurational bias, whereby the insertion of a molecule into a phase was “tested” to determine the most energy-favorable configuration. The 3 types of Monte Carlo (MC) moves which were considered by the GEMC program were: Translation/Rotation, volume change and interphase transfer. The end-bridging modification of the GEMC program introduced several different, polymer-specific moves: Reptation, end mer rotation, monomer flip, dimer flip and end-bridging.

The TraPPE model used in this work [7,8] handled each functional group as an individual pseudo-atom. In this way, the individual fluorine atoms on each CF_3 and CF_2 group were handled implicitly. This is primarily due to computational expediency. The TraPPE model accounted for all inter- and intra-molecular interactions: Bending, stretching, twisting (torsion), electrostatic forces and van der Waals forces. The modified torsional potential was a re-parametrization of the torsional potential energy according to a different functional form [7,8].

The water model used in this work was the SPC-E model [9,10]. This water model was preferred due to its sufficiently high critical temperature [17] of between 630 K and 640 K, which would exceed the maximum temperatures to be encountered in this work.

The van der Waals forces were handled by the TraPPE and SPC-E models in the form of a Lennard-Jones potential [14]. The classical Lorentz-Bertholet combining rules [15,16] were used to account for interactions between unlike molecular and atomic pairs.

The approach which was followed was used previously for the PE + water system [18,19,20]. This approach entailed two sets of simulations in order to determine the solubility of water in the polymer in terms of temperature and polymer chain length. The simulation of the n-C_{10} + water system at varying temperatures was performed, as per the aforementioned prior work [18,19,20] in order to determine the influence of temperature on the solubility of water in the polymer. The influence of polymer chain length was determined by simulations of the n-C_N + water systems at a fixed temperature and varying carbon numbers.

In order to study the phenomenon of water solubility in the polymer, it was necessary to study the condition of liquid-liquid equilibrium (LLE) occurring between the polymer and the water. This followed from the aforementioned water + polymer solubility analysis methodology [18,19,20]. The reason for investigating two liquid phases was that the crystalline portions of the polymer are impermeable, and thus any species absorbed into the polymer is absorbed into the amorphous portions [21]. To this end, it was necessary to investigate temperatures ranging up to 600 K, in order to ensure that the PTFE occurred as

an amorphous liquid [3,4]. That the perfluoroalkane crystals in particular should be impermeable can be seen in prior work on the interactions between perfluoro-n-eicosane crystals and water [22].

3. Results

In all simulations in this work, the systems consisted of 500 water molecules and 100 polymer/perfluoroalkane molecules. In each case, the system was initially allowed to equilibriate internally without swap moves occurring between the two phases. Once this was achieved, swap moves were allowed, and this was continued until the phase compositions had reached a state of equilibrium. After this point, the simulations were run further to produce data in order to reduce the statistical error. On average, this two-stage equilibriation period took ~ 90,000,000 MC moves. In each case, the production period consisted of no less than 60,000,000 MC moves.

The results of the simulations conducted in this work can be found in the following three figures;

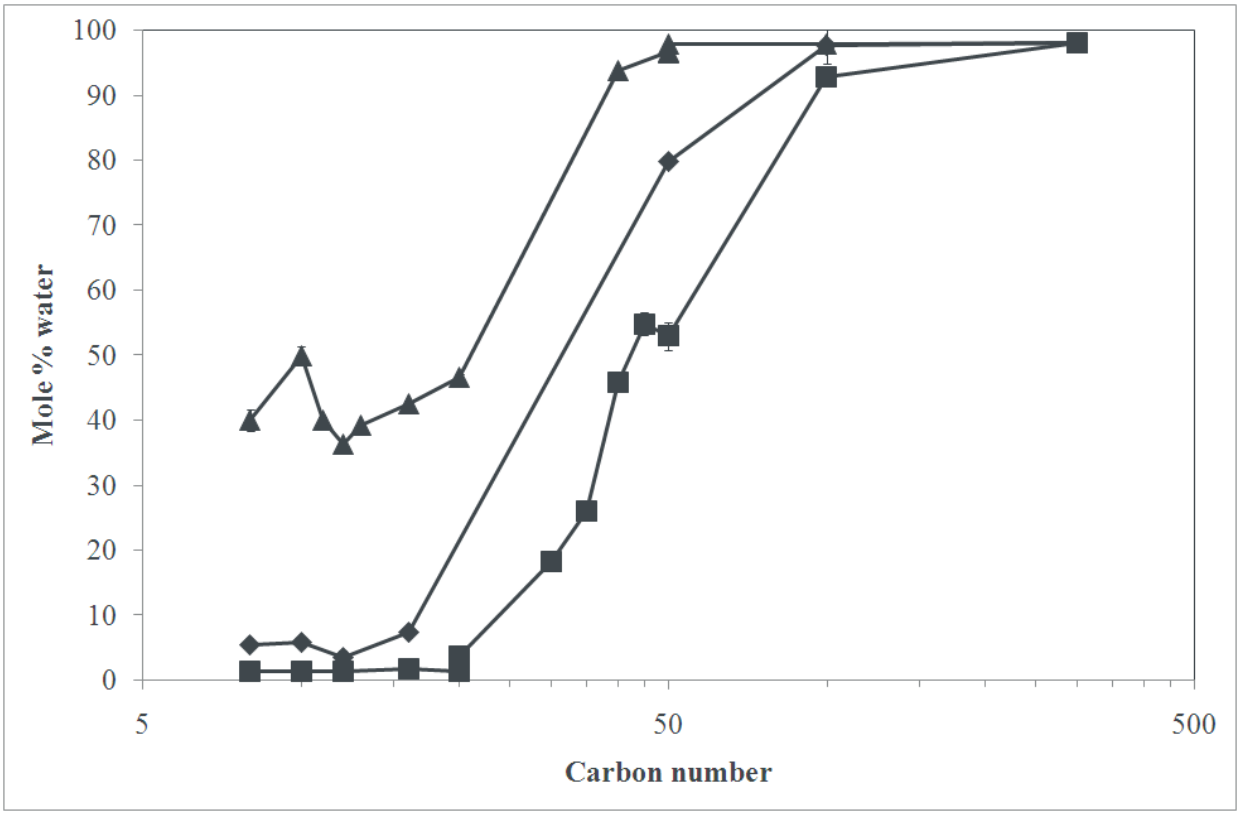

Figure 1. Solubility of water in PTFE as a function of carbon number, for three different temperatures, on a molar basis. (■) T = 450 K, (◆) T = 500 K, (▲) T = 600 K. Lines have been added between the points as guides for the eye. The x-axis has been made logarithmic for clarity at the smaller carbon numbers.

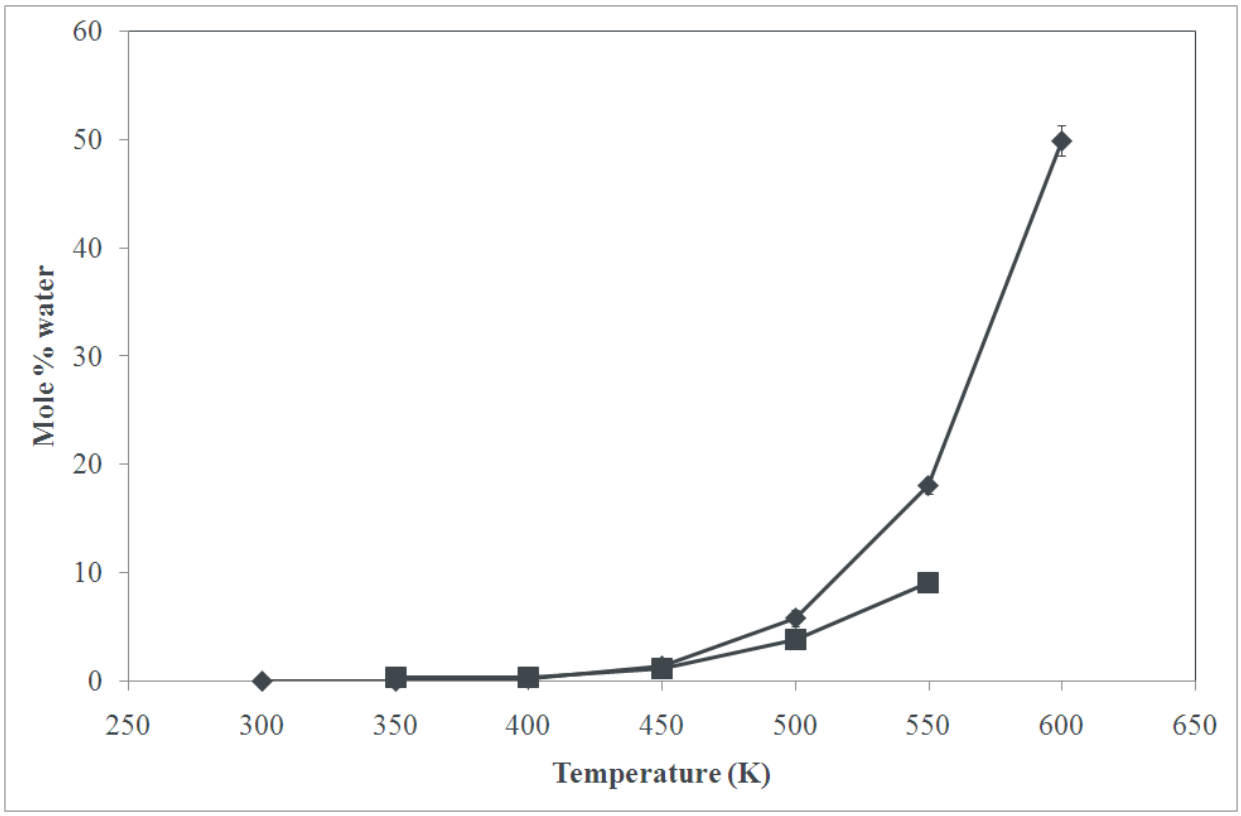

Figure 2. Solubility of water in n-decane and perfluorodecane over a temperature range from 300 K to 600 K. (■) n-alkanes (literature), (◆) perfluoroalkanes (this work). The literature data is from [19].

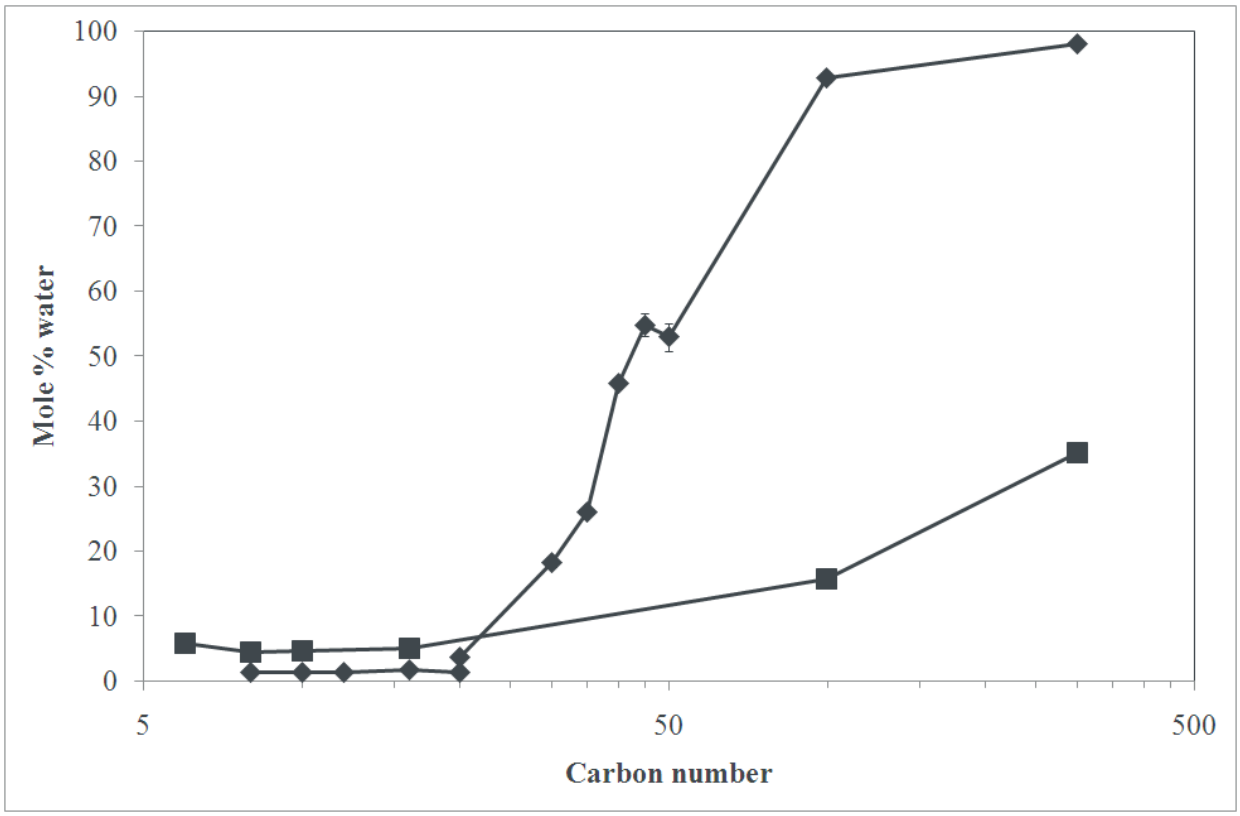

Figure 3. Graph of the solubility of water, at T = 450 K, as a function of carbon number in PTFE compared to PE, on a molar basis. (■) PE (literature), (◆) PTFE (this work).The literature data is from [19].. Lines have been added between the points as guides for the eye. The x- axis has been made logarithmic for clarity at the smaller carbon numbers.

4. Discussion

As is evident in figure 1, there is a trend towards increased solubility of water in the perfluoroalkane phase with increases in both temperature and perfluoroalkane chain length. There appears to be an asymptotic value of 98.0 mole percent water solubility in the perfluoroalkane phase. While this figure may seem high, given that the measured absorption of water in solid PTFE is < 0.01 wt% [3,4], it is important to note that once an approximate value for the crystallinity [6] and the high molar mass of the PTFE [23] are taken into account, a figure of ~ 0.09 wt% of water in the PTFE emerges. This is of the same order of magnitude as the aforementioned measurement. It is also important to note here that the PTFE in the simulations shown in figure 1 was at a temperature of 450 K (~ 177 ºC), whereas the measurements [3,4] were performed at 23 ºC [24], and thus it may be expected that the water may be slightly more soluble in the simulated PTFE as compared to the available measurements.

With regard to the effect of temperature on the solubility of water into the perfluoroalkane phase with the carbon number of the perfluoroalkane being held constant, figure 2 illustrates that similar trends may be observed. This trend is of an apparently exponential increase in solubility with temperature.

Previous work on clustering in perfluoroalkanes and alkanes [5] illustrated that there was greater supramolecular order in perfluoroalkanes than in alkanes at comparable conditions due to increased molecular rigidity. This may suggest that higher temperatures, as the polymer molecules move further away from each other, there would be an increase in the free volume apparent in the PTFE matrix as compared to the PE matrix. This would be due to the rigid perfluoroalkane molecules being less likely to bend and twist to occupy the free spaces formed as the molecules move further apart, due to their inherent rigidity. In addition, previous experiments [6] have shown that the average volume of a hole in the PTFE matrix is roughly twice the size of the average hole in the PE matrix (~ 0.37 nm^3 versus ~ 0.18 nm^3). This would then suggest that, based upon the radius of a water molecule of ~ 1.58 Å [25], there may be roughly twice as many water molecules per void in the PTFE matrix as compared to the PE matrix (~ 22 versus ~ 11). However, it should be noted that these same experiments [6] yielded an overall free volume fraction of ~ 70 percent for both PTFE and PE, suggesting that there are fewer and larger holes in the PTFE matrix as occur in the PE matrix. The increased solubility of water in PTFE/perfluoroalkanes as compared to PE/alkanes evident in figures 2 and 3 may illustrate this increased hole volume.

In addition to the simulations already discussed, figure 1 illustrates the effect of drastically increasing the temperature of the PE + water system. The simulated point of the PE + water system at 600 K illustrates that the relatively large solubility of water in PTFE as compared to PE are not totally inconceivable. By increasing the temperature to 600 K from 450 K, it can be seen that the solubility of water into the PE increased from ~ 30 mole percent to ~ 90 mole percent.

A further point to note is the apparent irregularity at a PTFE chain length of 12. This irregularity can be seen in figure 1, and it can be seen that it is more pronounced at higher temperatures (600 K in this case, as compared to 500 K and 450 K). A possible cause for this may be inferred from previous work on the energy contributions to the helical to all-trans conformation transformation [26]. From the data presented in this prior work, it can be seen that there was a change in the regime of the energy contributions towards the helical structuring of perfluoroalkanes, from a chain length of 8 to 12 carbon atoms. At carbon number 8, it was observed that the Coulombic energy contribution was greater than the total fluorine-fluorine interaction, whilst from carbon number 12 upwards, the Coulombic interactions became increasingly less significant. While it is apparent that the TraPPE model for perfluoroalkanes does not explicitly state electrical charges on the pseudo-atoms, the parameters describing the interactions such

as bending, torsion, etc may implicitly account for any Coulombic interactions.

5. Conclusions

The effects of perfluoroalkane chain length and temperature on the solubility of water into the perfluoroalkane phase have been investigated by GEMC simulations. The solubility of the water was observed to increase with both increasing temperature and increasing perfluoroalkane carbon number.

It was observed that increasing the temperature had an exponential-type effect on the solubility of water into the perfluoroalkane phase, similar to the effect observed for alkanes [18,19,20].

Increasing the PTFE chain length was observed to result in increased water solubility into the PTFE phase, similar to the trends observed for the water + PE system [18,19,20]. The solubility of water into the PTFE was found to have an asymptotic maximum of 98.0 mole percent.

Overall, the solubility of water into PTFE/perfluoroalkanes was observed to be significantly higher than that of water into PE/alkanes as presented in the literature [18,19,20].

An irregularity was observed at a perfluoroalkane chain length of 12, which may be due to a change in the regime of the energy contributions towards the helical to all-trans conformation transformation inferred from literature data [26].

Acknowledgements

We would like to thank the National Research Foundation (NRF) for their generous funding of this research project.

References

[1] H.L. Lin, T.L. Yu, L.N. Huang, L.C. Chen, K.S. Shen and G.B. Jung, *Nafion/PTFE Composite Membranes for Direct Methanol Fuel Cell Applications*, Journal of Power Sources 150 (2005) pp. 11-19.

[2] M. Courel, M. Dornier, G.M. Rios and M. Reynes, *Modeling of Water Transport in Osmotic Distillation Using Asymmetric Membrane*, Journal of Membrane Science 173 (2000) pp. 107-122.

[3] DuPont de Nemours (Nederland) B.V., *Safety Data Sheet: Teflon® PTFE*, available at http://msds.dupont.com/msds/pdfs/EN/PEN_09004a358023be41.pdf.

[4] DuPont de Nemours (Nederland) B.V., *Safety Data Sheet: Teflon™ AF Amorphous Fluoropolymer*, available at http://msds.dupont.com/msds/pdfs/EN/PEN_09004a35803537ac.pdf.

[5] R. Friedemann, S. Naumann and J. Brickmann, *Aggregation of Alkane and Fluoroalkane Clusters: Molecular Dynamics Simulation Results*, Phys. Chem. Chem. Phys. 3 (2001) pp. 4195-4199.

[6] G. Dlubek, K. Saarinen and H.M. Fretwell, *The Temperature Dependence of the Local Free Volume in Polyethylene and Polytetrafluoroethylene: A Positron Lifetime Study*, Journal of Polymer Science: Part B: Polymer Physics 36 (1998) pp. 1513-1528.

[7] S.T. Cui, J.I. Siepmann, H.D. Cochran and P.T. Cummings, *Intermolecular Potentials and Vapor-Liquid Phase Equilibria of Perfluorinated Alkanes*, Fluid Phase Equilibria 146 (1998) 51-61.

[8] L. Zhang and J.I. Siepmann, *Pressure Dependence of the Vapor-Liquid-Liquid Phase Behavior in Ternary Mixtures Consisting of n-Alkanes, n-Perfluoroalkanes, and Carbon Dioxide*, J. Phys. Chem. B 109 (2005) pp. 2911-2919.

[9] H.J.C. Berendsen, J.P.M. Postma, W.F. van Gunsteren and J. Hermans, *Interaction Models for Water in Relation to Protein Hydration*, in *Intermolecular Forces*, B. Pullman, ed., Reidel, Dordrecht, 1981, pp. 331-342.

[10] H.J.C. Berendsen, J.R. Grigera and T.P. Straatsma, *The Missing Term in Effective Pair Potentials* ,Phys. Chem. 91, (1987) pp. 6269-6271.

[11] J. Errington and A.Z. Panagiotopoulous, *Gibbs Ensemble Monte Carlo*; software available at http://kea.princeton.edu/jerring/gibbs/index.html.

[12] A.Z. Panagiotopoulos, *Direct Determination of Phase Coexistence Properties of Fluids by Monte Carlo Simulation in a New Ensemble*, Mol. Phys. 61 (1987) pp. 813-826.

[13] V.G. Mavrantzas, T.D. Boone, E. Zervopoulou and D.N. Theodorou, *End-Bridging Monte Carlo: A Fast Algorithm for Atomistic Simulation of Condensed Phases of Long Polymer Chains*, Macromolecules 32, (1999) pp. 5072-5096.

[14] J.E. Lennard-Jones, *Cohesion*, Proceedings of the Physical Society 43 (1931) pp. 461-482.

[15] H.A. Lorentz, *Ueber die Anwendung des Satzes vom Virial in der kinetischen Theorie der Gase*, Ann. Phys. 12 (1881) pp. 127-136.

[16] D.C. Berthelot, *Sur le Mélange des Gaz*, Compt. Rendus 126 (1898) pp. 1703-1706.

[17] C. Boulougouris, I.G. Economou and D.N. Theodorou, *Engineering a Molecular Model for Water Phase Equilibrium over a Wide Temperature Range*, J. Phys. Chem. B 102 (1998) pp. 1029-1035.

[18] E. Johansson and P. Ahlström, *Atomistic Simulation Studies of Polymers and Water*, Springer Lecture Notes in Computer Science 4966/2007 (2007) pp. 59-65.

[19] E.L. Johansson, *Simulations of Water Clustering in Vapour, Hydrocarbons and Polymers*, Ph.D. thesis, Chalmers University of Technology, 2007.

[20] E.L. Johansson, K. Bolton, D.N. Theodorou and P. Ahlström, *Monte Carlo Simulations of Equilibrium Solubilities and Structure of Water in n-Alkanes and Polyethylene*, J. Chem. Phys. 126 (2007) pp. 224902(1-7).

[21] U.W. Gedde, *Polymer Physics*, Chapman & Hall, London, 1995.

[22] S. Pal, H. Weiss, H. Keller and F. Müller-Plathe, *The Hydrophobicity of Nanostructured Alkane and Perfluoroalkane Surfaces: A Comparison by Molecular Dynamics Simulation*, Phys. Chem. Chem. Phys. 7 (2005) pp. 3191-3196.

[23] U. Lappan, U. Geißler, L. Häußler, G. Pompe and U. Scheler, *The Estimation of the Molecular Weight of Polytetrafluoroethylene Based on the Heat of Crystallisation. A Comment on Suwa's Equation*, Macromol. Mater. Eng. 289 (2004) pp. 420-425.

[24] Intertek Plastics Technology Laboratories, *Water Absorption 24Hour/Equilibrium*, available at http://www.ptli.com/testlopedia/tests/water_absorption-d570.asp.

[25] Y. Tamai, H. Tanaka and K. Nakanishi, *Molecular Simulation of Permeation of Small Penetrants through Membranes. 2. Solubilities*, Macromolecules 28 (1995) pp. 2544-2554.

[26] S.S. Jang, M. Blanco, W.A. Goddard III, G. Caldwell and R.B. Ross, *The Source of Helicity in Perfluorinated N-Alkanes*, Macromolecules 36 (2003) pp. 5331-5341.

APPENDIX 7: Paper III (manuscript to be submitted to *Journal of Cluster Science*)

Monte Carlo Simulations of Water Structures in Polytetrafluoroethylene

Matthew Lasich[a], *Erik L. Johansson*[a] *and Deresh Ramjugernath*[a,*]

[a]Thermodynamics Research Unit, University of KwaZulu-Natal, King George V Avenue, Durban, 4041, South Africa

[*]Corresponding author. Office: +27 31 260 2187. Fax: +27 31 260 1118. Email: matt.lasich@gmail.com

ABSTRACT

This project concerned the analysis of the clustering behaviour of water molecules within the polytetrafluoroethylene by varying the polymer carbon number from 8 to 300 and the temperature from 300 K to 600 K. It was found that data on the clustering behaviour of water molecules in polytetrafluoroethylene was lacking in the open literature. The Cartesian coordinate data was generated by Gibbs ensemble Monte Carlo simulations of the systems of interest. The cluster analysis was then conducted on the Cartesian coordinate data from these simulations. The cluster analysis was performed using Fotran90 software previously used for the polyethylene + water system. It was found that there were no clear trends in water clustering behaviour for polymer carbon numbers between 8 and 50. A marked decrease in the frequency of water clusters of all sizes was found to occur from a polymer carbon number of 50 to 300. A discontinuity was observed at a polymer carbon number of 12 which may be related to a change in the regime of the energy contributions to the helical to all-trans conformation transformation observed in a previous study. It was observed that increasing the temperature increased the frequency of all sizes of water clusters. Linear water clusters were found to account for up to 90

percent of all water clusters for tetramers and pentamers.

Keywords: molecular simulation, water, polymer

INTRODUCTION

Polytetrafluoroethylene (PTFE), more commonly known as Teflon®, can be found in many applications; pipe sealing tape, fuel cell membranes [1], osmotic distillation membranes [2] and frying pans, for example. Water is also frequently encountered, as it may have varied uses, such as solvent, heat transfer fluid and transport medium. Both species (i.e. PTFE and water) may therefore interact with one another regularly, yet the clustering behaviour of water within the PTFE was not found to be determined in the open literature.

Clustering amongst water molecules occurs due to the strongly polar nature of water molecules, as there are clearly separated negative and positive Coulombic charges on each molecule. The oxygen atom possesses a distinct negative charge, whilst the two hydrogen atoms possess distinct positive charges. These localized charges play a strong role in the geometric arrangements which water molecules may take when in contact with each other. It is these geometric arrangements, defined by their topologies, which are referred to as water clusters. These clusters may have different topological forms, such as linear, branched or cyclic, and may consist of different numbers of water molecules. This may then result in combinations of these two features such as linear tetramers or cyclic pentamers, for example. These water clusters are held together by a strong feature of aqueous systems: hydrogen bonding.

The importance of the clustering behaviour of water inside polymers may be seen in previous work on polyethylene (PE) and water [3, 4, 5, 6], for example. It was shown previously [6] that the deterioration of the PE insulation of electrical cables was strongly influenced by the clustering of water molecules around charged ions within the polymer matrix. Thus, a determination of the clustering behaviour of water within the PTFE matrix may yield more insight into the molecular interactions between two chemical species (PTFE and water) which may interact with one another on a regular basis.

To investigate the clustering behaviour of water within the PTFE matrix, the route of molecular simulation was selected for this study. In particular, the Monte Carlo approach to molecular simulation was used. The Monte Carlo approach entails random sampling of the system at various states, and as such is of interest in studies of chemical or phase equilibrium [7]. In addition, the computer simulation of

systems of individual molecules can provide insight at the molecular level that may otherwise be absent from laboratory experiments.

The conditions selected for this study on the PTFE + water system would be liquid-liquid equilibrium between the water and the PTFE at varying polymer carbon numbers and varying temperatures. The maximum temperature selected for this study was 600 K. This temperature is the stated melting point of commercial Teflon® [8, 9].

THEORY AND METHODS

Gibbs ensemble simulations were performed using Fortran90 computer programs run on Beowulf class computing clusters. The software used to generate coordinates for polymer carbon numbers less than or equal to 16 was an existing program written by Errington and Panagiotopoulos [10]. This program used the Gibbs ensemble developed by Panagiotopoulos [11]. A modified form of this program was used for polymer chains longer than 16 carbon atoms. This modified program employed an end-bridging algorithm [12].

With small systems of molecules (i.e. systems containing of the order of 10^2 or 10^3 molecules), surface effects may become overwhelmingly significant. This is a major drawback when data on the bulk properties are sought. The Gibbs ensemble overcomes this limitation by replacing the transfer of molecules across phase boundaries with the possibility of swapping molecules between “boxes” located within the bulk material of each phase under investigation. The Gibbs ensemble program used in this project made use of configurational bias, which involved the assembly (atom by atom) of molecules inserted from one phase into another such that the most energy-favourable configuration would be selected. The types of Monte Carlo moves which were considered in the unmodified Gibbs ensemble program were: Translation, rotation, volume change and swapping between phases. The modified Gibbs ensemble (incorporating the end-bridging algorithm) considered a different set of moves to be applied specifically to the polymer molecules: Reptation, end mer rotation, monomer flipping, dimer flipping and end-bridging.

The TraPPE model [13, 14] handled the ancilliary atoms contained within each functional group implicitly. This approach was taken for computational expediency. The types of interactions accounted for by the TraPPE model were both intra- and intermolecular in nature: Bond bending, bond stretching, dihedral twisting (torsion), Coulombic/electrostatic forces and the van der Waals forces. The TraPPE model in this work employed a torsional potential which was different in form to the usual torsional

potential function, and which was re-parametrized for greater accuracy in a previous study [13, 14].

The Simple Point Charge-Extended (SPC-E) model [15, 16] was used in this work to model to water molecules. This model was selected due to its critical temperature of 630 K to 640 K [17]. This critical temperature would exceed the maximum temperatures which would be encountered in this work (i.e. 600 K).

The van der Waals forces between the pseudo-atoms/molecules in this work were expressed by the TraPPE and SPC-E models in the form of the Lennard-Jones potential [18]. The classical Lorentz-Berthelot combining rules [19, 20] were used to handle the interactions between unlike pairs of pseudo-atoms/molecules.

This work followed an approach used previously for the polyethylene + water system [4, 5, 6]. This approach entailed the simulation of the the n-C_{10} + water system at varied temperatures. The n-C_N + water system was then simulated at varied carbon numbers.

As described in the introduction, the phenomenon of liquid-liquid equilibrium was necessary for this work. This phenomenon was also used in the approach used previously for the polyethylene + water system [4, 5, 6]. The reason for investigating the interactions between the two liquid phases (i.e. the water and the polymer) was that the species absorbed into a polymer would be absorbed into the amorphous portion of the polymer matrix [21]. The crystalline portions of the polymer would be impervious to the absorbed species [21]. The impermeability of these polymer/long carbon chain crystals to water may be further evidenced by a study on the interactions between water and perfluoro-n-eicosane [22].

The definition of a water cluster may significantly influence the results obtained by any cluster analysis. The cluster definition used in this work was that used previously for the polyethylene + water system [4, 5, 6]. This definition is that of an intermolecular oxygen-hydrogen distance of less than 2.4 Å coupled with an intermolecular energy of less than – 10 kJ/mol, based upon a previous definition of water clusters [23].

RESULTS

In all simulations in this work, the systems consisted of 500 water molecules and 100 polymer/perfluoroalkane molecules. In each case, the system was initially allowed to equilibriate internally without swap moves occurring between the two phases. Once this was achieved, swap moves were allowed, and this was continued until the phase compositions had reached a state of equilibrium.

After this point, the simulations were run further to produce data in order to reduce the statistical error. On average, this two-stage equilibriation period took ~ 90,000,000 MC moves. In each case, the production period consisted of no less than 60,000,000 MC moves.

For the production runs, the Cartesian coordinates of the water molecules in the polymer phase at each configuration were stored to disk. These coordinates were then analysed by the aforementioned cluster analysis program, based upon the aforementioned cluster definition.

Additional sources of information regarding the clustering of water molecules may be the frequency distributions of commonly occurring cluster types, the radial distribution function of water in relation to the polymer molecules, the water cluster binding energy, as well as a comparison between the clustering observed in PTFE and the clustering found in pure water.

The results of this cluster analysis study may found in the following figures;

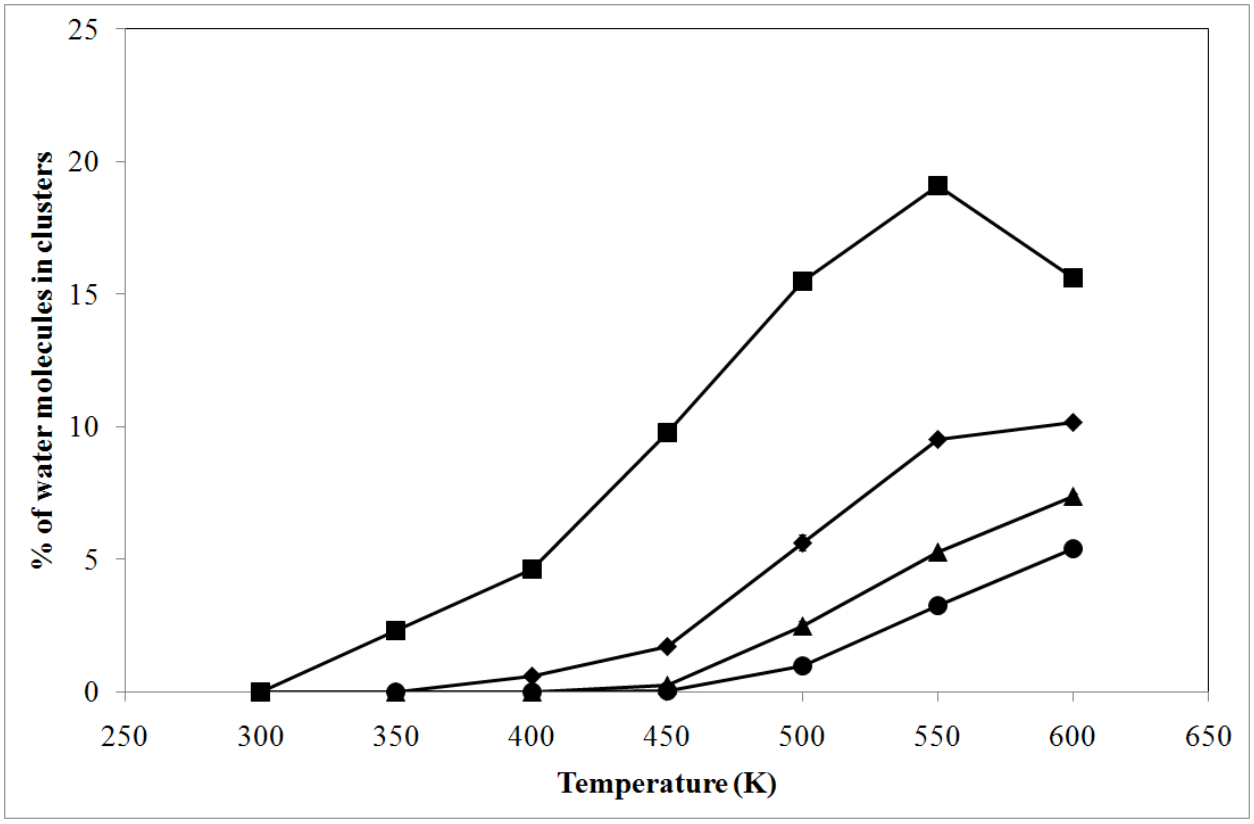

Fig. 1. Percentage of water molecules included in clusters in the perfluoroalkane phase as a function of temperature at a carbon number of 10. (■) n = 2, (◆) n = 3, (▲) n = 4, (●) n = 5. Lines joining the points have been added as guides for the eye.

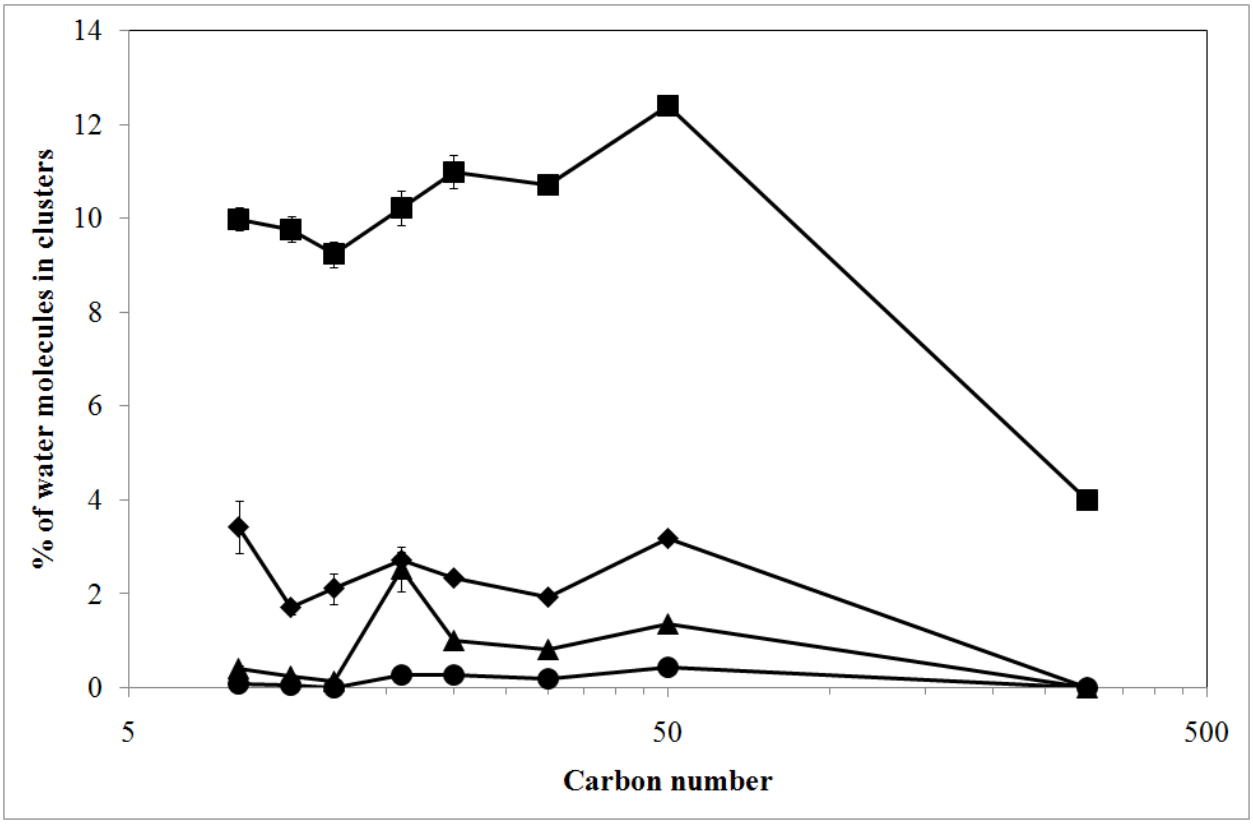

Fig. 2. Percentage of water molecules included in clusters in the perfluoroalkane phase as a function of carbon number at T = 450 K. (■) n = 2, (◆) n = 3, (▲) n = 4, (●) n = 5. The scale of the x-axis has been made logarithmic for clarity at the smaller carbon numbers. Lines joining the points have been added as guides for the eye.

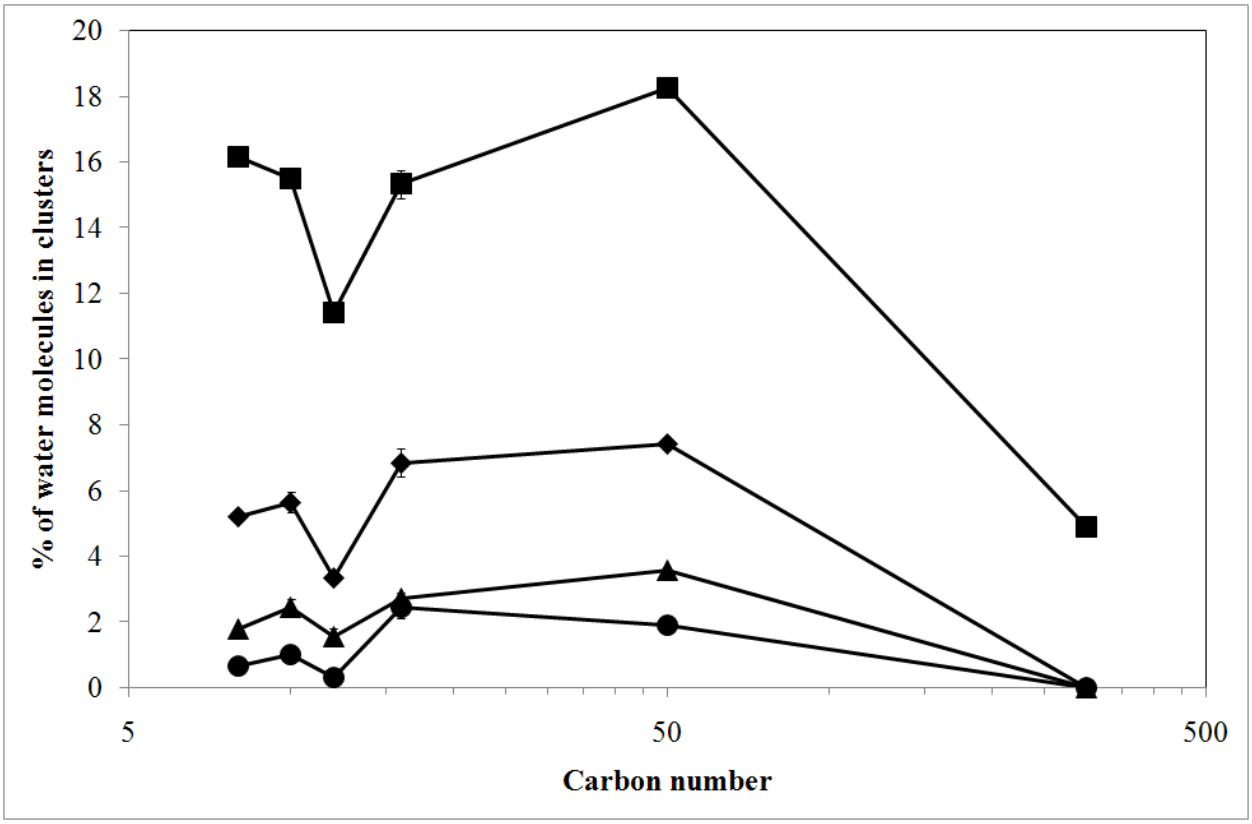

Fig. 3. Percentage of water molecules included in clusters in the perfluoroalkane phase as a function of carbon number at T = 500 K. (■) n = 2, (◆) n = 3, (▲) n = 4, (●) n = 5. The scale of the x-axis has been made logarithmic for clarity at the smaller carbon numbers. Lines joining the points have been added as guides for the eye.

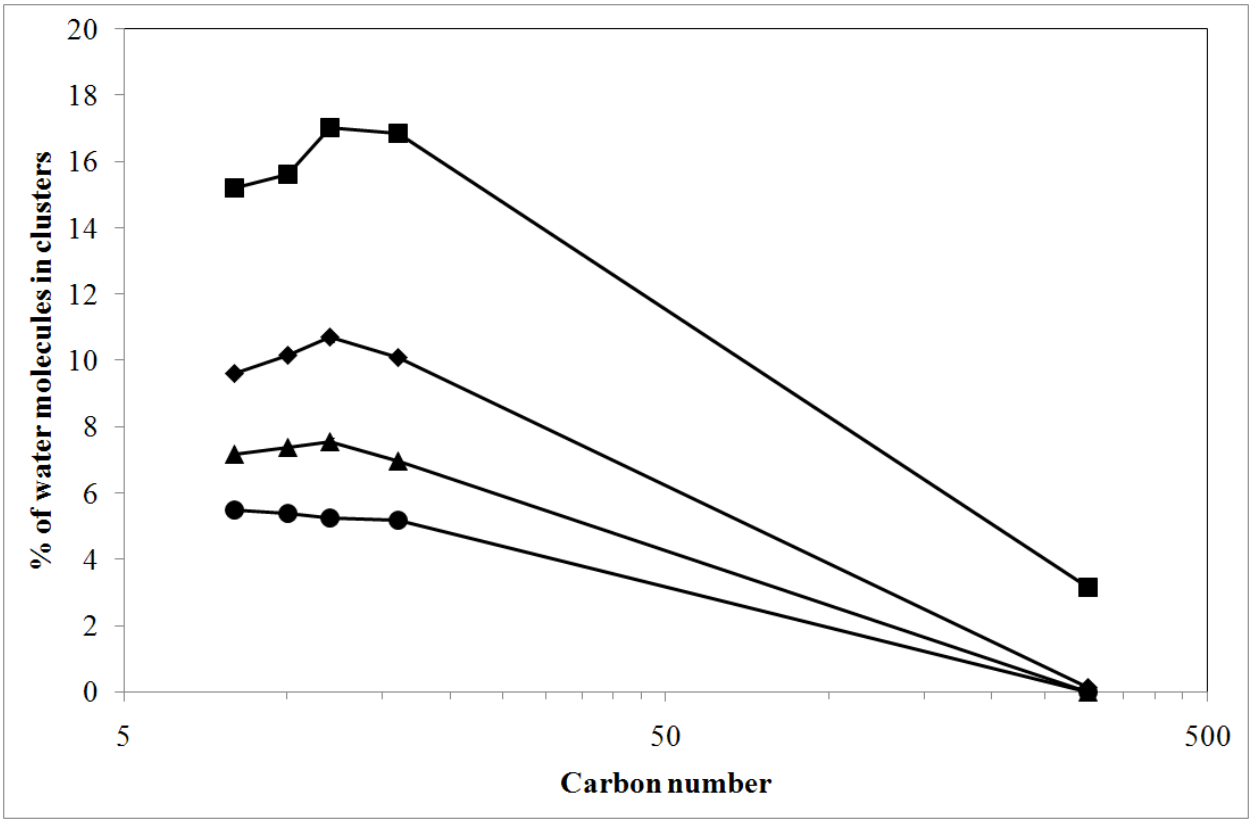

Fig. 4. Percentage of water molecules included in clusters in the perfluoroalkane phase as a function of carbon number at T = 600 K. (■) n = 2, (◆) n = 3, (▲) n = 4, (●) n = 5. The scale of the x-axis has been made logarithmic for clarity at the smaller carbon numbers. Lines joining the points have been added as guides for the eye.

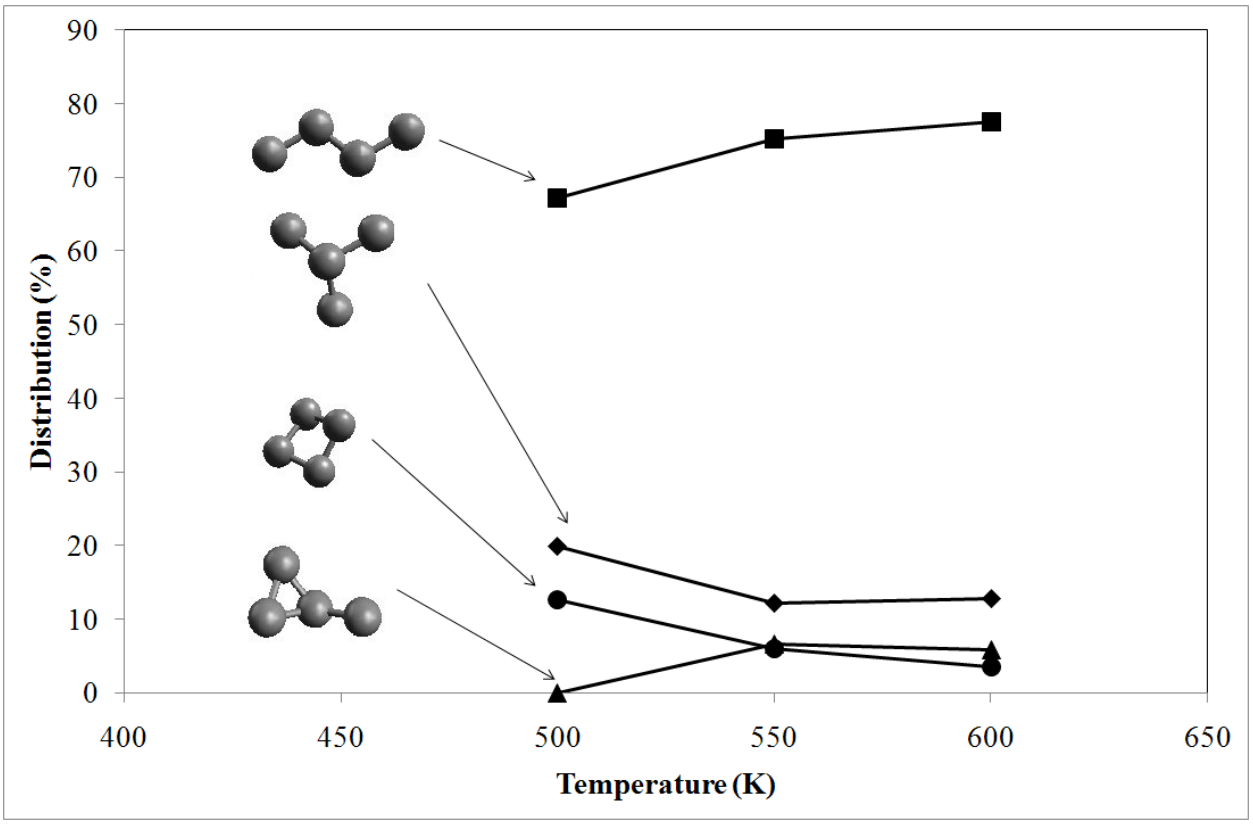

Fig. 5. Frequency distribution of the four most common tetramer configurations as a function of temperature. Lines joining the points have been added as guides for the eye.

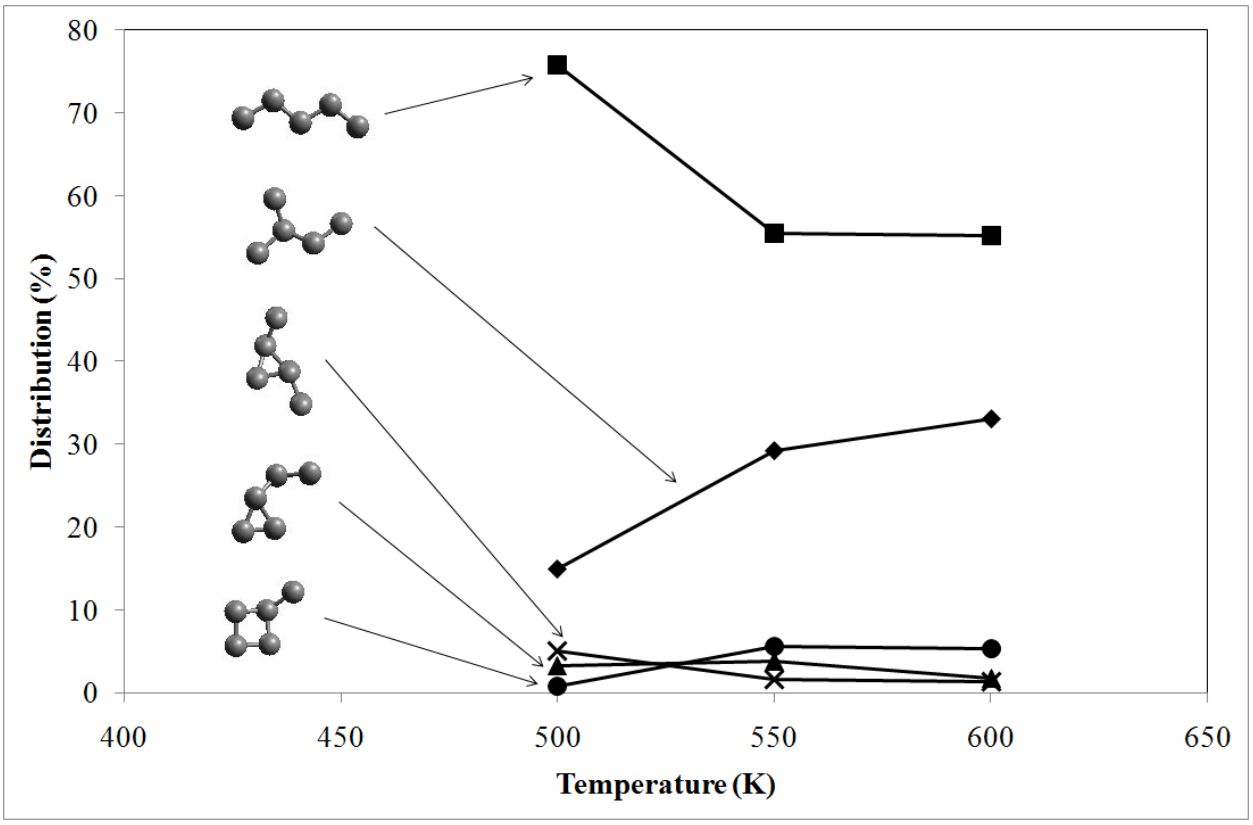

Fig. 6. Frequency distribution of the five most common pentamer configurations as a function of temperature. Lines joining the points have been added as guides for the eye.

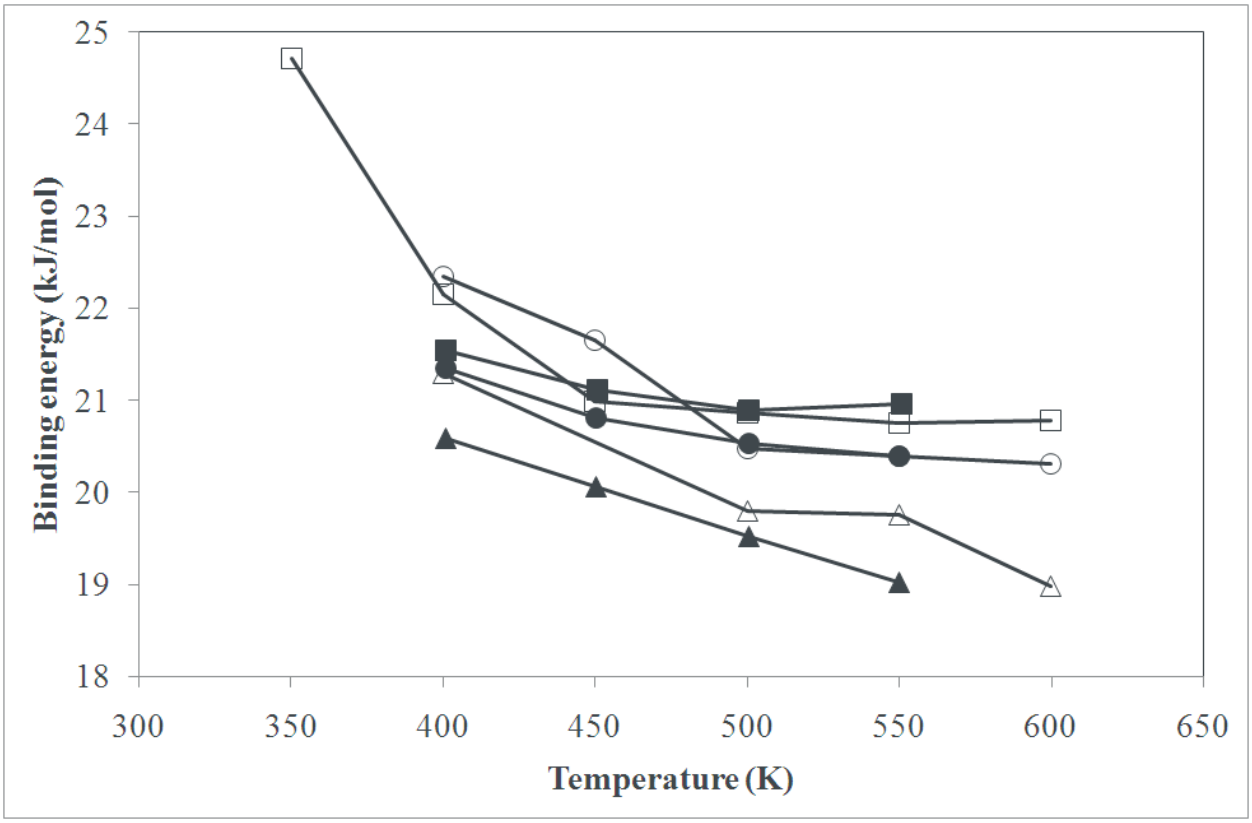

Fig. 7. Dimer and trimer water cluster binding energy versus temperature in perfluorodecane and decane. (■) dimers in decane, (□) dimers in perfluorodecane, (●) linear trimers in decane, (○) linear trimers in perfluorodecane, (▲) cyclic trimers in decane, (△) cyclic trimers in perfluorodecane. Lines have been added between the points as guides for the eye. The data for the decane is from [5].

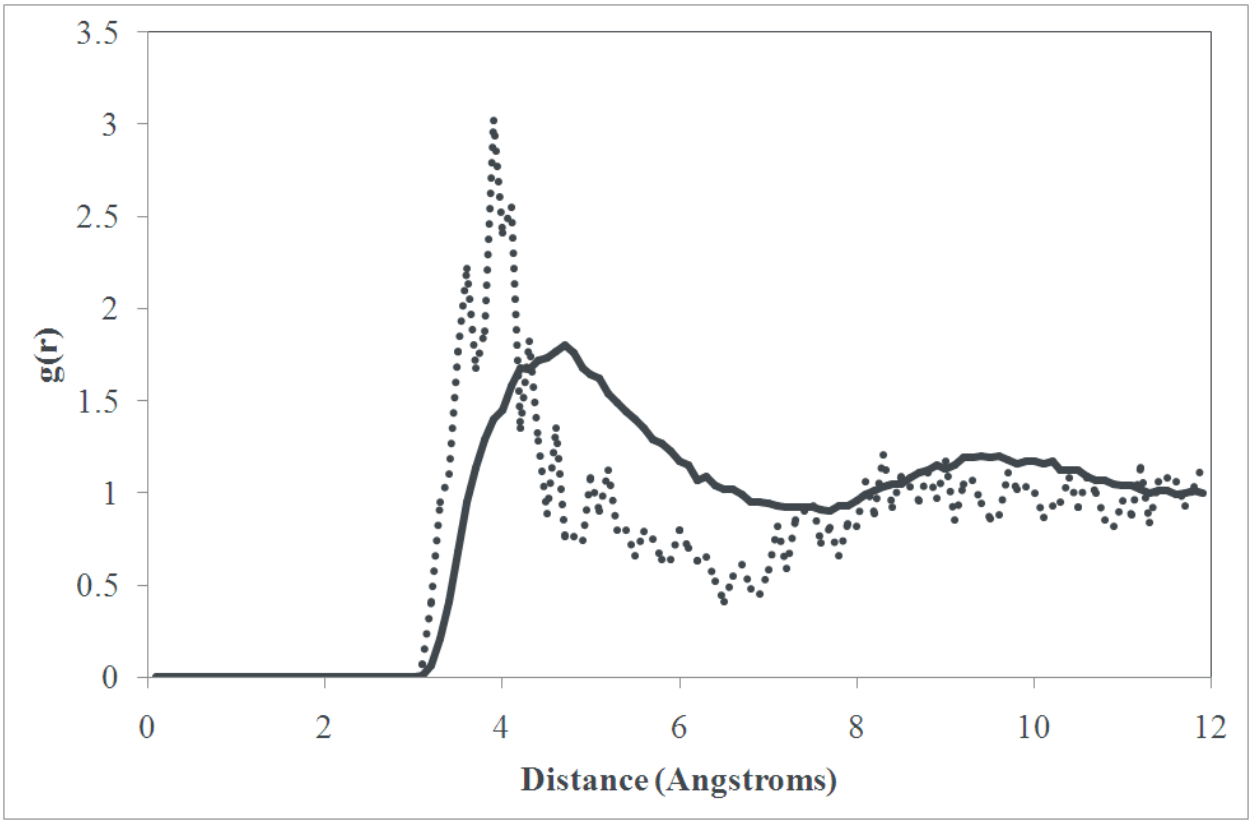

Fig. 8. Radial distribution function of water in PTFE, for a carbon number of 300 at conditions of T = 450 K and P = 2 MPa. Solid lines are for the H_2O-CF_2 pair, dashed lines are for the H_2O-CF_3 pair.

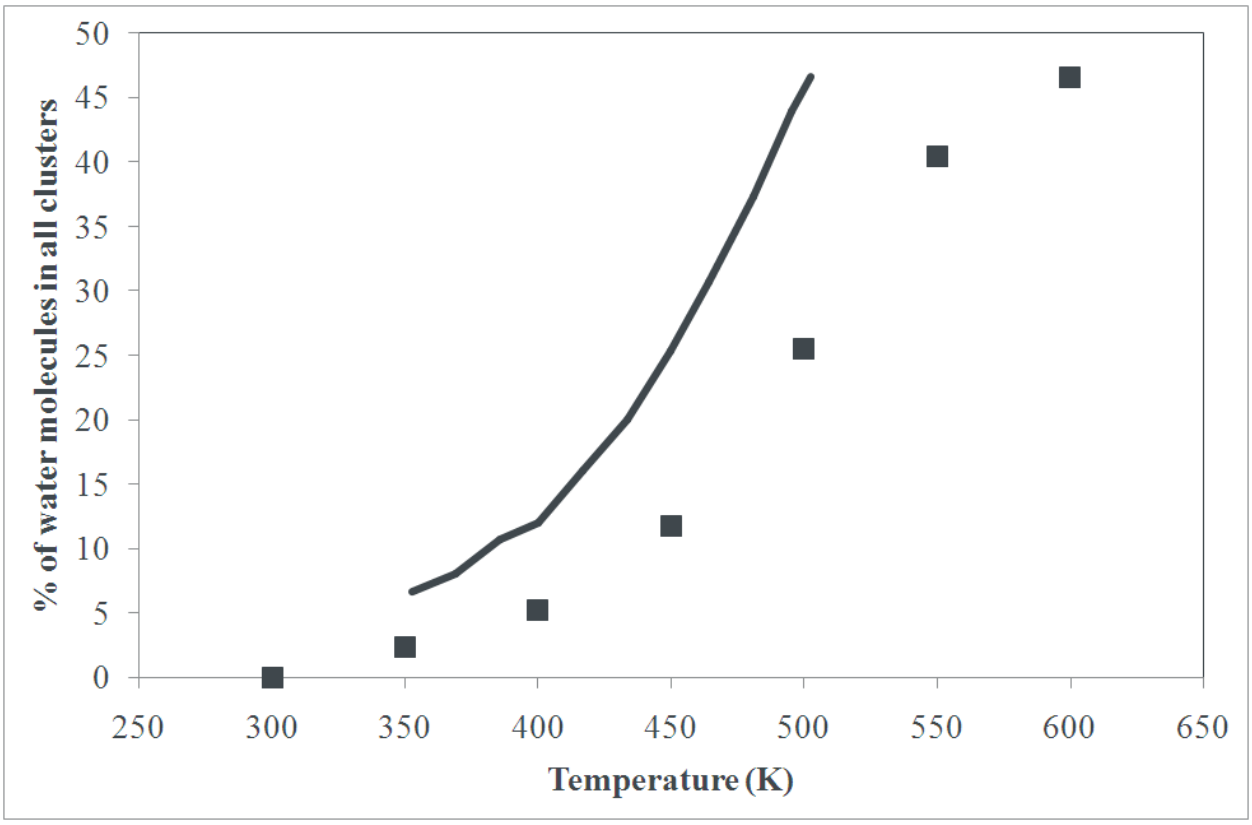

Fig. 9. Percentage of water molecules in all clusters as a function of temperature for the perfluorodecane + water system compared to pure saturated water vapor. (■) water in perfluorodecane, (-) pure saturated water vapor (literature data [6]).

DISCUSSION

As can be seen in fig. 1, there is an overall trend of an increasing fraction of water molecules found in all clusters with increasing temperature. This concurred with prior work on the polyethylene + water system [4, 5, 6]. The increasing presence of clustered water molecules with increasing temperature may also be connected with the increased solubility of water into PTFE with increasing temperature [24]. Since the solubility of water into PTFE increases with increasing temperatures, then of course there would be increasing numbers of water molecules in a confined space, and thus there may be an increased likelihood of water clusters forming.

It can also be seen in fig. 1 that there is a peak occurrence for the smallest water water clusters (consisting of 2 water molecules) at a temperature of 550 K. This may occur when the overall trend of increased water clustering with increasing temperature is taken into account. If increasing numbers of

water molecules in the system begin to group together into clusters, then it would only be natural for some clusters to begin to overlap with neighbouring clusters. This overlapping would naturally result in a larger net water cluster, and thus as more and more water molecules cluster together, it may be seen that smaller clusters may give way to larger and larger clusters.

Figs. 2 through 4 illustrate an inverse correlation of sorts between the polymer carbon number and the fraction of water molecules found in clusters. For polymer carbon numbers from 8 to 50, no clear trend may be seen in any of figs. 2 through 4. From a polymer carbon number of 50 to 300 though, there is an apparent decrease in the fraction of water molecules found in clusters. With reference to the high molar solubility (i.e. ~98 mole percent) of water into PTFE at a carbon number of 300 [24], what may be deduced from this trend at large carbon numbers is that there must be large amounts of free volume for a disproportionately low number of water molecules to occupy within the polymer matrix. This vast amount of free space would not lend itself to clustering of water molecules, and thus clustering would not be as likely to occur as with smaller polymer molecules.

Figs. 5 and 6 illustrate a trend of increasing linearity in the water clusters with increasing temperature. For both tetramers (fig. 5) and pentamers (fig. 6), it may be seen that linear water clusters account for up to ~90 percent of all water clusters. This trend was also observed in the polyethylene + water system [5, 6]. This observation may reveal that the free volume within the polymer matrix consisted of long “channels”. Based upon the cluster definition used in this work, these channels may be, on average, approximately 9 Å across. This value was determined by considering the “square” formed by 4 water molecules arranged in a cyclic fashion, as seen in figs. 5 and 6. If the length of the diagonal is calculated, and the width of two SPC-E water molecules is added to it (to account for the water molecules at each opposing corner of the “square”), then a value of ~ 9 Å emerges.

Fig. 7 illustrates the comparison in the water cluster binding energies of dimers, linear trimers and cyclic trimers between perfluorodecane and decane [6]. This binding energy is more commonly known as the hydrogen bond energy. It may be seen that at the lower temperatures in this figure (less than 500 K), the binding energy in perfluorodecane is significantly higher than in decane, whilst as the temperature increases, the binding energies become approximately equal. This suggests that at lower temperatures, the rigidity of the perfluorodecane chains coupled with the smaller spaces between molecules (due to the temperature) results in a lower probability of water molecules forming clusters with one another. Ultimately, this suggests that at lower temperatures, perfluorodecane may be more densely and rigidly packed than perfluorodecane. An additional observation is that the binding energy of the linear clusters (i.e. dimers and linear trimers) at the higher temperatures (greater than 500 K) is lower in perfluorodecane

than in decane. The reverse may also be observed in fig. 8 for the cyclic trimers. This may also suggest that the geometry of the free volume in perfluorodecane consists of long “channels”, as discussed previously, as voids shaped thusly would favour the formation of linear water clusters over cyclic water clusters.

The radial distribution function seen in fig. 8 illustrates than there may be a higher probability of locating a water molecule at the end of a polymer chain as opposed to along the length of a polymer chain. This may be expected if one takes into account the spatial geometry of a rod-like molecule. In addition, it may be seen that there is a noticeable second peak in the radial distribution function, both for the polymer ends and along the length of the polymer. Perfluoroalkane matrices have been found to possess significant supramolecular ordering [25] due the rigid nature of the perfluoroalkane molecule, and therefore there may be some degree of regularity in the placement of the perfluoralkane molecules along with the interspersed water molecules. This rigidity in the perfluoroalkane chains arises from the helical nature of the chain, brought about by the interaction of the fluorine atoms with one another [26].

Fig. 9 illustrates an increasing deviation with increasing temperature between water clustering in PTFE as compared to pure water vapour. This comparison may considered due to the similar densities of water in PTFE and pure water vapour. This may suggest that with decreasing temperature, the influence of the polymer molecules on the becomes decreasingly prevalent, with the water clustering behaving increasingly similarly to water clustering in pure water vapour. This comparison has also been performed for the polyethylene + water system [6] in which is was found that the water clustering within the polymer matrix behaved approximately similarly to water clustering in pure water vapour. In this work though, fig. 9 illustrates that at increasing temperatures, the presence of the perfluoroalkane chains increasingly influences that clustering behaviour of the water molecules within the polymer matrix. This may be due to the rigidity of the perfluoroalkane molecules dictating the nature of the spatial geometry within the polymer matrix.

CONCLUSIONS

It was found that increasing temperatures resulted in an increasing frequency of water clusters, as well an increasing frequency of large water clusters. A peak frequency for the smallest water cluster (consisting of 2 water molecules) was observed at a temperature of 500 K. This may be due to increased overcrowding of the polymer phase with water molecules at increasing temperatures.

No clear trend was observed regarding the effect of polymer carbon number on the water

clustering behaviour for polymer carbon numbers from 8 to 50. It was observed that from a polymer carbon number of 50 to 300, a significant decrease in the frequency of water clusters of all sizes occurred. This may be due to large amounts of free volume occurring between the rigid polymer molecules being filled with a disproportionately low number of water molecules which would not be conducive to water cluster formation.

It was found that linear water clusters accounted for up to ~ 90 percent of all water cluster tetramers and pentamers. This, coupled with the observation that the binding energies of linear water clusters was significantly lower than for cyclic water clusters, suggests that the geometry of the free volume in the PTFE matrix may be similar to long "channels". The diameter of these "channels" may be ~ 9 Å.

Significant supramolecular ordering of the PTFE matrix was observed by analysis of the radial distribution function of the water in relation to the polymer molecules. Significantly more water molecules were observed at the ends of the polymer molecules than along the length of the polymer molecules. This may be due to the spatial geometry of the scenario.

It was observed that with increasing temperatures, the clustering behaviour of water in the PTFE matrix deviated further and further from the clustering behaviour observed for pure water vapour. This suggests that with increasing temperature, the PTFE chains increasingly influence the geometry of the free volume in the PTFE matrix and the arrangement of water molecules therein.

ACKNOWLEDGEMENTS

We would like to thank the National Research Foundation (NRF) for their generous funding and the School of Engineering at University College of Borås in Sweden for allowing the use of their computing facilities, through which some of the simulations in this work was conducted.

REFERENCES

[1] H.L. Lin, T.L. Yu, L.N. Huang, L.C. Chen, K.S. Shen and G.B. Jung (2005). *Journal of Power Sources* **150**, 11.

[2] M. Courel, M. Dornier, G.M. Rios and M. Reynes (2000). *Journal of Membrane Science* **173**,107.

[3] E. Johansson, K. Bolton and P. Ahlström (2005). *J. Chem. Phys.* **123**, 024504.

[4] E. Johansson and P. Ahlström (2007). *Springer Lecture Notes in Computer Science* **4966/2007**, 59-65.

[5] E.L. Johansson, K. Bolton, D.N. Theodorou and P. Ahlström P (2007). *J. Chem. Phys.* **126**, 224902.

[6] E.L. Johansson, Simulations of Water Clustering in Vapour, Hydrocarbons and Polymers (Thesis for the Degree of Doctor of Philosophy, Chalmers University of Technology, Göteborg, 2007).

[7] K. Gubbins (1993). *Fluid Phase Equilibria* **83**, 1.

[8] DuPont de Nemours (Nederland) B.V., Safety Data Sheet: Teflon® PTFE **(a**vailable online: http://msds.dupont.com/msds/pdfs/EN/PEN_09004a358023be41.pdf, date accessed: 23/03/2010).

[9] DuPont de Nemours (Nederland) B.V., Safety Data Sheet: Teflon™ AF Amorphous Fluoropolymer **(**available online: http://msds.dupont.com/msds/pdfs/EN/PEN_09004a35803537ac.pdf, date accessed: 23/03/2010).

[10] J. Errington and A.Z. Panagiotopoulous, Gibbs Ensemble Monte Carlo Computer Program (available online: http://kea.princeton.edu/jerring/gibbs/index.html date accessed: 01/06/2010, 2000).

[11] A.Z. Panagiotopoulos (1987). *Mol. Phys.* **61**, 813.

[12] V.G. Mavrantzas, T.D. Boone, E. Zervopoulou and D.N. Theodorou (1999). *Macromolecules* **32**, 5072.

[13] S.T. Cui, J.I. Siepmann, H.D. Cochran and P.T. Cummings (1998). *Fluid Phase Equilibria* **146**, 51.

[14] L. Zhang and J.I. Siepmann (2005). *J. Phys. Chem. B* **109**, 2911.

[15] H.J.C. Berendsen, J.P.M. Postma, W.F. van Gunsteren and J. Hermans, in B. Pullman (ed.), Intermolecular Forces (Reidel, Dordrecht, 1981), pp. 331--342.

[16] H.J.C. Berendsen, J.R. Grigera and T.P. Straatsma (1987). *Phys. Chem.* **91**, 6269.

[17] C. Boulougouris, I.G. Economou and D.N. Theodorou (1998). *J. Phys. Chem. B* **102**, 1029.

[18] J.E. Lennard-Jones (1931). *Proceedings of the Physical Society* **43**, 461.

[19] H.A. Lorentz (1881). *Ann. Phys.* **12**, 127.

[20] D.C. Berthelot (1898). *Compt. Rendus* **126**, 1703.

[21] U.W. Gedde, Polymer Physics 1st Edition (Chapman & Hall, London, 1995).

[22] S. Pal, H. Weiss, H. Keller and F. Müller-Plathe (2005). *Phys. Chem. Chem. Phys*. **7**, 3191.

[23] A. G. Kalinichev and J. D. Bass (1997). *J. Phys. Chem. A* **101**, 9720.

[24] M. Lasich, E.L. Johansson and D. Ramjugernath (2011) *Molecular Simulation*, submitted for review.

[25] R. Friedemann, S. Naumann and J. Brickmann (2001). *Phys. Chem. Chem. Phys.* **3**, 4195.